ORGANIC CHEMISTRY

Sulfenylnitrene-mediated nitrogen-atom insertion for late-stage skeletal editing of *N*-heterocycles

Bidhan Ghosh†, Prakash Kafle†, Rishav Mukherjee†, Randall Welles, Deacon Herndon, Kenneth M. Nicholas, Yihan Shao, Indrajeet Sharma*

Given the prevalence of nitrogen-containing heterocycles in commercial drugs, selectively incorporating a single nitrogen atom is a promising scaffold hopping approach to enhance chemical diversity in drug discovery libraries. We harness the distinct reactivity of sulfenylnitrenes, which insert a single nitrogen atom to transform readily available pyrroles, indoles, and imidazoles into synthetically challenging pyrimidines, quinazolines, and triazines, respectively. Our additive-free method for skeletal editing employs easily accessible, benchtop-stable sulfenylnitrene precursors over a broad temperature range (−30 to 150°C). This approach is compatible with diverse functional groups, including oxidation-sensitive functionalities such as phenols and thioethers, and has been applied to various natural products, amino acids, and pharmaceuticals. Furthermore, we have conducted mechanistic studies and explored regioselectivity outcomes through density functional theory calculations.

Scaffold hopping, first introduced by Schneider and colleagues (*1*), began as a virtual strategy in drug discovery to identify novel pharmacophores by making simple structural modifications that alter a molecule's biological and pharmacological properties (*2*, *3*). In recent years, several scaffold hopping methods have been developed for the direct editing of drug molecules. (*4*). Among them, skeletal editing has taken center stage as it modifies the molecular frameworks by adding or removing individual atoms (*5*). In the late-stage functionalization of scaffolds, notable progress has been achieved by editing carbon, nitrogen, or oxygen atoms within a skeleton (*5*–*12*). This process enhances the chemical diversity of existing libraries, allowing access to uncharted regions of chemical space in drug discovery (*13*).

Nitrogen atoms play a pivotal role in medicinal chemistry and drug development (*14*, *15*). For example, pyrroles, indoles, and imidazoles are prevalent nitrogen-containing heterocycles, and direct incorporation of a single nitrogen atom into these structures offers a straightforward route to synthetically challenging heterocycles (quinazoline, pyrimidine, or triazine) without altering the rest of the molecule. Therefore, incorporating a single nitrogen atom could enhance late-stage diversification by adding key pharmacophores to drug discovery libraries (*16*).

The strategy of *N*-atom insertion into an aromatic compound goes back to 1964 when ammonium chloride was used as the source for a single nitrogen atom in the presence of oxidizing agents (*17*) (Fig. 1A). Despite advances in direct *N*-atom insertion (*18*–*28*), most methods rely on nitrene intermediates that require harsh reaction conditions to generate, involving heavy metals (*25*) or excessive use of potent oxidizing (*24*) or pyrophoric reagents (*28*), which constrains synthetic applicability. Additionally, some methods require the protection of free nitrogen in substrates such as indoles, necessitating a separate prefunctionalization step (*27*). Moreover, the direct insertion of nitrogen atoms into pyrroles, azaindoles, and imidazoles remains underexplored, with only a limited number of reports (*28*, *29*).

Department of Chemistry and Biochemistry, University of Oklahoma, 101 Stephenson Parkway, Norman, OK, USA.
***Corresponding author. Email: isharma@ou.edu**
†These authors contributed equally to this work.

Reaction development

Motivated by the potential of nitrenes bearing a leaving group to incorporate a single nitrogen atom, we aimed to uncover a mild protocol that does not depend on oxidizing agents. Our investigation led us to sulfenylnitrenes, which possess a thio-functionality known for its leaving group capabilities. Despite their discovery in 1967 (*30*), these nitrenes have not been extensively explored (*23*, *31*–*35*). Following a comprehensive literature survey, we identified sulfenylnitrene precursors (SNPs) **SNP-1**, **SNP-2**, and **SNP-3**, capable of generating sulfenylnitrenes over a broad temperature range (Fig. 1B). These thermal precursors have only been used in a few prior reports on aziridination (*32*, *33*, *36*, *37*).

Building upon the literature precedents, we hypothesized that the aziridine intermediate featuring an inbuilt thio-moiety as a leaving group would facilitate ring expansion and enable the selective incorporation of a single nitrogen atom. The S–N bond length in sulfenylnitrenes is approximately 1.51 Å, indicating the double bond character between sulfur and nitrogen (*32*). This implies that the metallomimetic properties of sulfur not only stabilize sulfenylnitrenes but also modulate their reactivity for a variety of synthetic transformations (Fig. 1B).

To insert a single nitrogen atom into pyrroles, indoles, and imidazoles, we envisioned using benchtop-stable precursors of sulfenylnitrenes, **SNP-1**, **SNP-2**, and **SNP-3**. These precursors allow the generation of nitrenes under additive-free conditions over a broad temperature range (−30 to 150°C) as described in Fig. 1B (see fig. S8 in the SM for differential scanning calorimetry analyses).

Our optimization studies commenced with the use of symmetric 2,5-diphenyl pyrrole **1a** as the model substrate to overcome the regioselectivity challenge. We employed two equivalents of **SNP-1**, which was generated in situ by the reaction of triphenyl sulfanenitrile with commercially available 2,4-dinitrobenzenesulfenyl chloride at low-temperature using dichloromethane as a solvent (Fig. 2A), following literature precedent for the aziridination (*37*). The reaction produced the corresponding pyrimidine **2a** at −30°C, albeit in a modest yield (15%, entry 1). To enhance the yield, we switched to chlorobenzene as the solvent, inspired by its successful application in aziridination by Atkinson and coworkers (*35*), and the yield improved to 30%. Further raising the reaction temperature to 0°C resulted in an increased yield of 50%; however, temperatures above this led to increased byproduct formation. We next examined the reaction with **SNP-2**. In this case, acetonitrile was initially chosen as the solvent, following the literature precedent for aziridination (*32*). Notably, the reaction resulted in the formation of the corresponding pyrimidine **2a** in 77% yield (Fig. 2B, entry 1). Changing the solvent to dichloromethane or toluene did not substantially improve the yield (entries 2 and 3). However, using chlorobenzene as the solvent led to a nearly quantitative yield of pyrimidine **2a** (99%) (entry 4).

We also tested industrially preferred solvents, including esters and alcohols, and found that the reaction proceeded in both with moderate yields (entries 5 to 8). Finally, we screened 1 and 1.5 equivalents of **SNP-2** precursors, but this resulted in slightly lower yields and left some pyrroles unreacted (entries 9 and 10). Moving forward, we investigated the reactivity of various **SNP-3** precursors in the *N*-insertion reaction with pyrrole **1a** (Fig. 2C). Three distinct nitrene precursors were synthesized and treated with pyrrole **1a**. **SNP-3a** demonstrated a moderate yield (70%) at 100°C (*33*) when chlorobenzene was used as the reaction solvent (entry 1). By contrast, **SNP-3b** and **SNP-3c** exhibited better reactivity with pyrrole **1a**, yielding the desired pyrimidine **2a** in nearly quantitative yield, with chlorobenzene as the solvent (entries 2 and 3). The decomposition temperatures of **SNP-3b** and **SNP-3c** were determined to be 120°C and 150°C, respectively. Other aromatic solvents, such as toluene and xylene, provided slightly lower yields (entries 4 and 5). However, the industrially preferred solvents (esters and alcohols) provided moderate yields of the desired pyrimidine **2a** (entries 6 and 7).

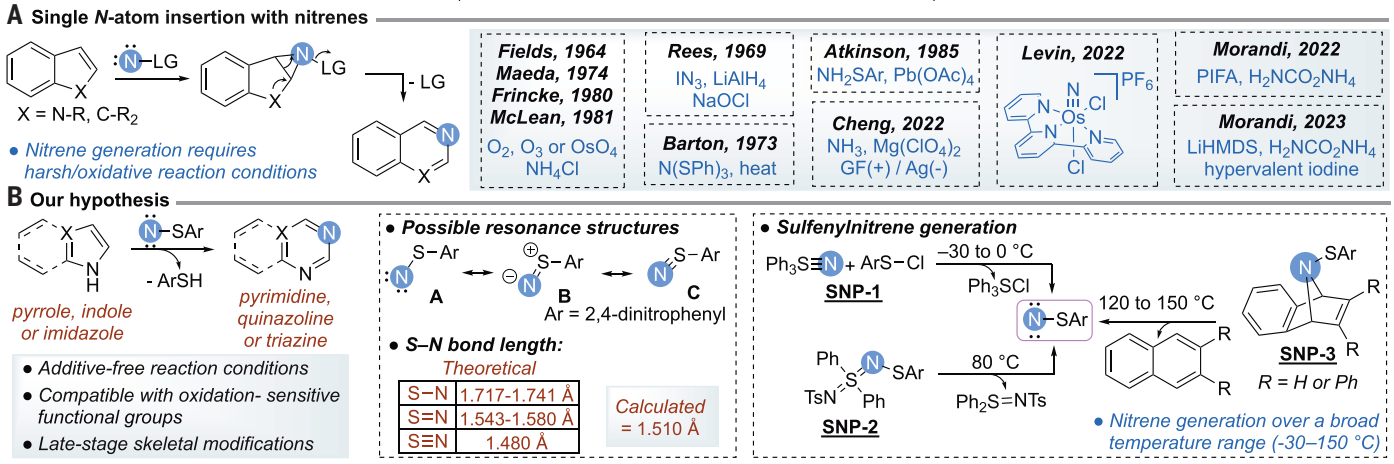

Fig. 1. Background and design. (**A**) Literature precedents for single *N*-atom insertion using nitrenes. (**B**) Our design using sulfenylnitrenes generated from SNPs to achieve tunable, protecting group-free single *N*-atom insertion over a broad temperature range (−30 to 150°C).

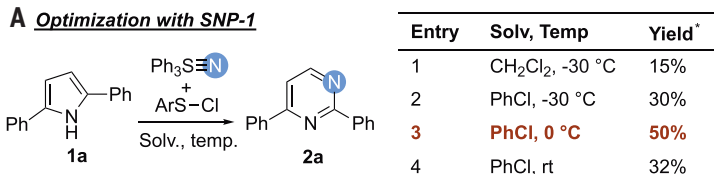

Entry	Solv, Temp	Yield*
1	CH_2Cl_2, -30 °C	15%
2	PhCl, -30 °C	30%
3	**PhCl, 0 °C**	**50%**
4	PhCl, rt	32%

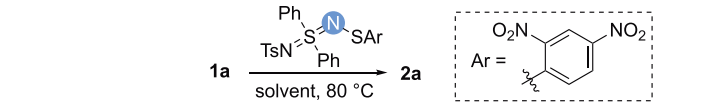

Entry	Solvent	Yield*
1	acetonitrile	77%
2	dichloroethane	75%
3	toluene	80%
4	**chlorobenzene**	**99%**
5	ethyl acetate	73%

Entry	Solvent	Yield*
6	*t*-butanol	48%
7	isopropanol	40%
8	ethanol	45%
9.†	chlorobenzene	68%
10.‡	chlorobenzene	82%

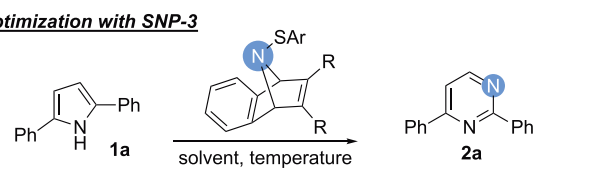

Entry	SNP	Solvent	Temperature	Yield*
1	SNP-3a	chlorobenzene	100 °C	70%
2	**SNP-3b**	**chlorobenzene**	**120 °C**	**99%**
3	**SNP-3c**	**chlorobenzene**	**150 °C**	**99%**
4	SNP-3b	toluene	120 °C	81%
5	SNP-3b	xylene	120 °C	92%
6	SNP-3b	*n*-butanol	120 °C	50%
7	SNP-3b	*n*-butyl acetate	120 °C	50%

SNP-3a: R = H, Ar = 4-nitrophenyl | **SNP-3b:** R = H, Ar = 2,4-dinitrophenyl | **SNP-3c:** R = Ph, Ar = 2,4-dinitrophenyl

Fig. 2. Optimization of the *N*-insertion reaction. (**A**) to (**C**) Reactions were carried out on a 0.03 to 0.1 mmol scale in a sealed vial with 2.0 equiv. of SNPs. *Yield was determined by ^{1}H-NMR using 1,3,5-trimethoxybenzene as an internal standard. †1 equiv. of SNP-2 was used. ‡1.5 equiv. of SNP-2 was used.

We selected **SNP-3b** as the optimal nitrene precursor due to the generation of sublimable naphthalene as a byproduct, easing the purification process at scale. Additionally, **SNP-3b** can be easily synthesized at a large scale (~10 to 20 g) in three simple steps (see SM for additional details).

Scope and application of *N*-insertion into pyrroles

With these optimized conditions, we next investigated the scope and regioselectivity of pyrroles (Fig. 3A). The *N*-insertion preferentially occurs adjacent to electron-donating over electron-withdrawing substituents. For instance, a pyrrole featuring an aryl group at the 3-position and various electron-withdrawing substituents at the 4-position consistently produced the corresponding pyrimidine in good to excellent yields favoring *N*-insertion next to the aryl side (**2b** to **2f**). We observed that a highly oxidation–sensitive thioether functional group underwent the expansion reaction smoothly with a satisfactory yield (**2g**). Next, various 3-substituted pyrroles were subjected to the reaction conditions, and the *N*-insertion predominantly occurred from the substituted side of pyrrole. We observed that phenyl rings bearing electron-donating and electron-withdrawing groups at the 3-position of pyrrole did not affect the regioselectivity outcome (**2h** to **2l**). As anticipated, 3-naphthyl-pyrrole produced the corresponding pyrimidine in high yield (90%) with 1:5 regioselectivity (**2m**). We observed that *di-* and *tri*-substituted pyrroles predominantly yielded a single regio-isomer, favoring the more substituted position (**2n** to **2r**). A pyrrole derivative featuring an 8-membered carbocycle furnished the corresponding pyrimidine in high yield (**2o**). We observed that *tri*-substituted pyrroles bearing a methyl ester and a carboxylic acid functionality were compatible (**2p** and **2q**). Furthermore, pyrrole with a Boc-protected aromatic amine underwent the ring expansion reaction with a nearly quantitative yield (**2r**), highlighting the robustness of this method. Pyrroles with electron-withdrawing esters provided lower regioselectivity, favoring the electron-rich side (**2s** to **2t**).

To further expand the utility of this methodology, we applied it to complex bioactive pyrroles (Fig. 3B). We found that a carbohydrate-bound pyrrole was compatible preserving the stereochemistry at the sensitive anomeric acetal functionality (**2u**). The reaction also proved effective with fenpiclonil, an agricultural phenylpyrrole fungicide (*38*), yielding the expansion product in a good yield (**2v**). Additionally, the antipsychotic drug elopiprazole (*39*) demonstrated compatibility with the reaction, providing a yield of 72%, with only one regioisomer

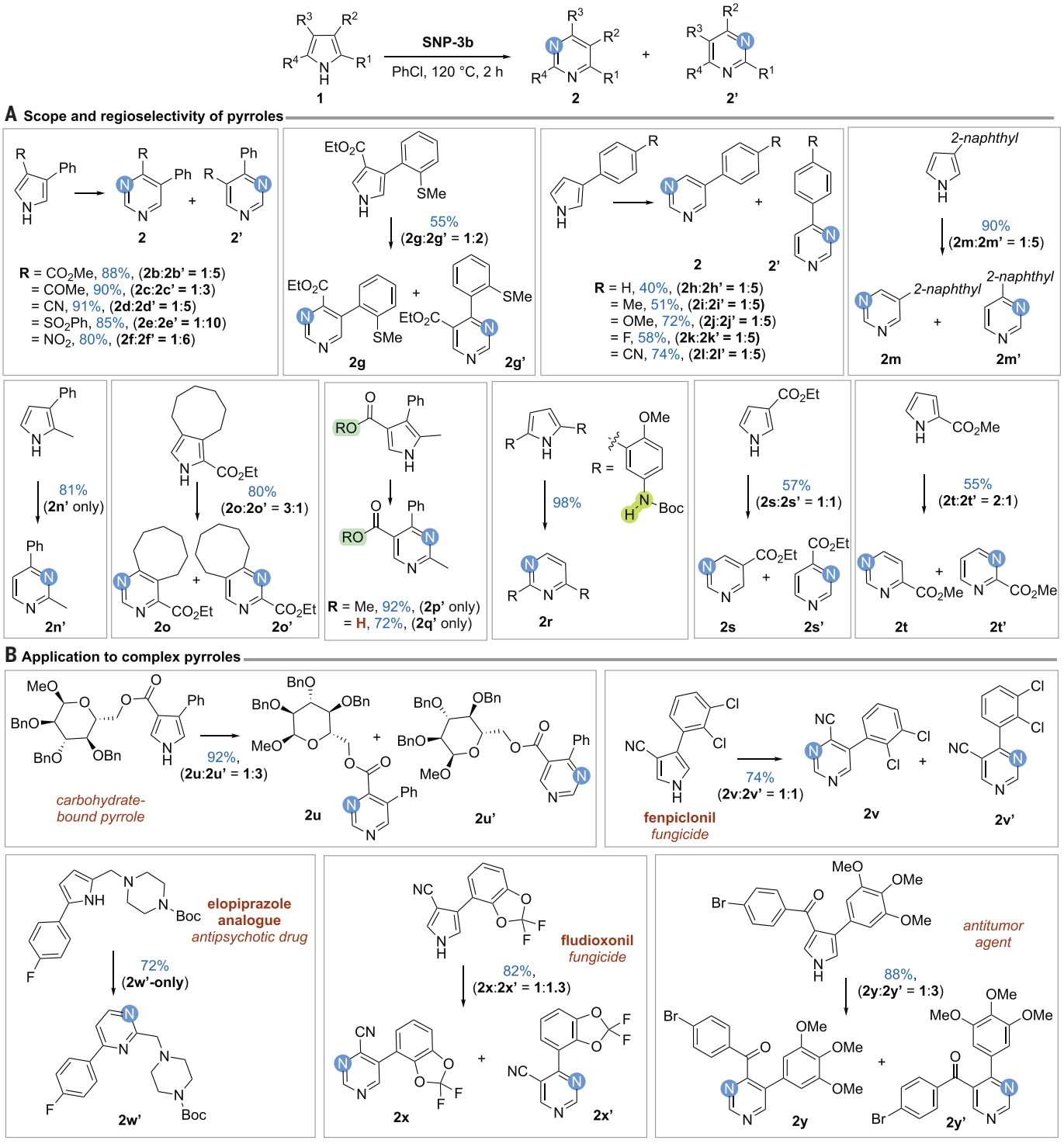

Fig. 3. Scope and regioselectivity. (**A**) Reaction with pyrroles. Conditions: 1 (1 equiv.), SNP-3b (2 equiv.), chlorobenzene (0.1 M), 120°C, two hours. Reactions were carried out on a 0.03 to 0.1 mmol scale and yields reported are isolated yields, except for the products having regioisomeric ratios, which were determined by ^{1}H-NMR using 1,3,5-trimethoxybenzene as an internal standard. (**B**) Application to complex pyrroles.

obtained (**2w**). Furthermore, fludioxonil, a fungicide used for seed treatment (*40*), was successfully transformed to the corresponding pyrimidine (**2x**). Finally, a trimethoxyphenyl substituted pyrrole, recognized as an antitumor agent (*41*), successfully expanded into the corresponding pyrimidine (**2y**) with a high yield of 88%.

Application to indole and azaindole scaffolds

Next, we harnessed the potential of sulfenylnitrenes to add a single *N*-atom to indoles, an important motif in numerous bioactive molecules (*42*) (Fig. 4A). Contrary to the literature reports, in which indole *N*-protection was necessary for the *N*-insertion, our methodology did not require any protection (*27*). This methodology accommodated various indoles, bearing both

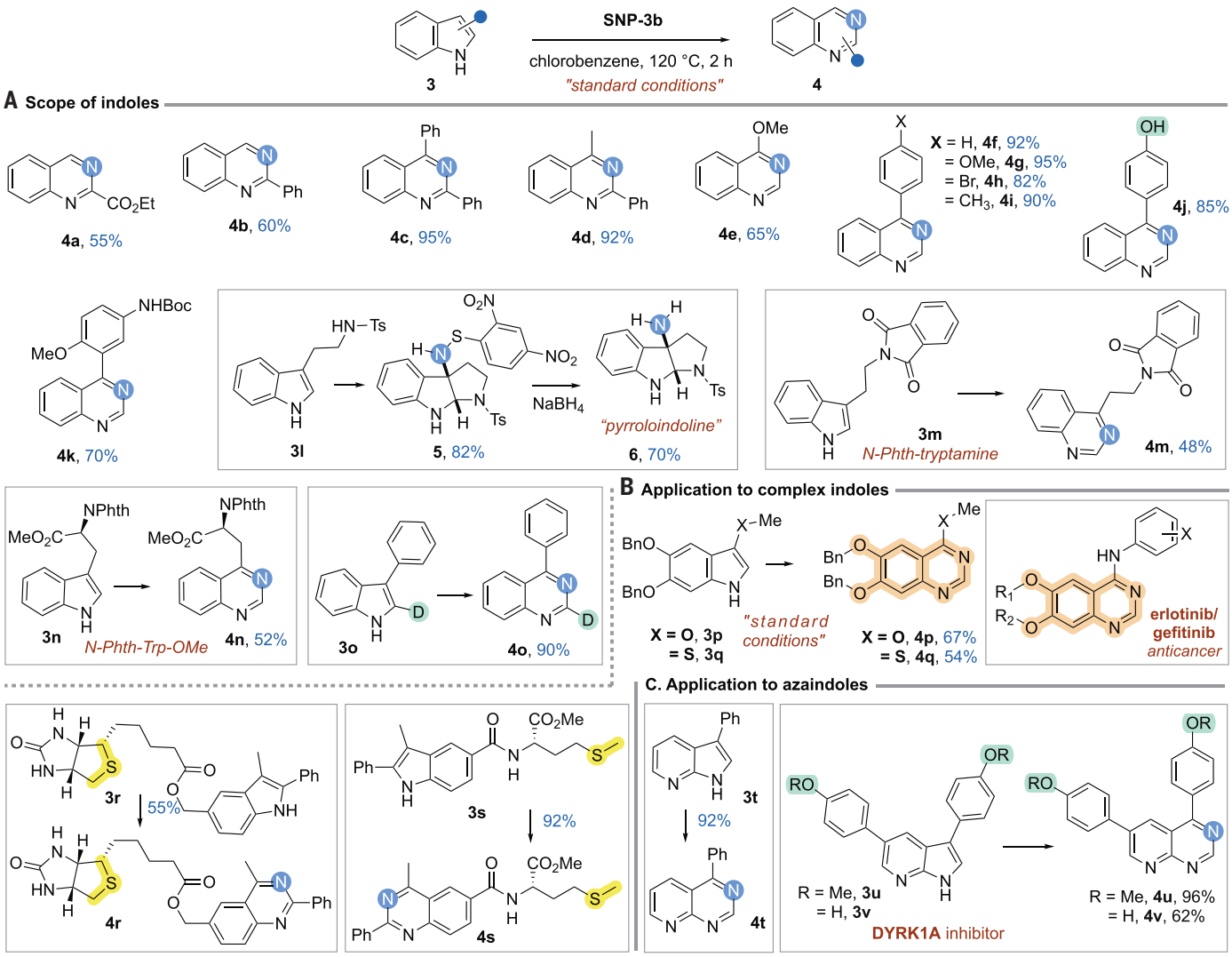

Fig. 4. Application to indoles and azaindoles. (**A**) Scope of indoles. Conditions: 3 (1 equiv.), SNP-3b (2 equiv.), chlorobenzene (0.1 M), 120°C, two hours. Reactions were carried out on a 0.03 to 0.1 mmol scale and yields reported are isolated yields. (**B**) Application to complex indoles. (**C**) Application to azaindoles.

electron-donating and electron-withdrawing groups, and provided the corresponding quinazolines in good to high yields (**4a** to **4i**). The method also exhibited compatibility with the oxidation-sensitive functionality phenol (**4j**), which was incompatible with the existing methods as they require potent oxidizing agents. An indole containing a Boc-protected amine was compatible (**4k**). The reaction with tosyl-protected tryptamine (**3l**) provided the corresponding pyrroloindoline **5** as a single diastereomer in high yield. Mechanistically, the opening of the aziridine intermediate was favored over ring expansion, occurring from the same side of the aliphatic chain at the 3-position of tryptamine, resulting in exclusive *cis*-selectivity (see SM for additional details). This suggests that sulfenylnitrenes can also be used to access bioactive pyrroloindolines, a diverse family of structurally complex polyindoline alkaloids derived from various natural sources including amphibians, plants, and marine algae (*43*). Additionally, the N–S bond of the thioether functionality was easily cleaved through reduction with sodium borohydride. To avoid the cyclization product pyrroloindoline, we used phthalimide-protected tryptamine and tryptophan and transformed them into their respective quinazoline products (**4m** and **4n**), thereby providing access to previously underexplored unnatural amino acids and their derivatives (*44*). We also attempted the reaction with 2-deuterated indole to understand the mechanism further. As expected, no loss of deuterium was observed in the product (**4o**), supporting the mechanistic hypothesis described in the computational simulations (see Fig. 5C and fig. S9).

We further demonstrated the potential of this method for synthesizing readily accessible starting materials for medicinally relevant compounds, such as the anticancer agents erlotinib and gefitinib (*45*), which could aid in developing a robust library of drugs leads. To access their analogs, a substituted indole bearing a thioether functionality **3q** was transformed into quinazoline **4q**, which could be readily converted into erlotinib or gefitinib analogs as outlined in the literature (*46*) (Fig. 4B). Biotinylated indoles serve as bifunctional probes for detecting indole-binding proteins, which are integral to numerous biological processes (*47*). Additionally, 23% of newly FDA-approved small-molecule drugs from 2013 to 2023 feature sulfur moieties (*48*). To demonstrate the compatibility with oxidation-sensitive sulfur-containing complex substrates, a biotin-containing indole **3r** was successfully transformed into the corresponding quinazoline **4r** with good yield. The reaction also showed effectiveness with methionine-derivatized indole **3s**. These results showcase the compatibility of our nitrene reaction conditions with

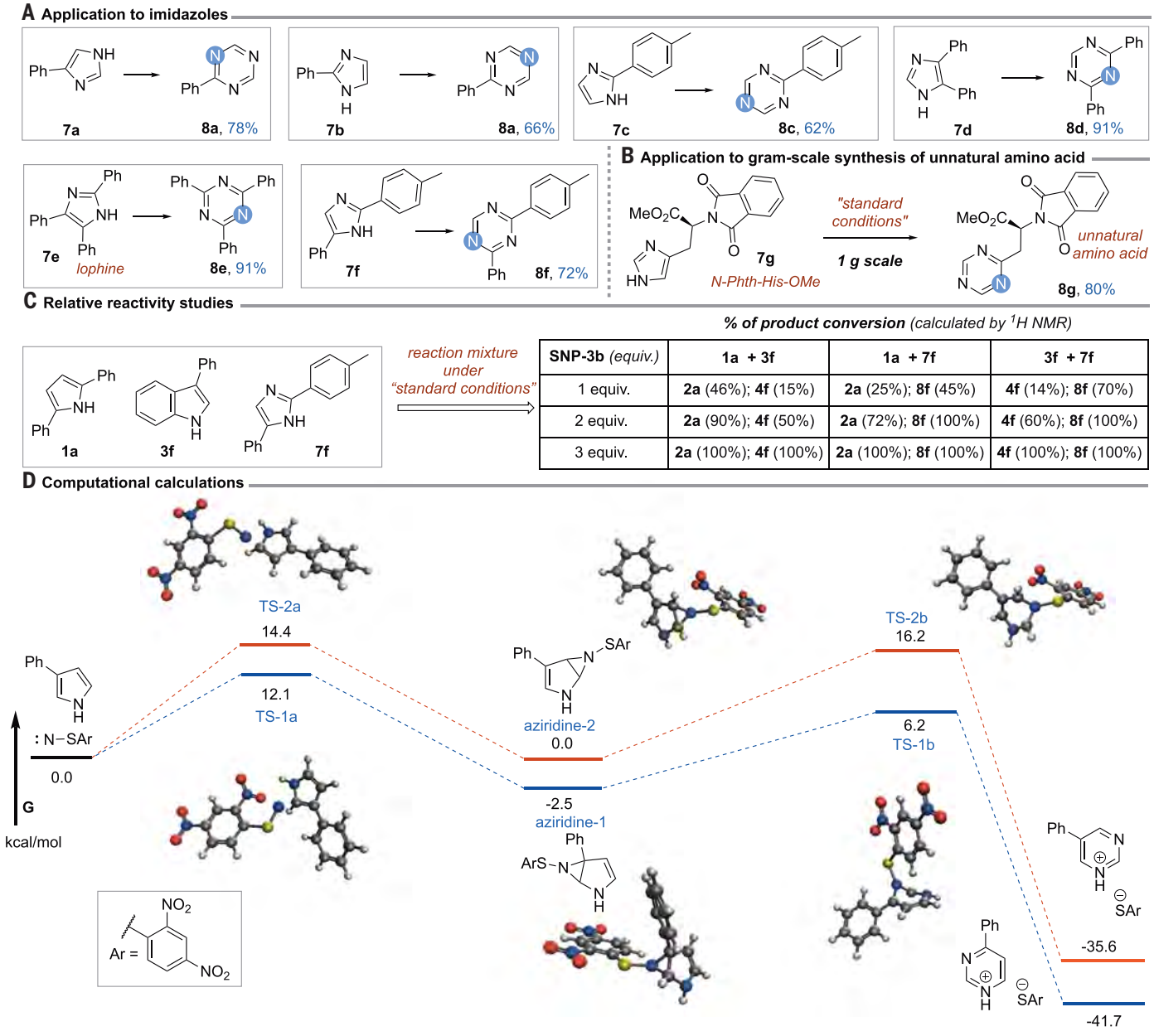

Fig. 5. Application to imidazoles and relative reactivity studies. (**A**) Applications to imidazoles. Conditions: 7 (1 equiv.), SNP-3b (2 equiv.), chlorobenzene (0.1 M), 120°C, two hours. Reactions were carried out on a 0.03 to 0.1 mmol scale and yields reported are isolated yields. (**B**) Gram-scale synthesis of unnatural amino acid. (**C**) Relative reactivity studies of pyrrole, indole, and imidazole. (**D**) Computational calculations. Free energy profile for reaction of 3-Ph pyrrole with sulfenylnitrene **SNP-3b**. Energies are in kcal/mol; atomic colors are as follows: C, gray; O, red; N, blue; S, yellow; H, light gray.

various functionalities including urea, amide, and thioether.

Furthermore, azaindoles are crucial core structures in pharmaceuticals and natural products, widely used in various areas of medicinal chemistry (*49*). However, existing *N*-insertion methods have proven inadequate for expanding azaindoles. Our methodology successfully expanded azaindoles to the corresponding 1,3,8-triazanaphthalenes (Fig. 4C; **4t** and **4u**) with high efficiency. We observed that a phenol-containing azaindole **3v**, a DYRK1A inhibitor (*50*), underwent a smooth *N*-insertion reaction, furnishing the desired product in high yield.

Application to imidazoles, relative reactivity studies, and computational calculations

Following the successful implementation of *N*-insertion into pyrroles and indoles, we also extended its application to imidazoles (Fig. 5A). We observed that various aryl-substituted imidazoles smoothly converted into the corresponding 1,3,5-triazenes, a privileged motif in drug discovery (**8a** to **8f**). Lophine, a chemiluminescent molecule known for its prolonged luminescence, readily underwent expansion in excellent yield (**8e**). Additionally, the phthalimide-protected L-histidine methyl ester (**7g**) was successfully transformed into the corresponding unnatural triazine amino acid (**8g**) at the gram scale (Fig. 5B).

We also investigated the relative reactivity of pyrrole, indole, and imidazole with sulfenylnitrene precursor **SNP-3b**. Combinations of equimolar amounts of pyrrole (**1a**), indole (**3f**), and imidazole (**7f**) were subjected to the standard reaction conditions with 1.0, 2.0, and 3.0 equiv. of **SNP-3b** (Fig. 5C). Rate of *N*-insertion

with 1.0 and 2.0 equiv. **SNP-3b** followed the order imidazole > pyrrole > indole (see figs. S21 to S23 for details). Notably, 3 equiv. of **SNP-3b** fully converted all combinations to the desired products.

Finally, we sought to elucidate the pathway for *N*-insertion to pyrroles by conducting density functional theory (DFT) calculations (B3LYP//6-31G(d)//D3-BJ//SMD-PhCl), resulting in the energy profile shown in Fig. 5D. The reaction begins with the rate-limiting release of 2,4-dinitrophenylsulfenylnitrene, likely a ground state singlet, from the precursor **SNP-3b** (ΔG^{*} = 31 kcal/mol, not shown). The sulfenylnitrene can react with a substituted pyrrole through asymmetric dipolar transition states **TS-1a** or **TS-2a** to form **aziridine-1** or **aziridine-2**. In this asynchronous concerted process, *C2/C5*-bond formation precedes *C3/C4*-bond formation. The insertion regioselectivity, which favors *N*-attack at *C2* over *C5*, can be explained by the more effective delocalization of the developing positive charge in **TS-1a** by the phenyl group at the *C3* position. The reverse regioselectivity observed for substrates **2s** and **2t** can also be explained by our DFT model. Here, the nitrene will preferentially add to the more electron rich side of the pyrrole, favoring the dipolar structure that avoids developing a positive charge adjacent to the electron-withdrawing ester group (see figs. S24 to S31 for details).

These SNPs can be synthesized at a large scale, highlighting their potential for commercial availability. Additive-free nitrene generation, an operationally simple protocol, and good functional group compatibility highlight the advantages of sulfenylnitrenes in creating distinct chemical entities to explore the uncharted chemical space in drug discovery.

REFERENCES AND NOTES

1. G. Schneider, W. Neidhart, T. Giller, G. Schmid, *Angew. Chem. Int. Ed.* **38**, 2894–2896 (1999).
2. Y. Hu, D. Stumpfe, J. Bajorath, *J. Med. Chem.* **59**, 4062–4076 (2016).
3. P. R. Lazzara, T. W. Moore, *RSC Med. Chem.* **11**, 18–29 (2019).
4. K. R. Campos *et al*., *Science* **363**, eaat0805 (2019).
5. J. Jurczyk *et al*., *Nat. Synth.* **1**, 352–364 (2022).
6. S. H. Kennedy, B. D. Dherange, K. J. Berger, M. D. Levin, *Nature* **593**, 223–227 (2021).
7. G. L. Bartholomew, F. Carpaneto, R. Sarpong, *J. Am. Chem. Soc.* **144**, 22309–22315 (2022).
8. B. W. Joynson, L. T. Ball, *Helv. Chim. Acta* **106**, e202200182 (2023).
9. Q.-H. Shi *et al*., *Org. Chem. Front.* **10**, 3307–3312 (2023).
10. M. Peplow, *Nature* **618**, 21–24 (2023).
11. P. Zhang, L. Hua, T. Takahashi, S. Jin, Q. Wang, *Synthesis* **56**, 55–70 (2024).
12. Q. Cheng *et al*., *Nat. Chem.* **16**, 741–748 (2024).
13. I. Sharma, D. S. Tan, *Nat. Chem.* **5**, 157–158 (2013).
14. N. Kerru, L. Gummidi, S. Maddila, K. K. Gangu, S. B. Jonnalagadda, *Molecules* **25**, 1909 (2020).
15. M. M. Heravi, V. Zadsirjan, *RSC Adv.* **10**, 44247–44311 (2020).
16. Y. Hu, D. Stumpfe, J. Bajorath, *J. Med. Chem.* **60**, 1238–1246 (2017).
17. M. I. Fremery, E. K. Fields, *J. Org. Chem.* **29**, 2240–2243 (1964).
18. D. C. Horwell, C. W. Rees, *J. Chem. Soc. D* **23**, 1428a (1969).
19. D. H. Barton, I. A. Blair, P. D. Magnus, R. K. Norris, *J. Chem. Soc., Perkin Trans. 1*1037–1040 (1973).
20. K. Maeda, T. Mishima, T. Hayashi, *Bull. Chem. Soc. Jpn.* **47**, 334–338 (1974).
21. R. B. Miller, J. M. Frincke, *J. Org. Chem.* **45**, 5312–5315 (1980).
22. D. S. Dime, S. McLean, *J. Org. Chem.* **46**, 4999–5000 (1981).
23. R. S. Atkin son, B. D. Judkins, D. R. Russell, L. J. Sherry, *J. Chem. Soc., Perkin Trans. 1*1967–1969 (1985).
24. P. R. Kumar, *Heterocycles* **26**, 1257–1262 (1987).
25. P. Q. Kelly, A. S. Filatov, M. D. Levin, *Angew. Chem. Int. Ed.* **61**, e202213041 (2022).
26. S. Liu, X. Cheng, *Nat. Commun.* **13**, 425 (2022).
27. J. C. Reisenbauer, O. Green, A. Franchino, P. Finkelstein, B. Morandi, *Science* **377**, 1104–1109 (2022).
28. J. C. R *et al*., *Org. Lett.* **25**, 8419–8423 (2023).
29. Y. Shinkai, "Hetarenes and Related Ring Systems" in *Science of Synthesis*, vol. 17 (Thieme Publishing Group, 2004).
30. F. Anet, R. D. Trepka, D. J. Cram, *J. Am. Chem. Soc.* **89**, 357–362 (1967).
31. T. Q. Davies *et al*., *J. Am. Chem. Soc.* **142**, 15445–15453 (2020).
32. T. Yoshimura, T. Fujie, T. Fujii, *Tetrahedron Lett.* **48**, 427–430 (2007).
33. R. S. Atkinson, B. D. Judkins, *J. Chem. Soc., Perkin Trans. 1* 2615–2619 (1981).
34. X. Tian *et al*., *Angew. Chem. Int. Ed.* **58**, 3589–3593 (2019).
35. R. S. Atkinson, M. Lee, J. R. Malpass, *J. Chem. Soc. Chem. Commun.* **14**, 919–920 (1984).
36. A. Lork *et al*., *J. Chem. Soc., Chem. Commun.* **12**, 898–899 (1992).
37. T. Fujii, T. Kousaka, T. Yoshimura, *Tetrahedron Lett.* **43**, 5841–5843 (2002).
38. A. B. Jespers, L. C. Davidse, M. A. Dewaard, *Pestic. Biochem. Physiol.* **45**, 116–129 (1993).
39. I. van Wijngaarden, C. G. Kruse, R. van Hes, J. A. van der Heyden, M. T. Tulp, *J. Med. Chem.* **30**, 2099–2104 (1987).
40. T. T. Brandhorst, I. R. L. Kean, S. M. Lawry, D. L. Wiesner, B. S. Klein, *Sci. Rep.* **9**, 5047 (2019).
41. X. P. Zhan *et al*., *Chem. Biodivers.* **14**, e1600219 (2017).
42. N. K. Kaushik *et al*., *Molecules* **18**, 6620–6662 (2013).
43. C. Sun, W. Tian, Z. Lin, X. Qu, *Nat. Prod. Rep.* **39**, 1721–1765 (2022).
44. T. Narancic, S. A. Almahboub, K. E. O'Connor, *World J. Microbiol. Biotechnol.* **35**, 67 (2019).
45. M. A. Bareschino *et al*., *Ann. Oncol.* **18**, vi35–vi41 (2007).
46. V. Chandregowda, G. V. Rao, G. C. Reddy, *Synth. Commun.* **37**, 3409–3415 (2007).
47. E. Dolusić, M. Kowalczyk, V. Magnus, G. Sandberg, J. Normanly, *Bioconjug. Chem.* **12**, 152–162 (2001).
48. C. M. Marshall, J. G. Federice, C. N. Bell, P. B. Cox, J. T. Njardarson, *J. Med. Chem.* **67**, 11622–11655 (2024).
49. D. R. Motati, R. Amaradhi, T. Ganesh, *Bioorg. Med. Chem.* **28**, 115830 (2020).
50. S. Gourdain *et al*., *J. Med. Chem.* **56**, 9569–9585 (2013).

ACKNOWLEDGMENTS

We thank N.G. Akhmedov and S. Foster from Research Support Services at the University of Oklahoma for NMR and mass spectral analyses, respectively. We gratefully acknowledge B.P. Grady and H. Aboukeila from the Department of Chemical, Biological, and Materials Engineering at the University of Oklahoma for their assistance with the DSC analyses. We also acknowledge support from the OU Supercomputing Center for Education & Research (OSCER). **Funding:** This work was supported by NSF CHE-1753187 (to I.S.). **Author contributions:** I.S. conceptualized the idea and supervised the research. B.G., P.K., R.M., and R.W designed and conducted synthetic experiments, including purification and characterization. D.H., K.M.N, and Y.S. conducted computational studies. B.G. and I.S. prepared the manuscript with input from all authors. **Competing interests:** The authors declare that they have no competing interests. **Data and materials availability:** All data are available in the supplementary materials.

SUPPLEMENTARY MATERIALS

Submitted 13 March 2024; resubmitted 26 September 2024
Accepted 19 November 2024
10.1126/science.adp0974

nature communications

Article

https://doi.org/10.1038/s41467-025-56445-1

Fe(OTf)3 or Photosensitizer-free blue light activated diazo-thioglycoside donors for Iterative and stereoselective glycosylations

Received: 20 September 2024

Accepted: 20 January 2025

Published online: xx xx 2025

Check for updates

Surya Pratap Singh, Umesh Chaudhary, Adrienne Daróczi & Indrajeet Sharma

Conventional methods for thioglycoside activation often rely on precious and toxic platinum group metals. Here, we report a catalytic glycosylation strategy employing diazo-thioglycoside donors activated by earth-abundant iron or photosensitizer-free blue light conditions. It confers orthogonal reactivity relative to most glycosyl donors, including widely used thioglycosides and alkyne-based donors, thereby enabling one-pot orthogonal synthesis of glycans. The Thorpe-Ingold-like effect drives the proximity of iron- or blue-light-generated carbenes to the sulfur atom of thioglycosides. This approach accommodates diverse protecting groups and nucleophiles. It applies to various glycosyl donors derived from glucose, mannose, galactose, rhamnose, xylose, lactose, 2-deoxyamino glucose, and furanose derivatives such as ribose and arabinose. Moreover, we demonstrate the robustness of this methodology through challenging 1,2-*cis* furanosides, late-stage modifications of biomolecules like cholesterol, and the drug simvastatin on a gram scale, along with the iterative synthesis of challenging hexasaccharides.

Carbenes are versatile reactive intermediates in organic synthesis, widely employed in various transformations such as cyclopropanations, cycloadditions, X − H, X − R (X = O, N, S) insertions, and cascade reactions.[1–5] Traditionally, diazo compounds have been the most common carbene precursors, but their activation typically required harsh thermal conditions, often resulting in limited selectivity.[6–13] The introduction of transition metal catalysis, specifically rhodium[14,15] (Rh) and gold[16,17] (Au), has dramatically improved the efficiency of carbene-based transformations.[14,18–21] However, the reliance on these precious and platinum group metals [PGMs] presents environmental and human health concerns,[22] posing substantial challenges in developing sustainable synthetic methods.

Q1 – Q5

Iron (Fe) is the second most abundant metal (5%) in the Earth's crust, after aluminum (8%),[19] and offers a cost-effective and non-toxic alternative to these precious and platinum group metals [PGMs] in catalytic processes (Fig. 1a).[23–26] Significantly less expensive than precious metals (Rh, Au) frequently used in carbene chemistry, making it a more sustainable choice for large-scale applications. For instance, mining 1 kg of rhodium and gold produces 35,100 and 12,500 kilograms of CO_2, respectively, while mining the same amount of iron emits only 1.5 kilograms of CO_2.[27] Moreover, all these PGMs are primarily responsible for global terrestrial acidification, freshwater eutrophication, and human toxicity, compared to earth-abundant metals like iron,[27] underscoring the importance of developing iron-catalyzed organic transformations. Iron catalysts also operate under milder conditions, exhibit lower toxicity, and are environmentally benign, making them attractive in both industrial and academic fields. By utilizing iron in catalytic transformations, chemists can adopt greener, more cost-effective methodologies without compromising efficiency or selectivity. Moreover, using blue light to generate carbenes offers an eco-friendly approach, further boosting the sustainability of these transformations (Fig. 1a).[2,28–30] The iron and blue light-initiated carbene generation provides a promising platform for developing synthetic methods that are both cost-effective and environmentally sustainable.

In this context, our group and others have developed carbene-based transformations using iron catalysis[26,31] or blue light.[2,32] Focusing

Department of Chemistry and Biochemistry, University of Oklahoma, 101 Stephenson Parkway, Norman, OK 73019, USA. e-mail: isharma@ou.edu

https://doi.org/10.1038/s41467-025-56445-1

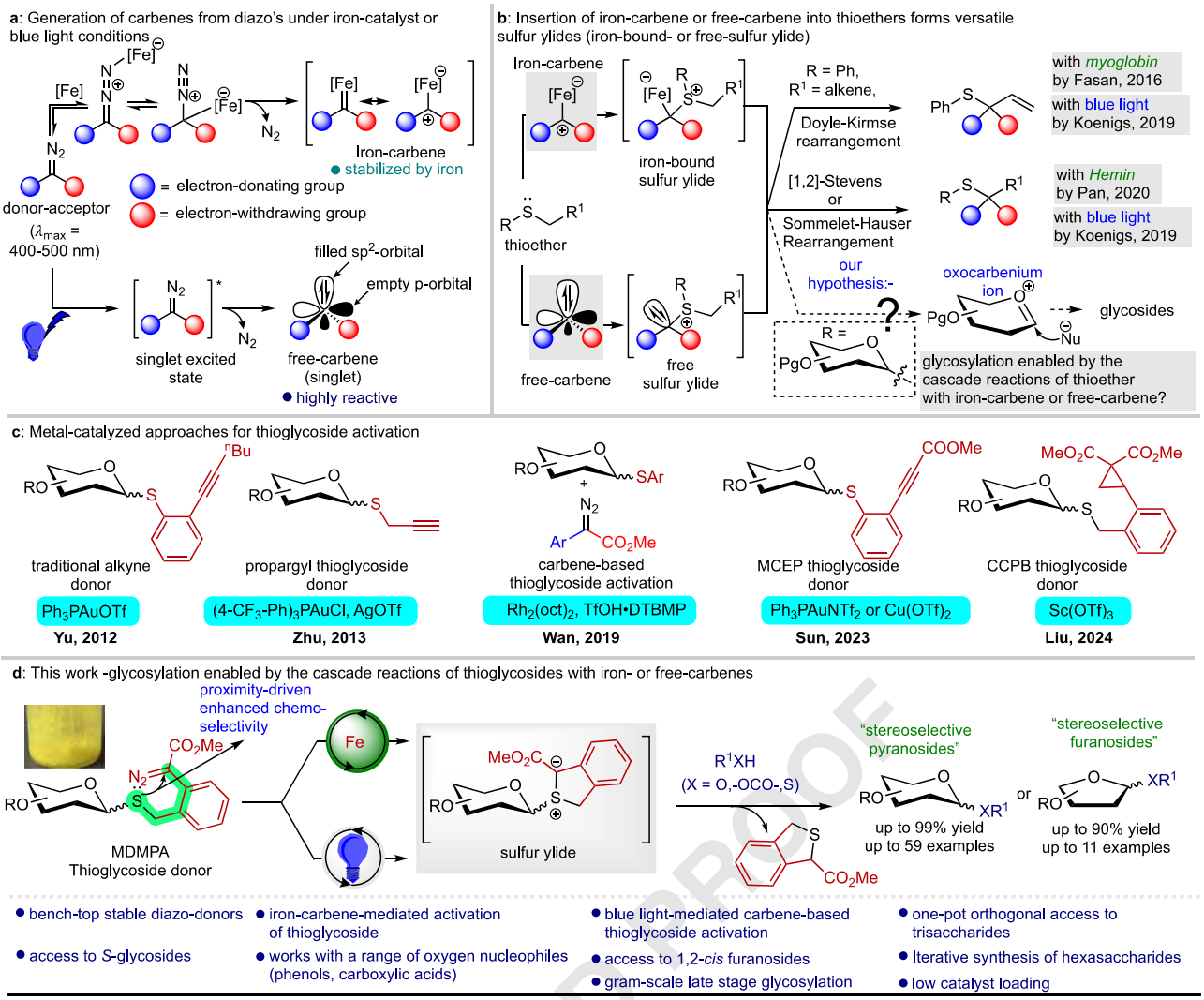

Fig. 1 | Iron-, or Free-carbenes in organic transformations by activating thioethers. a Generation of iron- or free-carbenes from donor-acceptor diazo's, (**b**) application of thioethers with carbenes, and our hypothesis, (**c**) metal-catalyzed activation of various thioglycoside donors, (**d**) This work: iron- or free-carbene-mediated proximity-driven glycosylations. Pg protecting group, MDMPA methyl 2-diazo-2-(2-((methyl)phenyl)acetate, Me methyl, Tf trifluoromethanesulfonate, Ph phenyl, oct octanoate.

on applying carbenes in carbohydrate chemistry,[33–36] we turned our attention to thioglycoside activations. Due to their prolonged stability, thioglycosides are the most widely used glycosyl donors in automated glycan assembly (AGA). However, the inherent stability of thioglycosides often necessitates the use of stoichiometric amounts of promoters or harsh reaction conditions for activation, limiting their applicability and compatibility with various functional groups.[37–39] Over the past decade, several catalytic strategies have been developed to overcome the limitations of traditional thioglycoside activation (Fig. 1c).[40–43] Notably, Wan and coworkers introduced an innovative method in 2019 utilizing rhodium carbenes.[44] In their report, once rhodium carbene reacts with the thioglycoside functionality, it transforms into sulfur ylide. Then, the sulfur ylide gets eliminated to form oxocarbenium ion, eventually leading to access to the glycosidic linkages. While these methods represent significant advancements, their reliance on PGMs and precious metals such as Au,[40,43] Ag,[41] Rh,[44] and Sc,[42] along with the requirement of harsh reaction conditions continues to present challenges for the synthetic community and calls for more sustainable and environmentally benign alternatives.

The thioaryl group in thioglycoside donors is a valuable functionality in organic synthesis, inspiring the development of numerous synthetic transformations. A literature survey revealed that substituted thioether derivatives can react with iron-carbenoids or free carbenes to form unique sulfur ylides. These ylides are crucial intermediates in significant transformations such as the Doyle-Kirmse reaction,[45] [1,2]-Stevens rearrangement,[46] and Sommelet-Hauser rearrangement.[2,26] Fasan and coworkers reported the iron carbene-mediated sulfur-ylide reaction in 2016, utilizing an iron-biocatalyst, *myoglobin (Mb)*, to produce allylic or allenyl sulfides (Fig. 1b).[47] Following Fasan's pioneering work, only a few other reports have emerged, notably from Koenigs and colleagues,[48,49] Bi and coworkers,[50,51] and the Pan group.[52] They further investigated these iron-bound sulfur-ylides in various transformations.

The reaction between blue light-initiated free carbenes and thioethers was reported by Koenigs and coworkers in 2019, where they demonstrated free sulfur ylide-derived Doyle-Kirmse rearrangement to produce allylic sulfides.[53] Since then, only a few groups have utilized these free sulfur ylides.[54–57] While these iron-bound or free sulfur ylides have been primarily used to access benzylic or allylic sulfides and allenes, their potential remains largely untapped. Expanding sulfur-ylides' application, mainly through activating thioglycosides (a class of thioethers) using iron or blue light to synthesize glycosides, represents a significant advancement in this area.

We propose an approach to meet the synthetic community's urgent need for more sustainable methods in catalytic stereoselective glycosylations. We hypothesize that environmentally friendly, iron- or photosensitizer-free blue-light-promoted carbenes can activate thioglycosides via intramolecular pathways, enabling the development of orthogonal and stereoselective glycosylation strategies under mild conditions. These approaches offer a milder, more cost-effective alternative to expensive and environmentally harmful PGMs (Fig. 1d). These carbene intermediates can fragment to generate an oxocarbenium ion, a key intermediate, and easily removable thioether byproducts. The mild, carbene-based activation provides orthogonal reactivity compared to traditional glycosyl donors. The proximity-driven, intramolecular design will accommodate a range of nucleophiles, including primary, secondary, and tertiary alcohols, carboxylic acids, phenols, and sulfur-based nucleophiles. Ultimately, this methodology will offer a new platform for thioglycoside activation, enhancing automated glycan assembly (AGA) for synthesizing oligosaccharides.

Results

Reaction development

In our initial studies, we synthesized perbenzoylated thioglucopyranoside (**3a**) as a donor, methyl 6-OH tri-*O*-benzyl glucopyranoside (**2a**) as an acceptor, and methyl 2-diazo-2-phenylacetate as a carbene precursor. We utilized our previously developed diazo-activation method using $Fe(BF_4)_2{\bullet}6H_2O$ as a catalyst and $NaBAr^F$ as an additive.[31] As expected, the diazo decomposed and generated iron-carbene. However, we observed a direct insertion of the acceptor O–H into the diazo- derived iron carbene, producing product **5** as a major product and only a minimal amount of the desired product **4aa** (see optimization table S1 from supporting information). After screening multiple iron salts and additives, we found that $Fe(OTf)_3$ was the most optimized catalyst, and camphorsulfonic acid (CSA) was the best additive, yielding 54% of the desired product. However, there was still a significant amount of insertion byproduct (Fig. 2a).

Our exploration of photosensitizer-free blue-light-mediated diazo activation successfully generated free carbenes. However, the primary outcome was the insertion of the carbene into the acceptor O–H bond, yielding product **5** as the major product, with only a minor amount of the desired glycoside **4aa**. The direct insertion of a free carbene into the O–H bond can be explained by the work of Koenigs and coworkers.[58] They demonstrated that free carbenes interact significantly with the hydroxyl group through hydrogen bonding, which prefers the formation of O–H insertion products. These preliminary findings with both reaction conditions (Fe-catalyst and photochemical) highlighted a competitive interaction between two nucleophilic systems within the same reaction vessel. Based on the observed byproducts and the reduced yield of the target glycoside, we proposed a plausible reaction pathway for the intermolecular activation of thioglycosides (see Figure S-11 in SI for more details). In this pathway, diazo compounds react with $Fe(OTf)_3$ to form an iron-carbene intermediate, which then interacts with nucleophiles present in the reaction mixture, namely the thioglycoside and glycosyl acceptor. This competition leads to relatively low yields of the desired product alongside significant byproduct formation. Nevertheless, these findings validate and strengthen our hypothesis of developing a carbene-based methodology for thioglycoside activation. To avoid the direct O–H insertion of acceptor alcohols into carbenes to achieve chemoselective thioglycoside activation, we designed an intramolecular thioglycoside donor featuring a diazo functionality **3b** (Fig. 2b).

This donor was synthesized using a readily available, literature-known glycosyl thiol as the glycosyl donor,[59] which reacted with 2-bromomethyl 2-diazo-2-phenylacetate (EDPA) via an S_N2 mechanism with triethylamine as the base and acetonitrile as the solvent. We anticipated that this donor would undergo an intramolecular reaction with the carbene to form a six-membered sulfonium ylide (either iron-bound or free), which would then transform into a glycosyl sulfonium ion, ultimately leading to the formation of an oxocarbenium ion and a glycosidic bond upon coupling with a glycosyl acceptor (see Figure S-14 in the SI for mechanistic details). Upon introducing donor **3b** and acceptor **2a** to the catalytic conditions of $Fe(OTf)_3$ without any additives, we observed the insertion of acceptor **2a** into the iron carbene, producing a major byproduct (**7**) and yielding only a small amount of the desired glycoside (**4aa**). Similarly, irradiation of donor **3b** under

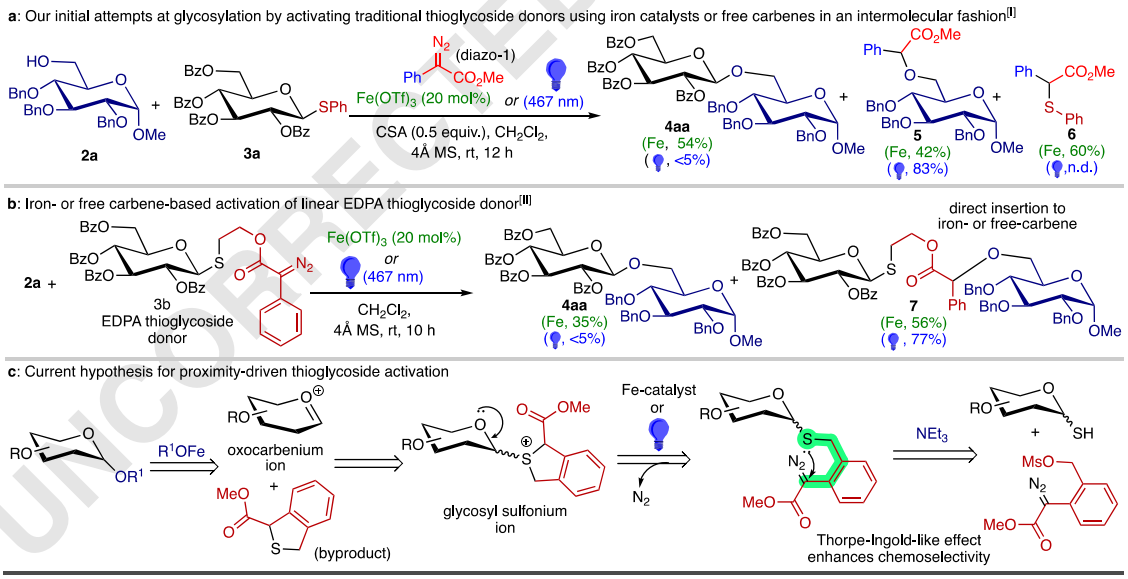

Fig. 2 | Reaction development. a Carbene-based iron-catalyzed or blue-light initiated intermolecular activation of traditional thioglycosides for glycosylation, (**b**) iron-catalyzed or blue-light initiated intramolecular diazo-based thioglycoside activations for glycosylation, (**c**) retrosynthetic analysis for the proximity driven diazo-based thioglycoside activation. [I] acceptor (0.025 mmol), donor (0.037 mmol), $Fe(OTf)_3$ (0.05 mmol, 20 mol%) or Blue-light (467 nm, 50% intensity), CSA (0.012 mmol), CH_2Cl_2 (0.05 M), and diazo-1 (0.063 mmol). [II] acceptor (0.025 mmol), donor (0.050 mmol), $Fe(OTf)_3$ (0.05 mmol, 20 mol%) or Blue-light (467 nm, 50% intensity), and CH_2Cl_2 (0.05 M). Yields in green are for $Fe(OTf)_3$, and those in blue are for blue light. CSA camphorsulfonic acid, n.d. not detected, Bn benzyl, Bz, benzoyl, Ph phenyl, Me methyl, Tf trifluoromethanesulfonate, EDPA ethyl 2-diazo-2-phenylacetate, rt room temperature, MS molecular sieves.

https://doi.org/10.1038/s41467-025-56445-1

blue light in the presence of acceptor **2a** exclusively produced byproduct **7**. These results suggest that, despite the intramolecular design, the sulfur and diazo groups may not be in close enough proximity to achieve the desired reaction.

We hypothesize that the linearity of the linker in this donor could be responsible for the unproductive pathways leading to byproducts and the low chemoselectivity favoring alcohol over sulfur for carbene insertion. While preliminary results demonstrated successful glycoside formation using iron- or blue-light-promoted carbenes, the key challenge remained the chemoselective activation of the thioglycoside in the presence of acceptor alcohol.

To enhance chemoselectivity, we propose leveraging the Thorpe-Ingold-like effect[60] to bring the sulfur atom of the thioglycoside and the carbene closer together. We hypothesize that introducing a phenyl ring with thioether and diazo groups at the *ortho* position will address this issue, promoting chemoselective activation due to the improved spatial alignment of the reactive centers.

Synthesis of MDMPA thioglycoside donors

After a better understanding of reactivity, we resumed our studies by synthesizing designed thioglycoside donors. These donors were easily synthesized using readily accessible glycosyl thiols, which could be synthesized in two steps from the perbenzoylated glycosyl bromide to form glycosyl thiourea salt or thioacetate and their hydrolysis. The crude thiols[59] were light brown solid and significantly pure to use in the last step of donor synthesis, where they were coupled with methyl 2-diazo-2-(2-(((methylsulfonyloxy)methyl) phenyl) acetate[61] (MDMPA) in an S_N2 fashion (Fig. 3).[42] These donors were yellow solid and benchtop stable. Overall, the synthesis of these donors required mainly four main steps, starting from perbenzoylated sugars, but the purification was needed only in the last step, producing overall high yields. We

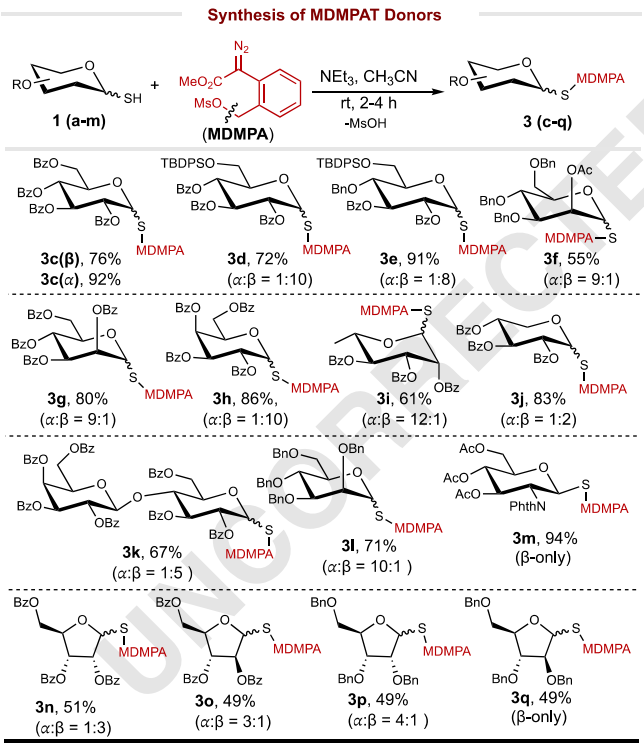

Fig. 3 | Synthesis of MDMPA thioglycoside donors. Reactions were performed with glycosyl thiol (1 equiv.), MDMPA linker (diazo-3) (1.15–1.2 equiv.), triethylamine (1.5 equiv.), and CH_3CN (0.3 M). MDMPAT methyl 2-diazo-2-(2-((methyl)phenyl) acetate, Me methyl, Ms methanesulfonate, Bz benzoyl, TBDPS *tert*-butyldiphenylsilyl, Bn benzyl, Ac acetyl.

synthesize various classes of glycosyl donors, including D-glucose, D-mannose, D-galactose, L-rhamnose, D-xylose, lactose, 2-deoxyamino glucose, D-ribose, and D-arabinose, in good to excellent yields.

Optimization of the reaction conditions

After successfully synthesizing the MDMPA thioglycoside donors, we optimized the reaction conditions. In our initial studies, we selected perbenzoylated (disarmed) MDMPAT **3c** as the model glycosyl donor and **2a** as the model glycosyl acceptor. Based on previous optimizations (see optimization Table S1 from SI), we used $Fe(OTf)_3$ as a catalyst at 20 mol%, CH_2Cl_2 as a solvent, and 4 Å molecular sieves for the initial trial. After stirring the reaction at ambient temperature for 4 h, we were delighted to see an excellent yield of the desired product (entry 1, Table 1). To our delight, the major byproduct (**10**) and other byproducts were easily separated from the desired glycoside **4aa** by a small plug of column chromatography (see Figure S-8 in the SI). To understand and determine the exact stereochemistry at the anomeric position of the product, we performed the 2D-NMR studies. More specifically, the coupled $^1H,^{13}C$-HSQC (Heteronuclear Single Quantum Coherence) provides the $^1J_{C1\text{-}H1}$ values for the anomeric carbon and hydrogen. In this case, we found that the $^1J_{C1\text{-}H1}$ value at the newly formed glycosidic bond was 161 Hz, and at the acceptor, the $^1J_{C1\text{-}H1}$ value was recorded 169 Hz. These values were consistent with the standard known values.[62] We also screened other iron salts as catalysts, such as $Fe(OTf)_2$ (entry 2) and $FeCl_2$ (entry 3), but after stirring the reaction mixture for 24 h, no product formation was observed, and the starting thioglycoside donor remained unreactive. In the case of $FeCl_3$ (entries 4 and 5) and $Fe(BF_4)_2{\cdot}6H_2O$ (entry 6), the donor decomposed into unproductive pathways to produce significant endo glycal (**9**) as the major outcome, highlighting the importance of triflate counter anion in glycosylation reactions.[63] We also screened $Rh_2(esp)_2$ (entry 7) as a catalyst; the reaction was completed in just 2 h, producing the major byproducts with no product formation. Superacids such as trifluoromethanesulfonic acid (TfOH) can also decompose the donor-acceptor diazo and generate carbene, so we performed two experiments with and without molecular sieves (entries 8 and 9). Molecular sieves quenched the TfOH, and the starting material remained unreactive, but without sieves, the starting donor decomposed into undesired products. This experiment was crucial for understanding the role of iron (III) and the triflate counterion in forming disaccharide **4aa**. We then screened various solvents, including THF (entry 10), CH_3CN (entry 11), toluene (entry 12), acetone (entry 13), and ethyl acetate (entry 14). Among these solvents, toluene was found to produce the desired compound, but dichloromethane remained the optimal solvent. We also examined the effect of temperature on the reaction conditions. We observed that lower temperatures, such as −20 °C and −10 °C, did not produce a product, but at 0 °C, the product was observed after a prolonged time of 36 h with slightly lower yields. We varied the amount of donor and catalyst loading and found that 1.5 equivalents of donor and 20 mol% of catalyst were optimal for the reaction. Then, we also examined the different sizes of molecular sieves (MS) 3 Å (entry 15) and 5 Å (entry 16). 3 Å molecular sieves work as efficiently as 4 Å MS, while 5 Å MS produces slightly less yield. Finally, we experimented in the absence of molecular sieves (entry 17), which also led to a slight decrease in yields, further highlighting the importance of molecular sieves.

Simultaneously, we optimized the reaction conditions for blue-light-promoted activation of thioglycosides, using superarmed MDMPAT **3 f** as a model glycosyl donor. During these studies, we primarily screened three wavelengths of blue light (467, 456, and 440 nm) known to decompose donor/acceptor diazo under photosensitizer-free conditions.[32] We also tested various additives to improve the efficiency of the glycoside formation. Ultimately, for donor **3 f**, we found that the 456 nm wavelength combined with LiOTf as an additive produced the best results, highlighting the importance of triflate

https://doi.org/10.1038/s41467-025-56445-1

Table 1 | Optimization of the reaction conditions[a]

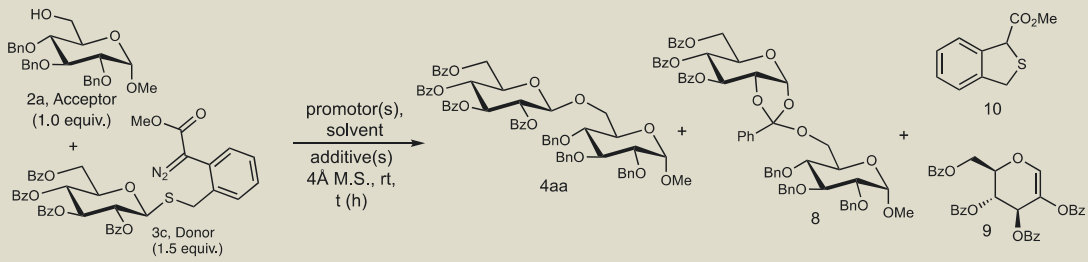

Entry	Promotor (s) [mol%]	Solvent (s)	Additive (s) [equiv.]	t (h)	Yields (%)[b]
1.	$Fe(OTf)_3$ [20]	CH_2Cl_2	-	4	4aa (91)[c], 10 (76)[c]
2.	$Fe(OTf)_2$ [20]	CH_2Cl_2	-	24	n.r.
3.	$FeCl_2$ [20]	CH_2Cl_2	-	24	n.r.
4.	$FeCl_3$ [20]	CH_2Cl_2	-	8	4aa (<5), 9 (81)
5.[d]	$FeCl_3$ [20]	CH_2Cl_2	-	22	4aa (<5), 9 (83)
6.	$Fe(BF_4)_2{\cdot}6H_2O$ [20]	CH_2Cl_2	-	24	4aa (<5), 9 (72)
7.	Rh_2esp_2 [20]	CH_2Cl_2	-	4	8 (34)[c], 9 (70)[c], 10 (74)[c]
8.	TfOH [100]	CH_2Cl_2	-	24	n.r.
9.[e]	TfOH [100]	CH_2Cl_2	-	2	4aa (<10), 8 (28)
10.	$Fe(OTf)_3$ [20]	THF	-	24	n.r.
11.	$Fe(OTf)_3$ [20]	CH_3CN	-	12	4aa (11)
12.	$Fe(OTf)_3$ [20]	toluene	-	18	4aa (83), 10 (92)
13.	$Fe(OTf)_3$ [20]	acetone	-	24	n.r.
14.	$Fe(OTf)_3$ [20]	ethyl acetate	-	24	n.r.
15.[f]	$Fe(OTf)_3$ [20]	CH_2Cl_2	-	4	4aa (90)[c], 10 (73)[c]
16.[g]	$Fe(OTf)_3$ [20]	CH_2Cl_2	-	4	4aa (82)[c], 10 (73)[c]
17.[e]	$Fe(OTf)_3$ [20]	CH_2Cl_2	-	4	4aa (79)[c], 10 (73)[c]
18.	Blue LED (456 nm)	CH_2Cl_2	-	2	4aa (<5), 9 (91)
19.	Blue LED (456 nm)	CH_2Cl_2	LiOTf [1.0]	3	4aa (29), 9 (91), 10 (82)
20.	Blue LED (456 nm)	CH_2Cl_2	LiOTf [1.0] + CSA [0.5]	3	4aa (49), 10 (80)
21.[h]	Blue LED (456 nm)	CH_2Cl_2	LiOTf [1.0] + CSA [0.5]	3	4aa (65), 10 (73)
22.[i]	Blue LED (456 nm)	CH_2Cl_2	LiOTf [1.0] + CSA [0.5]	4	4aa (72), 10 (86)
23.	Blue LED (456 nm)	CH_2Cl_2	CSA [0.5]	4	4aa (<5)
24.	none	CH_2Cl_2	LiOTf [1.0] + CSA [0.5]	24	n.r.

[a] Unless otherwise specified, all reactions were conducted with acceptor 2a (0.025 mmol), donor 3c (0.037 mmol), promotors (0.005 mmol, 20 mol%) or blue-light (456 nm), and CH_2Cl_2 (0.05 M). [b]Yield was determined by ^1H NMR using 1,3,5-trimethoxybenzene as the internal standard. [c]Isolated yields, The yield of byproduct 10 was calculated based on the initial amount of the donor. [d]reactions were performed at 0 °C temperature. [e]Molecular sieves (MS) were not added. [f]3 Å MS were added. [g]5 Å MS were added. [h]2.0 equiv. of a donor was added. [i]2.5 equiv. of a donor was added. *n.r.* no reaction, *n.d.* not detected, *Bz* benzoyl, *Bn* benzyl, *Tf* trifluoromethanesulfonate, *CSA* camphorsulfonic acid, *THF* tetrahydrofuran, *rt* room temperature, *esp* ethylsorbate propionate, *M.S.* molecular sieves; t, time.

counteranion in glycosylation[63] (refer to Table S2 in the SI). We then applied the same optimized conditions to the disarmed donor **3c**, and to our great satisfaction, we observed the desired product, though with significantly low yields (entry 19). The ambiphilic nature of this free carbene[2] and the electron-withdrawing nature of the disarmed[64] donor **3c** resulted in the elimination product (**9**) as the major outcome. This issue was addressed by introducing a Brønsted acid, which significantly increased the yields, presumably protonating the free carbene to enhance its electrophilicity (entry 20, see Figure S-26 in SI for a plausible mechanism). By increasing the donor's equivalents and adding them in portions to the ongoing reaction, we further optimized the conditions for disarmed donor **3c** (entries 21 and 22). Finally, we conducted experiments without LiOTf (entry 23) and no blue light irradiation (entry 24). We concluded that $Fe(OTf)_3$ or blue light (456 nm) works equally well as an efficient promoter for activating MDMPA thioglycoside donors.

In our continued investigation into the effects of protecting groups on MDMPA thioglycoside donors under optimized conditions, we selected a range of donors with varying levels of moderately armed (**3e**), and superarmed (**3 f**). $Fe(OTf)_3$ works protection at each position: fully disarmed (**3c**), disarmed (**3 d**), equally efficiently across all donor classes, although electronic variations influence reaction time. Under blue-light-mediated activation, however, we noted changes in reactivity (Fig. 4a). Specifically, electronically rich MDMPAT donors (**3 d, 3 f**) exhibited similar reactivity, requiring only LiOTf as an additive.

Conversely, electronically deficient MDMPAT donors reacted slightly differently, necessitating a combination of CSA and LiOTf as additives. To explain these reactivity differences under blue light, we propose a plausible mechanism (refer to Figure S-26 in SI). It is well known that carbenes, generated from diazo compounds under blue light, are less electrophilic than metal carbenes. Once free carbene is formed, it reacts quickly with the most acidic site nearby. In the case of disarmed donors, it reacts with the C2 proton, producing endo-glycal **9**. A proton source is introduced into the reaction, and it first protonates the carbene, generating a carbocation intermediate, which is then captured by the sulfur atom of thioglycoside to form an

https://doi.org/10.1038/s41467-025-56445-1

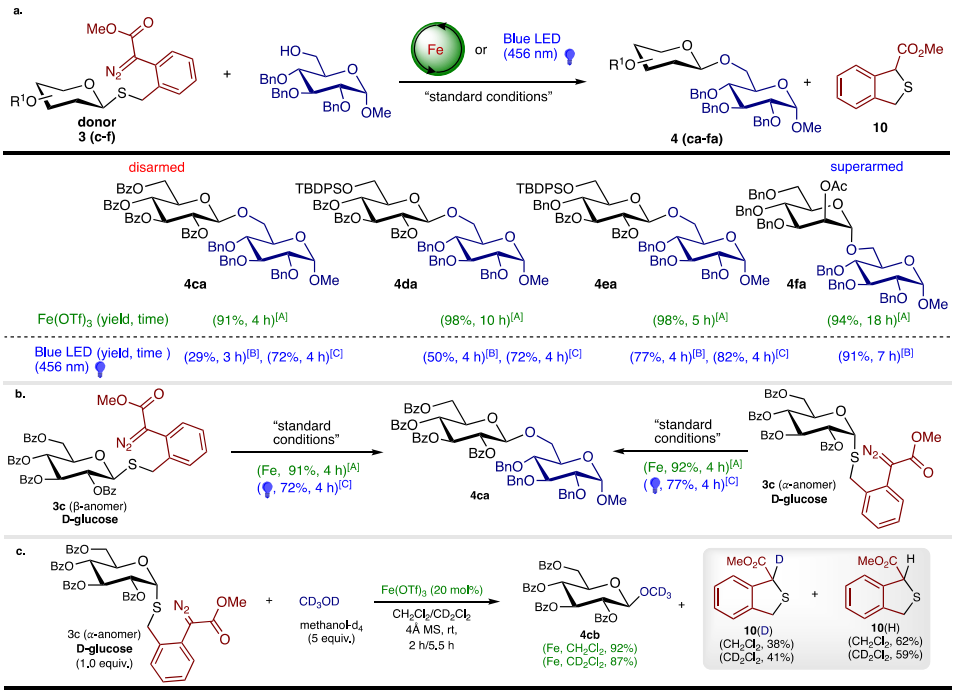

Fig. 4 | Effect of electronics on the reactivity of MDMPAT donors under iron- and blue-light activation conditions. a Effect of protecting groups (disarmed, armed, and superarmed) on the reactivity of MDMPAT donors under standard conditions. **b** Effect of anomeric stereochemistry of the MDMPAT donor (**3c**) under standard conditions. **c** A deuterium labeling experiment was conducted to elucidate the reaction pathway. [A] acceptor (0.025 mmol), donor (0.037 mmol), $Fe(OTf)_3$ (0.005 mmol, 20 mol%), and CH_2Cl_2 (0.05 M). [B] acceptor (0.025 mmol), donor (0.050 mmol), LiOTf (0.025 mmol), Blue-light (456 nm, 50% intensity), and CH_2Cl_2 (0.05 M). [C] acceptor (0.025 mmol), donor (0.062 mmol), CSA (0.012 mmol), LiOTf (0.025 mmol), blue-light (456 nm, 50% intensity), and CH_2Cl_2 (0.05 M). Yields in green are for $Fe(OTf)_3$, and those in blue are for blue light. CSA camphorsulfonic acid, Bz benzoyl, Bn benzyl, Tf trifluoromethanesulfonate, TBDPS *tert*-butyldiphenylsilyl, rt room temperature, MS molecular sieves, Ac acetyl.

oxocarbenium ion. Notably, in the case of superarmed donors, only LiOTf sufficiently stabilizes the carbene and facilitates efficient glycosylation.

To further investigate the impact of electronic effects at the anomeric position, we conducted experiments with anomerically pure donors. Specifically, we synthesized anomerically pure donors **3c(α)** and **3c(β)**. Upon treatment with acceptor **2a** under standard reaction conditions, both donors exhibited identical reactivity patterns (Fig. 4b), yielding the desired disaccharide **4ca** in excellent yield. These results indicate that the stereochemistry at the anomeric position does not influence the reactivity of MDMPA thiofuranoside donors, and the reaction proceeds through the common oxocarbenium intermediate.

To gain further insight into the reaction pathway, we performed deuterium-labeling experiments. Using donor **3c(α)** as a model and methanol-d_4 as the glycosyl acceptor, we observed excellent yields of the desired glucoside **4cb**, accompanied by a 38–41% yield of the deuterated byproduct (**10**) (Fig. 4c). These findings suggest that the protonation of the glycosyl sulfonium ylide can occur via two pathways: (1) proton donation from the glycosyl acceptor or (2) protonation from residual moisture in the reaction solvent (see Figure S-27 in the Supporting Information). This series of experiments not only elucidated the mechanistic pathways but also enhanced our understanding of MDMPA donor reactivity. Encouraged by these insights, we extended our investigation to screen various substrates, aiming to develop a comprehensive library of glycosylated molecules.

Scope of glycosyl acceptors

After optimizing the reaction conditions, we investigated various nucleophiles, including *O*-nucleophiles (alcohols, phenols, carboxylic acids) and *S*-nucleophiles, as glycosyl acceptors to demonstrate the effectiveness of this methodology. We chose the perbenzoylated (disarmed) MDMPA thioglycoside **3c** to investigate the glycosyl acceptors as a model donor. Initially, we utilized primary sugar alcohols with different protecting groups such as benzyl mannopyranoside **2b**, benzoyl glucopyranoside **2c**, mannopyranoside **2 d**, galactose acetonide **2e**, and acetyl glucopyranoside **2 f**. We were pleased to observe excellent yields of the disaccharides (**4cc-4cg**) (Fig. 5). Subsequently, we examined sterically hindered secondary sugar alcohols (**2g-2i**), producing pyranosides (**4ch, 4ci**) and furanosides (**4cj**) in excellent yields with expedited reaction times. The chiral secondary alcohol menthol provided an excellent yield of the desired product **4ck**. Additionally, the highly sterically bulky alcohol 1-adamantanol **4cl** yielded excellent results under standard reaction conditions.

After successfully screening various alcohols, we then investigated other *O*-nucleophiles. Specifically, we used 4-methoxyphenol as a phenol, which produced an excellent yield of **4 cm** despite being less nucleophilic. Typically, synthesizing glycosyl esters requires stoichiometric amounts of coupling reagents,[65,66] but our methodology efficiently formed glycosyl ester **4cn** quantitatively from its corresponding carboxylic acid. Glycopeptides, often found in pharmaceutically active compounds,[67] pose a significant challenge for carbohydrate chemists due to their complex synthesis. We attempted OH–*Z*–ser–OMe and OH–*Z*–ser–OAllyl as acceptors, successfully obtaining their corresponding glycopeptides **4co** and **4cp** in excellent yields. This suggests our methodology could be useful for the synthesis of late-stage glycopeptides. Following the successful screening of the oxygen nucleophiles, we turned our attention to sulfur nucleophiles as glycosyl acceptors. Fortunately, we obtained the corresponding thioglycosides (**4cq-4cr**) in moderate to good yields. To further test the robustness of our methodology, we synthesized glycosyl acceptors with thioglycoside and alkyne functionalities at the activated anomeric position. Upon treatment with MDMPA

https://doi.org/10.1038/s41467-025-56445-1

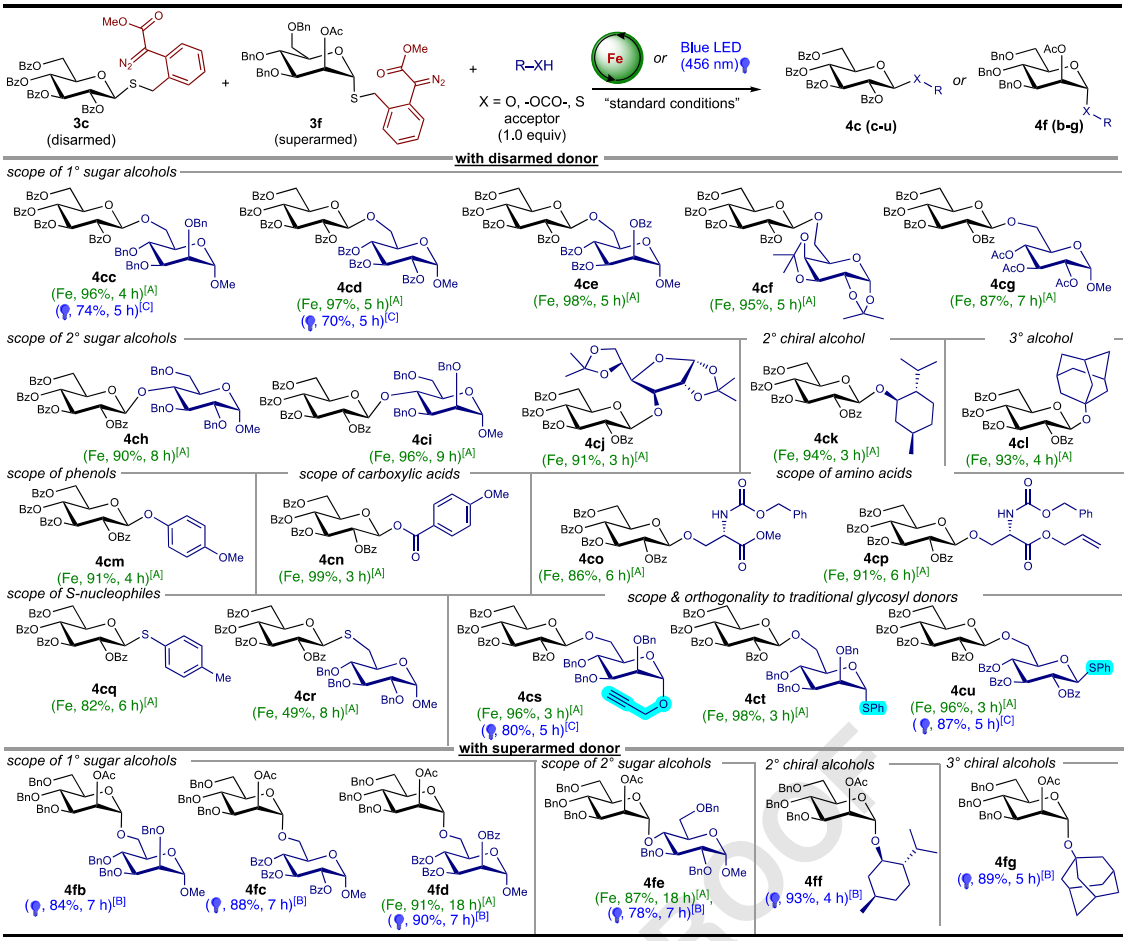

Fig. 5 | Scope of glycosyl acceptors. [A] acceptor (0.025 mmol), donor (0.037 mmol), $Fe(OTf)_3$ (0.005 mmol), and CH_2Cl_2 (0.05 M). [B] acceptor (0.025 mmol), donor (0.050 mmol), LiOTf (0.025 mmol), Blue LED (456 nm, 50% intensity), and CH_2Cl_2 (0.05 M). [C] acceptor (0.025 mmol), donor (0.062 mmol), CSA (0.012 mmol), LiOTf (0.025 mmol), and Blue LED (456 nm, 50% intensity), CH_2Cl_2 (0.05 M). Yields in green are for $Fe(OTf)_3$, and those in blue are for blue light. Note: In the product numbering system, the first number and letter (e.g., 4c) represent the donor's identity, while the second (e.g., d in 4 cd) indicates the product's identity. Bz, benzoyl; Bn, benzyl; Ac, acetyl.

thioglycoside donor **3c**, both functionalities remained unreactive under our reaction conditions (Fig. 5). We were delighted to observe excellent yields of the desired disaccharides **4cs**-**4cu**. We then focused on the reactivity of superarmed donors[64] with various nucleophiles. Using primary sugar alcohols with different protecting groups, such as benzyl mannopyranoside **2b**, benzoyl glucopyranoside **2c**, and mannopyranoside **2 d**, we observed excellent yields of disaccharides **4fb**-**4cd**. Similarly, sterically hindered secondary sugar alcohols **2 g** produced pyranosides **4fe** in excellent yield. The chiral secondary alcohol menthol yielded the desired product **4ff** with high efficiency. The sterically bulky alcohol 1-adamantanol was tolerated well, yielding the desired product **4fg** in excellent yield under standard reaction conditions.

Overall, our methodology is robust and cost-effective for all classes of glycosyl acceptors. Given its robustness, this approach can more efficiently synthesize various complex molecules such as glycosyl esters and glycopeptides and complement other known methods.

Scope of MDMPA thioglycoside donors

After successfully investigating glycosyl acceptors, we expanded our studies to include MDMPA thioglycoside donors. We resumed testing different protecting groups from Fig. 4a, using the MDMPA thioglucopyranoside donor **3 d** with a tert-butyldiphenylsilyl (TBDPS) group protecting the C6 oxygen. Under standard conditions, this donor produced excellent yields with a benzoylated mannopyranoside acceptor **2 d** and a sterically hindered glucosyl acceptor **2 g**, yielding **4db** and **4dc** (Fig. 6). We then used an MDMPAT mannosyl donor **3 g** with various acceptors, including primary sugar alcohols, thiols, and phenols. Sugar alcohols were successfully transformed into disaccharides (**4ga**-**4ge**) with excellent yields. While sugar thiols produced the desired product **4gd** in moderate yields, phenols yielded product **4fe** in excellent quantities. We then activated our MDMPAT galactose donor (**3 h**) with primary glycosyl acceptors (**2a, 2 d**) and secondary glycosyl acceptor (**2 g**) to produce excellent yields of the desired disaccharides (**4ha**-**4hc**). It is well known that the protecting group at the C6 position of sugars affects the reactivity at the anomeric position. To further investigate the effect of C6 protection, we used our synthesized MDMPAT rhamnose donor **3i**. We were pleased to find that this donor worked well with various primary and secondary sugar alcohols, yielding rhamnose disaccharides (**4ia**-**4ic**) in excellent quantities. Next, we explored the effect of C5 substitution on the reactivity at the anomeric position. We used our xylose donor **3j**, which has no substitution at the C5 position. We found it worked well with both primary (**2a, 2 d**) and secondary (**2 g**) sugar acceptors without affecting the reactivity of the thioglycoside donor, producing excellent yields of the xylose disaccharides (**4ja**-**4jc**). After testing monosaccharide donors, we examined the effect of disaccharide donors on the reactivity at the anomeric position. We used our synthesized lactose donor **3k** and exposed it to glycosyl (1°, 2°) acceptors under our standard conditions. We were pleased to find it produced the

https://doi.org/10.1038/s41467-025-56445-1

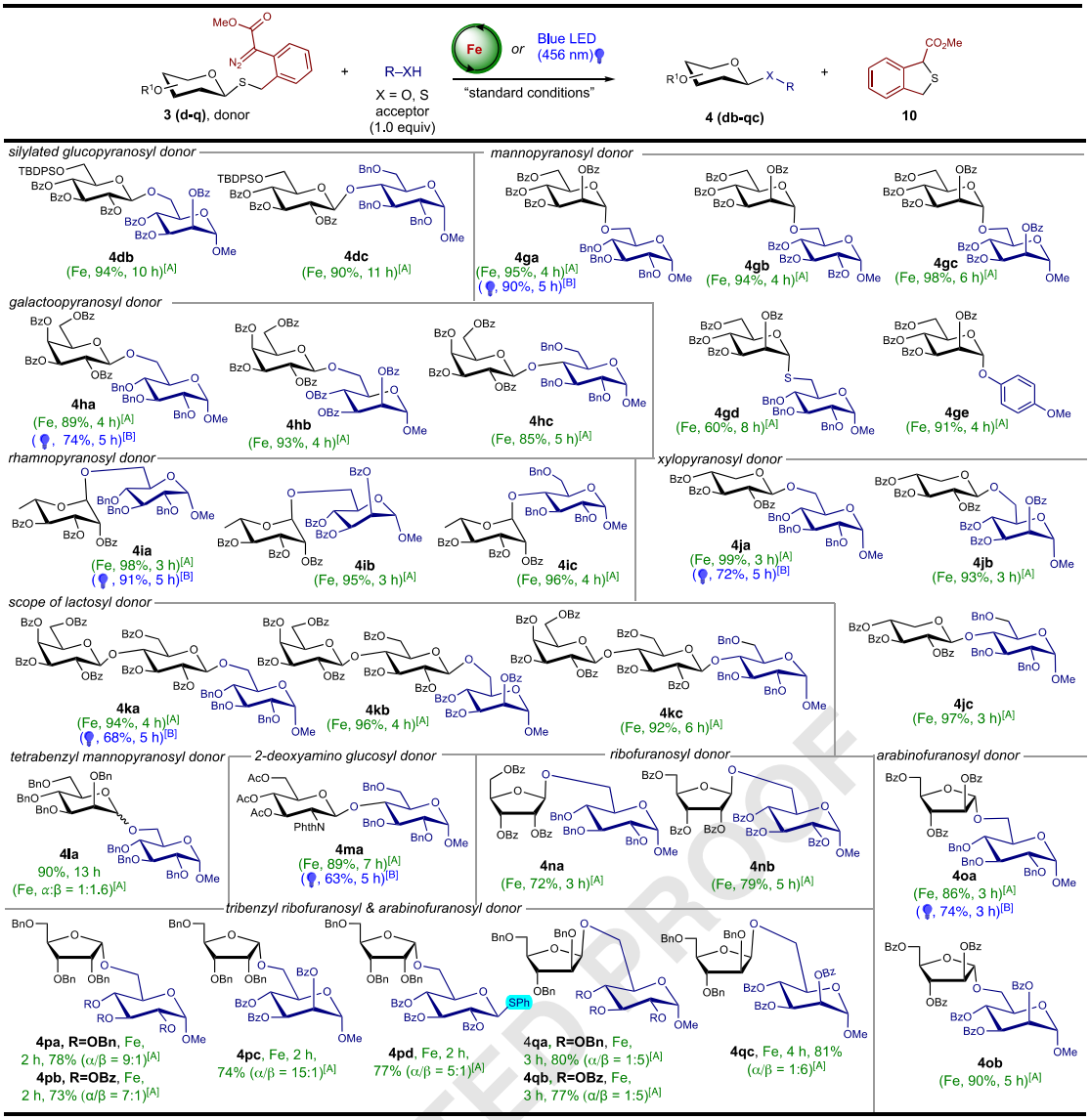

Fig. 6 | Scope of MDMPA thioglycoside donors. [A] Acceptor (0.025 mmol), donor (0.037 mmol), $Fe(OTf)_3$ (0.005 mmol), and CH_2Cl_2 (0.05 M). [B] Acceptor (0.025 mmol), donor (0.062 mmol), CSA (0.012 mmol), LiOTf (0.025 mmol), and Blue LED (456 nm, 50% intensity), CH_2Cl_2 (0.05 M). Yields in green are for $Fe(OTf)_3$, and those in blue are for blue light. Bz, benzoyl; Bn, benzyl; Ac, acetyl; Ph, phenyl; Phth, phthalimido; TBDPS, tert-butyldiphenylsilyl; Me, methyl.

respective trisaccharides (**4ka-4kc**) in excellent yields. So far, we only used benzoyl protection, which worked excellently with our standard conditions. However, we aimed to test our methodology with various protection groups to increase its applicability. In the realm of this, we synthesized a perbenzylated mannose donor **3 l** and found it worked with sugar alcohol to produce the desired disaccharide **4la** in good yield and with a mixture of diastereomers. Furthermore, we activated our MDMPAT 2-deoxyamino glucose donor **3 m** with secondary glycosyl alcohol (**2 g**) under standard conditions. We also found this to work well, producing the desired 2-deoxy amino disaccharide (**4ma**) in excellent yields. After successfully exploring the scope of pyranose donors, we shifted our focus to a different class of carbohydrates, the five-membered furanosides.

Furanosides are crucial components of many oligosaccharides of biological importance, and interest in the stereoselective synthesis of furanose-containing glycans has gained significant attention from the carbohydrate community.[68–73] Furanosides often feature 1,2-*trans* and 1,2-*cis* linkages, essential for their biological function.[74–76] We envision the synthesis of these linkages using MDMPA thiofuranoside donors. The reactivity of pyranose and furanose differ due to their conformational stability and rigidity; applying the same methodology to thiofuranosides is challenging. Following our strategy, we synthesized a perbenzoylated ribose MDMPA thiofuranoside donor **3n** and reacted it under standard conditions using primary sugar alcohols having benzyl (**2a**, activated) and benzoyl (**2c**, deactivated) protecting groups. We were ecstatic to find the formation of the desired products (**4na, 4nb**) in excellent yields. Building on these results, we also synthesized an arabinose MDMPA thiofuranoside donor **3o** and reacted it under standard reaction conditions using glucose (**2a**) and mannose (**2 d**) glycosyl acceptors. Expectedly, we observed similar results and produced excellent yields of desired products (**4oa, 4ob**). After successfully achieving the *trans* linkage, we considered applying our methodology to access the *cis* linkages. The synthesis of 1,2-*cis* linkage in furanosides is challenging due to the higher oxocarbenium ion stability. It is well known that the activation of furanose donors proceeds via an oxocarbenium ion, which favors the S_N1 pathway, making 1,2-*cis*-selectivity challenging to access.[77,78] Few literature reports have achieved 1,2-*cis* furanosides by utilizing chelation either by metal- or

https://doi.org/10.1038/s41467-025-56445-1

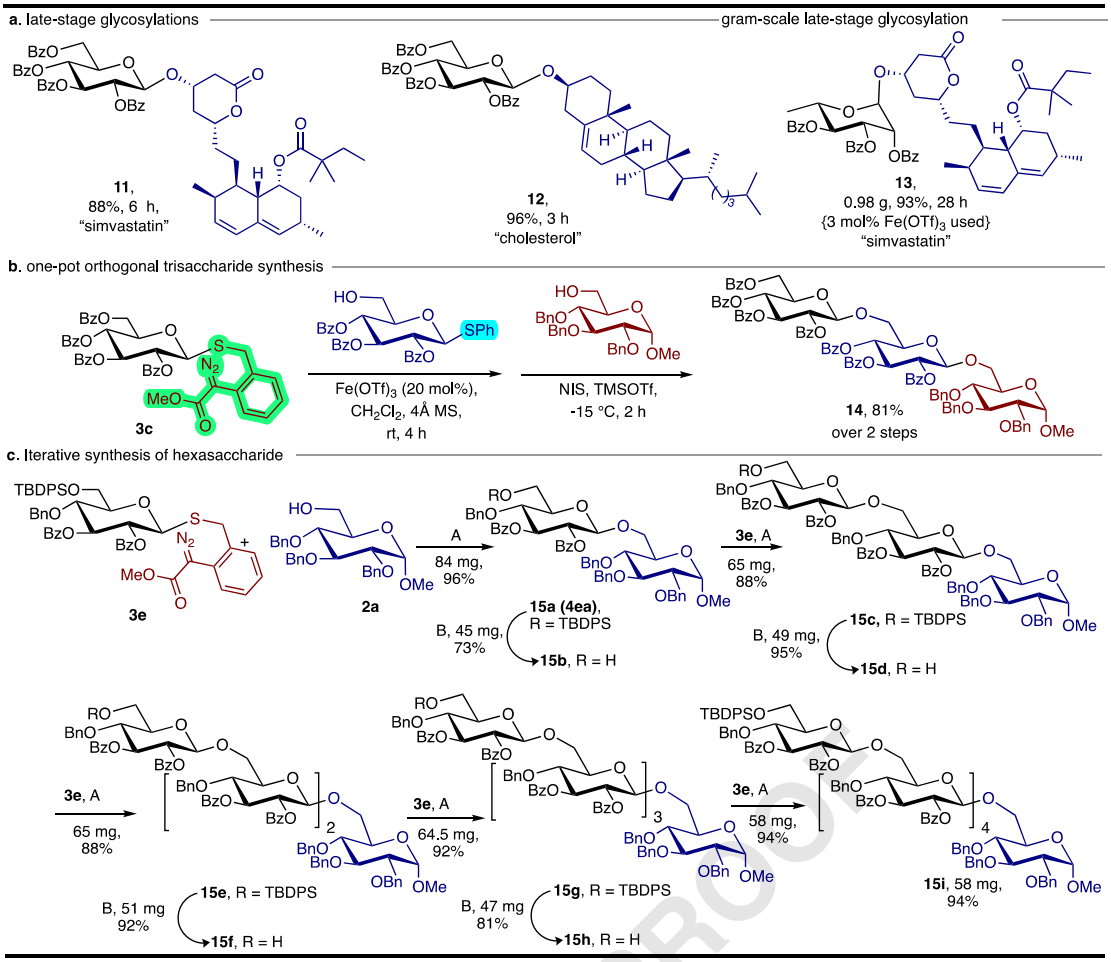

Fig. 7 | Applications of our methodology. a Late-stage glycosylations and gram-scale synthesis (**b**) One-pot orthogonal access to trisaccharides. **c** Iterative synthesis of hexasaccharides (A) acceptor (1.0 equiv.), donor (1.5 equiv.) $Fe(OTf)_3$ (20 mol%), CH_2Cl_2, time = 5 h, (B) TBAF in THF (1 mol/L, 1.5 equiv.), THF (2.0 mL). Bz benzoyl, Bn benzyl, Ac acetyl, TBDPS tert-butyldiphenylsilyl, THF tetrahydrofuran, Tf trifluoromethanesulfonate, Me methyl, NIS N-Iodosuccinimide, TBAF tetrabutylammonium fluoride.

organo-catalysts.[35,79–81] We could also leverage C2-*O* coordination with iron in this design to help deliver upcoming acceptors from the same face (see Figure S-31 in SI for mechanistic pathways). We started investigating our synthesized tri-*O*-benzyl ribose MDMPA thiofuranoside donor **3p** to probe our hypothesis. In our initial studies, we introduced donor **3p** under the optimized conditions along with glycosyl acceptor **2a**; upon completion, we were ecstatic to observe the good yield of the desired product **4pa** (68%, $\alpha/\beta = 9/1$), but with the high 1,2-*cis* selectivity (Fig. 6). The exact stereochemistry of the 1,2-*cis* furanosides was confirmed through NMR analysis, particularly using $^{1}H,^{13}C$-HSQC studies.[62] After this encouraging result, attention was directed towards other glycosyl alcohol acceptors with different protecting groups. Encouragingly, reaction yields, and selectivity were unaffected by the influence of protecting groups for benzyl-and benzoyl-protected glycosyl acceptors (**4pb, 4 pc**). Specifically, thioglycoside moiety at the anomeric position of the acceptor **4pd** was also found to work efficiently and orthogonal to our conditions. Building on the success observed with the ribose MDMPAT donor, we explored the range of substrates using an arabinose MDMPAT donor **3q**. Like our investigation with ribose, we began with primary sugar alcohols; encouragingly, benzyl-and benzoyl-protected glucose acceptors demonstrated easy reactivity in our system, yielding products **4qa** and **4qb** with high yields and good β-1,2-*cis*-selectivity. Notably, acceptors derived from mannose were unreactive with the well-established furanosylation protocols. Our method achieved the intended product with high yields and selectivity when employing the mannosyl acceptor (**4 pc** and **4qc**). Overall, this extensive exploration of donors and acceptors further supports our methodology as one of the best for activating thioglycoside donors.

Applications of MDMPA thioglycoside donors

Late-stage modification of pharmaceuticals has been an exciting topic for developing a chemical library of biologically active compounds.[82] Similarly, we successfully performed late-stage glycosylation of biologically relevant compounds such as simvastatin[83] **11** and cholesterol[84] **12** in excellent yields with perbenzoylated MDMPA glucosyl donor **3c**. Often, methods developed in academic labs are found difficult to scale up. To test the robustness of our methodology, we did a gram-scale late-stage glycosylation of simvastatin **13** with rhamnosyl donor **3i**. Specifically, in this transformation, we only used 3 mol% of the $Fe(OTf)_3$, highlighting the efficiency of the catalytic cycle. Furthermore, we performed the one-pot access to trisaccharide using other traditional thioglycoside donors to demonstrate the orthogonal nature of our activation conditions. We first activated our MDMPAT donor **3c** under optimized conditions in the presence of an acceptor bearing traditional thioglycoside, followed by the activation of in situ formed disaccharide thioglycoside under established literature conditions[85] to achieve trisaccharide in 81% yield over two steps.

Despite the numerous glycosylation strategies available, only a few methods can effectively accommodate the synthesis of

oligosaccharides.[86] To address this challenge, we synthesized donor **3e** for hexasaccharide synthesis. We were pleased to observe the formation of the hexasaccharide using our strategy, achieving a 31% yield after 9 steps (Fig. 7c). Our experience synthesizing hexasaccharides indicates that this methodology could be readily adapted for synthesizing larger oligosaccharide assemblies.

In conclusion, this study presents a catalytic glycosylation method that leverages diazo-thioglycoside donors activated by earth-abundant iron or photosensitizer-free blue light conditions, offering a sustainable alternative to traditional activation methods, which typically use precious and platinum-group metals (PGMs). The orthogonal reactivity provided by this approach opens new pathways for glycosylation reactions, distinct from widely used thioglycosides and alkyne-based donors. By capitalizing on a Thorpe-Ingold-like effect, this system facilitates proximity-induced *S*-insertion into carbenes, ensuring high chemoselectivity and efficiency. The versatility of carbene-based thioglycoside donors is demonstrated through their compatibility with a wide range of protecting groups, nucleophiles, and glycosyl donors, including mannose, galactose, rhamnose, xylose, 2-deoxyamino glucose, lactose, and furanose derivatives. This broad applicability highlights the potential of this method for diverse glycan syntheses. Additionally, the robustness of the approach is underscored by successful late-stage modifications of biomolecules, such as cholesterol and the drug simvastatin, even at the gram-scale. Furthermore, the methodology has been validated through the iterative synthesis of complex hexasaccharides, showcasing its utility in constructing intricate glycan structures. Overall, this work not only advances the field of glycosylation by providing an iron- and light-driven catalytic strategy but also sets the stage for further development of sustainable and chemoselective approaches in carbohydrate chemistry. The broad applicability and potential for late-stage functionalization render this method a valuable tool for both fundamental research and practical applications in the synthesis of complex glycoconjugates.

Methods

General Procedure(s) for activating MDMPA thioglycoside donor by utilizing Fe-catalyst or Blue LED in intramolecular fashion

General procedure A. In an oven-dried vial equipped with a stir bar, a glycosyl acceptor (0.025 mmol) was combined with MDMPA thioglycoside donors **3 (c-q)** (0.037 mmol, 1.5 equiv.), 4 Å molecular sieves (50 mg or 100 wt.%), and $Fe(OTf)_3$ (0.005 mmol, 0.2 equiv.) dissolved in CH_2Cl_2 (0.05 M). Upon complete addition, the reaction mixture was stirred at the ambient temperature, and the reaction progress was monitored by TLC and quenched with saturated aqueous $NaHCO_3$ upon completion. The layers were separated, and the aqueous layer was washed with ethyl acetate. The organic layers were combined, dried over Na_2SO_4, filtered, and evaporated under reduced pressure. The crude product was dissolved in ethyl acetate and passed through a short silica pad to remove traces of iron (to check the crude material via ^{1}H-NMR). The filtrate was evaporated, and the resulting crude material was purified by column chromatography.

General procedure C. In an oven-dried vial equipped with a stir bar, a glycosyl acceptor (0.025 mmol) was mixed with MDMPA thioglycoside donors **3 (c-o)** (0.025 mmol, 2 equiv.), LiOTf (0.025 mmol, 1.0 equiv.), and 4 Å molecular sieves (50 mg or 100 wt.%), all dissolved in a solvent (0.05 M). The reaction mixture was then irradiated under blue LED light (456 nm) for 1 h at the same temperature. Progress was monitored by TLC, and once the starting donor was fully consumed, an additional portion of donor **3 (c-o)** (0.0125 mmol, 0.5 equiv.) was added, followed by another 1 h of irradiation under blue LED light (456 nm). This step was repeated with another addition of donor **3 (c-o)** (0.0125 mmol, 0.5 equiv.) and subsequent irradiation until the starting glycosyl acceptor was completely consumed. The reaction mixture was then filtered through a Celite pad, with no additional workup required. The filtrate was evaporated, and the resulting crude product was purified by column chromatography.

General procedure C. In an oven-dried vial equipped with a stir bar, a glycosyl acceptor (0.025 mmol) was mixed with thioglycoside donors **3 (c-o)** (0.025 mmol, 2 equiv.), LiOTf (0.025 mmol, 1.0 equiv.), camphorsulfonic acid (0.0125 mmol, 0.5 equiv.), and 4 Å molecular sieves (50 mg or 100 wt.%), all dissolved in a solvent (0.05 M). The reaction mixture was then irradiated under blue LED light (456 nm) for 1 h at the same temperature. Progress was monitored by TLC, and once the starting donor was fully consumed, an additional portion of donor **3 (c-o)** (0.0125 mmol, 0.5 equiv.) was added, followed by another 1 h of irradiation under blue LED light (456 nm). This step was repeated with another addition of donor **3 (c-o)** (0.0125 mmol, 0.5 equiv.) and subsequent irradiation until the starting glycosyl acceptor was completely consumed. The reaction mixture was then filtered through a celite pad, with no additional workup required. The filtrate was evaporated, and the resulting crude product was purified by column chromatography.

Data availability

The authors declare that all additional data supporting the findings of this study are provided within the article and Supplementary Information files. These data can also be obtained from the corresponding author upon request.

References

1. Gillingham, D. & Fei, N. Catalytic X–H insertion reactions based on carbenoids. *Chem. Soc. Rev.* **42**, 4918–4931 (2013).
2. Zhang Z., Gevorgyan V. Visible Light-Induced Reactions of Diazo Compounds and Their Precursors. *Chem. Rev.* (2024). Q6
3. Xia, Y., Qiu, D. & Wang, J. Transition-metal-catalyzed cross-couplings through carbene migratory insertion. *Chem. Rev.* **117**, 13810–13889 (2017).
4. Jia, M. & Ma, S. New approaches to the synthesis of metal carbenes. *Angew. Chem. Int. Ed.* **55**, 9134–9166 (2016).
5. Bergstrom, B. D., Nickerson, L. A., Shaw, J. T. & Souza, L. W. Transition metal catalyzed insertion reactions with donor/donor carbenes. *Angew. Chem.* **133**, 6940–6954 (2021).
6. Regitz, M. New methods of preparative organic chemistry. Transfer of diazo groups. *Angew. Chem. Int. Ed.* **6**, 733–749 (1967).
7. REGITZ, M. Recent synthetic methods in diazo chemistry. *Synthesis* **1972**, 351–373 (1972).
8. Kirmse W. *Carbene chemistry*. Elsevier (2013).
9. Curtius, T. Ueber die Einwirkung von salpetriger Säure auf salzsauren Glycocoläther. *Ber. Dtsch. Chem. Ges.* **16**, 2230–2231 (1883).
10. Arndt, F. & Amende, J. Synthesen mit Diazo-methan, V.:¨ aurechloride mit Dia-Uber die Reaktion der S¨ zomethan. *Ber. Dtsch. Chem. Ges.* **61**, 1122 (1928).
11. Ye, T. & McKervey, M. A. Organic synthesis with. alpha.-diazo carbonyl compounds. *Chem. Rev.* **94**, 1091–1160 (1994).
12. Patrick, T. B., Scheibel, J. J. & Cantrell, G. L. Geminal fluorination of diazo compounds. *J. Org. Chem.* **46**, 3917–3918 (1981).
13. Mata, E. G., Setti, E. L. & Mascaretti, O. A. Stereoselective synthesis of 6-fluoropenicillanate analogs of. beta.-lactamase inhibitors. *J. Org. Chem.* **55**, 3674–3677 (1990).
14. Davies, H. M. & Hedley, S. J. Intermolecular reactions of electron-rich heterocycles with copper and rhodium carbenoids. *Chem. Soc. Rev.* **36**, 1109–1119 (2007).
15. Padwa, A. Domino reactions of rhodium (II) carbenoids for alkaloid synthesis. *Chem. Soc. Rev.* **38**, 3072–3081 (2009).
16. Qian, D. & Zhang, J. Gold-catalyzed cyclopropanation reactions using a carbenoid precursor toolbox. *Chem. Soc. Rev.* **44**, 677–698 (2015).

17. Seidel, G. & Fürstner, A. Structure of a reactive gold carbenoid. *Angew. Chem. Int. Ed.* **53**, 4807–4811 (2014).
18. Archambeau, A., Miege, F., Meyer, C. & Cossy, J. Intramolecular cyclopropanation and C–H insertion reactions with metal carbenoids generated from cyclopropenes. *Acc. Chem. Res.* **48**, 1021–1031 (2015).
19. Bolm, C. A new iron age. *Nat. Chem.* **1**, 420 (2009).
20. Maas, G. Ruthenium-catalysed carbenoid cyclopropanation reactions with diazo compounds. *Chem.Soc. Rev.* **33**, 183–190 (2004).
21. Zhang, X., Liu, Z., Sivaguru, P. & Bi, X. Silver carbenoids derived from diazo compounds: A historical perspective on challenges and opportunities. *Chem Catal* **1**, 599–630 (2021).
22. Bullock, R. M. et al. Using nature's blueprint to expand catalysis with Earth-abundant metals. *Science* **369**, eabc3183 (2020).
23. Wenger, O. S. Is iron the new ruthenium? *Chem. Eur. J.* **25**, 6043–6052 (2019).
24. Damiano, C., Sonzini, P. & Gallo, E. Iron catalysts with N-ligands for carbene transfer of diazo reagents. *Chem. Soc. Rev.* **49**, 4867–4905 (2020).
25. Empel, C., Jana, S. & Koenigs, R. M. CH functionalization via iron-catalyzed carbene-transfer reactions. *Molecules* **25**, 880 (2020).
26. Carreras, V., Tanbouza, N. & Ollevier, T. The power of iron catalysis in diazo chemistry. *Synthesis* **53**, 79–94 (2021).
27. Nuss, P. & Eckelman, M. J. Life Cycle Assessment of Metals: A Scientific Synthesis. *PLoS one* **9**, e101298 (2014).
28. Yang, Z., Stivanin, M. L., Jurberg, I. D. & Koenigs, R. M. Visible light-promoted reactions with diazo compounds: a mild and practical strategy towards free carbene intermediates. *Chem. Soc. Rev.* **49**, 6833–6847 (2020).
29. Ciszewski ŁW, Rybicka-Jasińska, K. & Gryko, D. Recent developments in photochemical reactions of diazo compounds. *Org. Biomol. Chem.* **17**, 432–448 (2019).
30. Durka, J., Turkowska, J. & Gryko, D. Lightening diazo compounds? *ACS Sustain. Chem. Eng.* **9**, 8895–8918 (2021).
31. Kafle, P. et al. Iron-Carbene Initiated O–H Insertion/Aldol Cascade for the Stereoselective Synthesis of Functionalized Tetrahydrofurans. *ACS Catal* **14**, 1292–1299 (2024).
32. Jurberg, I. D. & Davies, H. M. L. Blue light-promoted photolysis of aryldiazoacetates. *Chem. Sci.* **9**, 5112–5118 (2018).
33. Singh, S. P., Chaudhary, U. & Sharma, I. Catalytic Thioglycoside Activation with Diazo-Derived Copper Carbenes. *Molecules* **29**, 5367 (2024).
34. Ghosh, B. et al. Catalytic Activation of Thioglycosides with Copper-Carbenes for Stereoselective 1,2-Cis-Furanosylations. *Org. Lett.* **26**, 9436–9441 (2024).
35. Ghosh, B. et al. Catalytic Stereoselective 1,2-cis-Furanosylations Enabled by Enynal-Derived Copper Carbenes. *ACS Catal* **14**, 1037–1049 (2024).
36. Pratap Singh, S., Ghosh, B. & Sharma, I. Catalytic Orthogonal Glycosylation Enabled by Enynal-Derived Copper Carbenes. *Adv. Synth. Catal.* **366**, 1847–1856 (2024).
37. Xiong, D. C., Zhang, L. H. & Ye, X. S. Bromodimethylsulfonium Bromide-Silver Triflate: A New Powerful Promoter System for the Activation of Thioglycosides. *Adv. Synth. Catal.* **350**, 1696–1700 (2008).
38. Crich, D. & Smith, M. 1-Benzenesulfinyl piperidine/trifluoromethanesulfonic anhydride: a potent combination of shelf-stable reagents for the low-temperature conversion of thioglycosides to glycosyl triflates and for the formation of diverse glycosidic linkages. *J. Am. Chem. Soc.* **123**, 9015–9020 (2001).
39. Nakanishi, M., Takahashi, D. & Toshima, K. Light-induced O-glycosylation of unprotected deoxythioglycosyl donors. *Org. Biomol. Chem.* **11**, 5079–5082 (2013).
40. Yang, F., Wang, Q. & Yu, B. ortho-Alkynylphenyl thioglycosides as a new type of glycosylation donors under the catalysis of Au(I) complexes. *Tetrahedron Lett* **53**, 5231–5234 (2012).
41. Adhikari, S., Baryal, K. N., Zhu, D., Li, X. & Zhu, J. Gold-Catalyzed Synthesis of 2-Deoxy Glycosides Using S-But-3-ynyl Thioglycoside Donors. *ACS Catal* **3**, 57–60 (2013).
42. Ding, H. et al. Efficient O- and S-glycosylation with ortho-2,2-dimethoxycarbonylcyclopropylbenzyl thioglycoside donors by catalytic strain-release. *Chem. Sci.* **15**, 3711–3720 (2024).
43. Liu, H. et al. ortho-Methoxycarbonylethynylphenyl Thioglycosides (MCEPTs): Versatile Glycosyl Donors Enabled by Electron-Withdrawing Substituents and Catalyzed by Gold(I) or Cu(II) Complexes. *J. Am. Chem. Soc.* **145**, 3682–3695 (2023).
44. Meng, L. et al. Glycosylation Enabled by Successive Rhodium(II) and Brønsted Acid Catalysis. *J. Am. Chem. Soc.* **141**, 11775–11780 (2019).
45. Doyle, M. P., Griffin, J. H., Chinn, M. S. & Van Leusen, D. Rearrangements of ylides generated from reactions of diazo compounds with allyl acetals and thioketals by catalytic methods. Heteroatom acceleration of the [2,3]-sigmatropic rearrangement. *J. Org. Chem.* **49**, 1917–1925 (1984).
46. Ollis, W. D., Rey, M. & Sutherland, I. O. Base catalysed rearrangements involving ylide intermediates. Part 15. The mechanism of the Stevens [1,2] rearrangement. *J. Chem. Soc., Perkin Trans.* **1**, 1009–1027 (1983).
47. Tyagi, V., Sreenilayam, G., Bajaj, P., Tinoco, A. & Fasan, R. Biocatalytic Synthesis of Allylic and Allenyl Sulfides through a Myoglobin-Catalyzed Doyle–Kirmse Reaction. *Angew. Chem. Int. Ed.* **55**, 13562–13566 (2016).
48. Hock, K. J., Mertens, L., Hommelsheim, R., Spitzner, R. & Koenigs, R. M. Enabling iron catalyzed Doyle–Kirmse rearrangement reactions with in situ generated diazo compounds. *Chem. Commun.* **53**, 6577–6580 (2017).
49. Jana, S., Guo, Y. & Koenigs, R. M. Recent Perspectives on Rearrangement Reactions of Ylides via Carbene Transfer Reactions. *Chem. Eur. J.* **27**, 1270–1281 (2021).
50. Zhang, X. et al. Use of trifluoroacetaldehyde N-tfsylhydrazone as a trifluorodiazoethane surrogate and its synthetic applications. *Nat. Commun.* **10**, 284 (2019).
51. Ning, Y. et al. Difluoroacetaldehyde N-Triftosylhydrazone (DFHZ-Tfs) as a Bench-Stable Crystalline Diazo Surrogate for Diazoacetaldehyde and Difluorodiazoethane. *Angew. Chem. Int. Ed.* **59**, 6473–6481 (2020).
52. Yan, X., Li, C., Xu, X., Zhao, X. & Pan, Y. Hemin Catalyzed Dealkylative Intercepted [2, 3]-Sigmatropic Rearrangement Reactions of Sulfonium Ylides with 2, 2, 2-Trifluorodiazoethane. *Adv. Synth. Catal.* **362**, 2005–2011 (2020).
53. Hommelsheim, R., Guo, Y., Yang, Z., Empel, C. & Koenigs, R. M. Blue-Light-Induced Carbene-Transfer Reactions of Diazoalkanes. *Angew. Chem. Int. Ed.* **58**, 1203–1207 (2019).
54. Yang, Z., Guo, Y. & Koenigs, R. M. Photochemical, Metal-Free Sigmatropic Rearrangement Reactions of Sulfur Ylides. *Chem. Eur. J.* **25**, 6703–6706 (2019).
55. Yang, J. et al. gem-Difluoroallylation of Aryl Diazoesters via Catalyst-Free, Blue-Light-Mediated Formal Doyle–Kirmse Reaction. *Org. Lett.* **21**, 2654–2657 (2019).
56. Orłowska, K., Rybicka-Jasińska, K., Krajewski, P. & Gryko, D. Photochemical Doyle–Kirmse Reaction: A Route to Allenes. *Org. Lett.* **22**, 1018–1021 (2020).
57. Muthusamy, S. & Ramesh, C. Blue LED-Mediated Synthesis of 3-Arylidene Oxindoles. *J. Org. Chem.* **88**, 5609–5621 (2023).
58. Pei, C., Empel, C. & Koenigs, R. M. Photochemical Intermolecular Cyclopropanation Reactions of Allylic Alcohols for the Synthesis of [3.1.0]-Bicyclohexanes. *Org. Lett.* **25**, 169–173 (2023).
59. Doyle, L. M. et al. Stereoselective epimerizations of glycosyl thiols. *Org. Lett.* **19**, 5802–5805 (2017).
60. Beesley, R. M., Ingold, C. K. & Thorpe, J. F. CXIX.—The formation and stability of spiro-compounds. Part I. spiro-Compounds from cyclohexane. *J. Chem. Soc., Trans.* **107**, 1080–1106 (1915).

61. Zhu, S.-F., Song, X.-G., Li, Y., Cai, Y. & Zhou, Q.-L. Enantioselective copper-catalyzed intramolecular O– H insertion: an efficient approach to chiral 2-carboxy cyclic ethers. *J. Am. Chem. Soc.* **132**, 16374–16376 (2010).
62. Fontana, C. & Widmalm, G. Primary Structure of Glycans by NMR Spectroscopy. *Chem. Rev.* **123**, 1040–1102 (2023).
63. Crich, D. Mechanism of a Chemical Glycosylation Reaction. *Acc. Chem. Res.* **43**, 1144–1153 (2010).
64. Fraser-Reid B. O., López JCb, Aubry S. *Reactivity tuning in oligosaccharide assembly*. Springer (2011).
65. Liu, Z., Liu, D., Zhu, D. & Yu, B. Stereoselective Synthesis of β-glycosyl Esters via 1-Hydroxybenzotriazole Mediated Acylation of Glycosyl Hemiacetals. *Org. Lett.* **25**, 5372–5377 (2023).
66. Ma, X. et al. A "Traceless" Directing Group Enables Catalytic SN2 Glycosylation toward 1,2-cis-Glycopyranosides. *J. Am. Chem. Soc.* **143**, 11908–11913 (2021).
67. Butler, M. S., Hansford, K. A., Blaskovich, M. A. T., Halai, R. & Cooper, M. A. Glycopeptide antibiotics: Back to the future. *J. Antibiot.* **67**, 631–644 (2014).
68. Lindberg B. Components of Bacterial Polysaccharides. In: *Adv. Carbohydr. Chem. Biochem.* (eds Tipson RS, Horton D). Academic Press (1990).
69. Brennan, P. J. & Nikaido, H. The envelope of mycobacteria. *Annu. Rev. Biochem.* **64**, 29–63 (1995).
70. Crick, D. C., Mahapatra, S. & Brennan, P. J. Biosynthesis of the arabinogalactan-peptidoglycan complex of Mycobacterium tuberculosis. *Glycobiology* **11**, 107r–118r (2001).
71. Peltier, P., Euzen, R., Daniellou, R., Nugier-Chauvin, C. & Ferrières, V. Recent knowledge and innovations related to hexofuranosides: structure, synthesis and applications. *Carbohydr. Res.* **343**, 1897–1923 (2008).
72. Tefsen, B., Ram, A. F., van Die, I. & Routier, F. H. Galactofuranose in eukaryotes: aspects of biosynthesis and functional impact. *Glycobiology* **22**, 456–469 (2012).
73. Lowary, T. L. Twenty Years of Mycobacterial Glycans: Furanosides and Beyond. *Acc. Chem. Res.* **49**, 1379–1388 (2016).
74. Varki, A. Biological roles of oligosaccharides: all of the theories are correct. *Glycobiology* **3**, 97–130 (1993).
75. Dwek, R. A. Glycobiology: Toward Understanding the Function of Sugars. *Chem. Rev.* **96**, 683–720 (1996).
76. In: *Essentials of Glycobiology* (eds Varki A., et al.). Cold Spring Harbor Laboratory Press Copyright 2015-2017 by The Consortium of Glycobiology Editors, La Jolla, California. All rights reserved. (2015).
77. Nigudkar, S. S. & Demchenko, A. V. Stereocontrolled 1,2-cis glycosylation as the driving force of progress in synthetic carbohydrate chemistry. *Chem. Sci.* **6**, 2687–2704 (2015).
78. Mensink, R. A. & Boltje, T. J. Advances in Stereoselective 1,2-cis Glycosylation using C-2 Auxiliaries. *Chem. Eur. J* **23**, 17637–17653 (2017).
79. Mayfield, A. B., Metternich, J. B., Trotta, A. H. & Jacobsen, E. N. Stereospecific Furanosylations Catalyzed by Bis-thiourea Hydrogen-Bond Donors. *J. Am. Chem. Soc.* **142**, 4061–4069 (2020).
80. Xu, H., Schaugaard, R. N., Li, J., Schlegel, H. B. & Nguyen, H. M. Stereoselective 1,2-cis Furanosylations Catalyzed by Phenanthroline. *J. Am. Chem. Soc.* **144**, 7441–7456 (2022).
81. Ma, X., Zhang, Y., Zhu, X. & Zhang, L. An S(N)2-Type Strategy toward 1,2-cis-Furanosides. *CCS Chem.* **4**, 3677–3685 (2022).
82. Batra, J. & Rathore, A. S. Glycosylation of monoclonal antibody products: Current status and future prospects. *Biotechnol. Prog.* **32**, 1091–1102 (2016).
83. Simões, R. G., Bernardes, C. E. S., Diogo, H. P., Agapito, F. & Minas da Piedade, M. E. Energetics and Structure of Simvastatin. *Mol. Pharm.* **10**, 2713–2722 (2013).
84. Coisne, C. et al. Cyclodextrins as Emerging Therapeutic Tools in the Treatment of Cholesterol-Associated Vascular and Neurodegenerative Diseases. *Molecules* **21**, 1748 (2016).
85. Tanifum, C. T. & Chang, C.-W. T. Sonication-Assisted Oligomannoside Synthesis. *J. Org. Chem.* **74**, 634–644 (2009).
86. Le Mai Hoang, K. et al. Traceless Photolabile Linker Expedites the Chemical Synthesis of Complex Oligosaccharides by Automated Glycan Assembly. *J. Am. Chem. Soc.* **141**, 9079–9086 (2019).

Acknowledgements

We sincerely thank the National Science Foundation (NSF, CHE-1753187) for their generous support of this work. We also thank Dr. Novrus G. Akhmedov and Dr. Steven Foster from the Research Support Services at the University of Oklahoma for their assistance with NMR and mass spectral analyses, respectively.

Author contributions

I.S. and S.P.S. designed the project, and S.P.S. developed both activation methods (iron-catalyzed and photochemically initiated). S.P.S., U.C., and A.D. synthesized the MDMPAT donors and expanded the scope of donors and acceptors. S.P.S. performed gram-scale, one-pot orthogonal, and iterative synthesis of hexasaccharide experiments. I.S. and S.P.S. completed the manuscript writing. All the co-authors have approved the final version of the manuscript.

Competing interests

The authors declare no competing interests.

Additional information

Supplementary information The online version contains supplementary material available at https://doi.org/10.1038/s41467-025-56445-1.

Correspondence and requests for materials should be addressed to Indrajeet Sharma.

Peer review information *Nature Communications* thanks the anonymous reviewer(s) for their contribution to the peer review of this work. A peer review file is available.

ACS Catalysis

pubs.acs.org/acscatalysis

Research Article

Catalytic Stereoselective 1,2-*cis*-Furanosylations Enabled by Enynal-Derived Copper Carbenes

Bidhan Ghosh, Adam Alber, Chance W. Lander, Yihan Shao, Kenneth M. Nicholas, and Indrajeet Sharma*

Cite This: *ACS Catal.* 2024, 14, 1037−1049

Read Online

ACCESS | Metrics & More | Article Recommendations | Supporting Information

ABSTRACT: 1,2-*cis*-Furanosides are present in various biomedically relevant glycosides, and their stereoselective synthesis remains a significant challenge. In this vein, we have developed a stereoselective approach to 1,2-*cis*-furanosylations using earth-abundant copper catalysis. This protocol proceeds under mild conditions at room temperature and employs readily accessible benchtop stable enynal-derived furanose donors. This chemistry accommodates a variety of alcohols, including primary, secondary, and tertiary, as well as mannosyl alcohol acceptors, which have been incompatible with most known methods of furanosylation. The resulting 1,2-*cis*-furanoside products exhibit high yields and anomeric selectivity with both the ribose and arabinose series. Furthermore, the anomeric selectivity is independent of the C2 oxygen-protecting group and the anomeric configuration of the starting donor. Experimental evidence and computational studies support our hypothesis that copper chelation between the C2 oxygen of the furanose donor and an incoming alcohol nucleophile is responsible for the observed 1,2-*cis*-stereoselectivity.

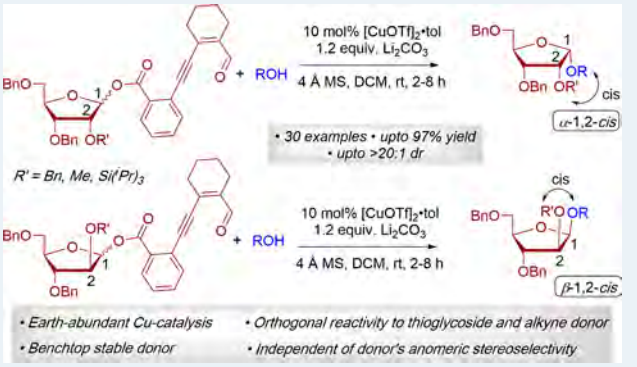

KEYWORDS: *copper catalysis, 1,2-cis-furanosides, stereoselective glycosylation, enynal-derived metal carbenes, earth-abundant catalysis, carbohydrate chemistry*

INTRODUCTION

Carbenes are versatile synthetic intermediates capable of novel transformations, leading to the rapid generation of molecular complexity with high efficiency, selectivity, and atom economy.[1] Diazo compounds are commonly employed to generate these species by extruding elemental nitrogen. Other frequently used precursors include hydrazones, triazoles, sulfonium ylides, cyclopropenes, and alkynes (Figure 1a). These carbenes, or metal carbenoid species, readily partake in a range of synthetically appealing transformations, including cyclopropanations,[2] dipolar cycloadditions,[3] insertions into XH bonds (X = C, Si, O, S, N, etc.),[4] reactions with nucleophiles, as well as migratory insertions involving various metals.[5] Moreover, carbenes find applications in polymerization,[6] olefin metathesis,[7] and labeling biomolecules (including proteins, RNA, and DNA) for research and diagnostic purposes.[8] While carbenes have found diverse applications across multiple domains, their potential in carbohydrate chemistry has been largely untapped. Carbenes are, in fact, rarely utilized in glycoscience transformations.[9]

The first report on the utilization of carbenes in glycosylation goes back to 1989, when the Vasella group synthesized glycosylidene carbenes from the corresponding diazirines.[9a] Because of the instability of diazirines, they then employed the anomeric *N*-tosylhydrazone donors, which are benchtop stable carbene precursors. The sodium salts of these *N*-tosylhydrazones under photochemical conditions generate the corresponding anomeric carbenes, which undergo an O−H insertion reaction with alcohols to form *O*-glycosides (Figure 1b).[10] However, the glycosylidene carbenes generated from the sodium salts of *N*-tosylhydrazones require an excess of alcohol acceptors to synthesize *O*-glycosides. Additionally, product yields in these transformations were remarkably low, and the scope was found to be very limited. The same anomeric carbene has also been applied to protecting group-free phosphorylation.[11] The necessity for a substantial excess of nucleophiles restricted the use of these highly reactive anomeric carbenes in glycosylation; however, it paved the way for potential applications of carbenes to achieve stereoselective glycosylation. In 2019, the Wan group activated thioglycosides using rhodium carbenes (Figure 1c).[9m]

Received: November 1, 2023
Revised: December 18, 2023
Accepted: December 20, 2023
Published: January 8, 2024

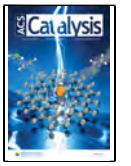

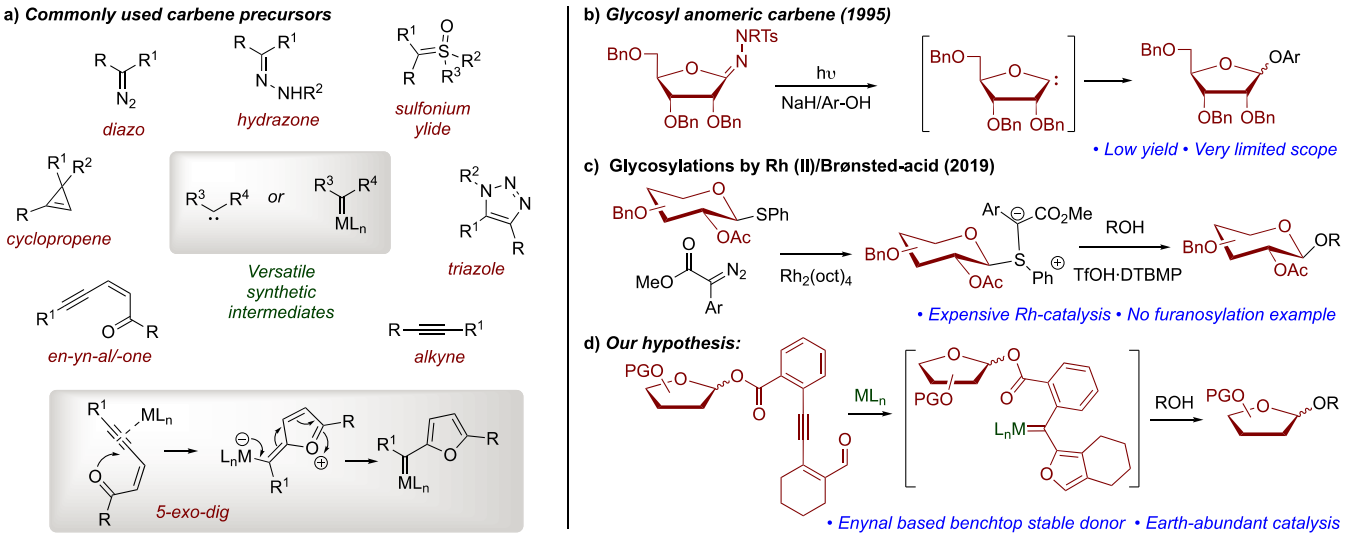

Figure 1. (a) Common carbene precursors. (b) Glycosyl anomeric carbene. (c) Catalytic glycosylation with Rh-carbene. (d) Our approach.

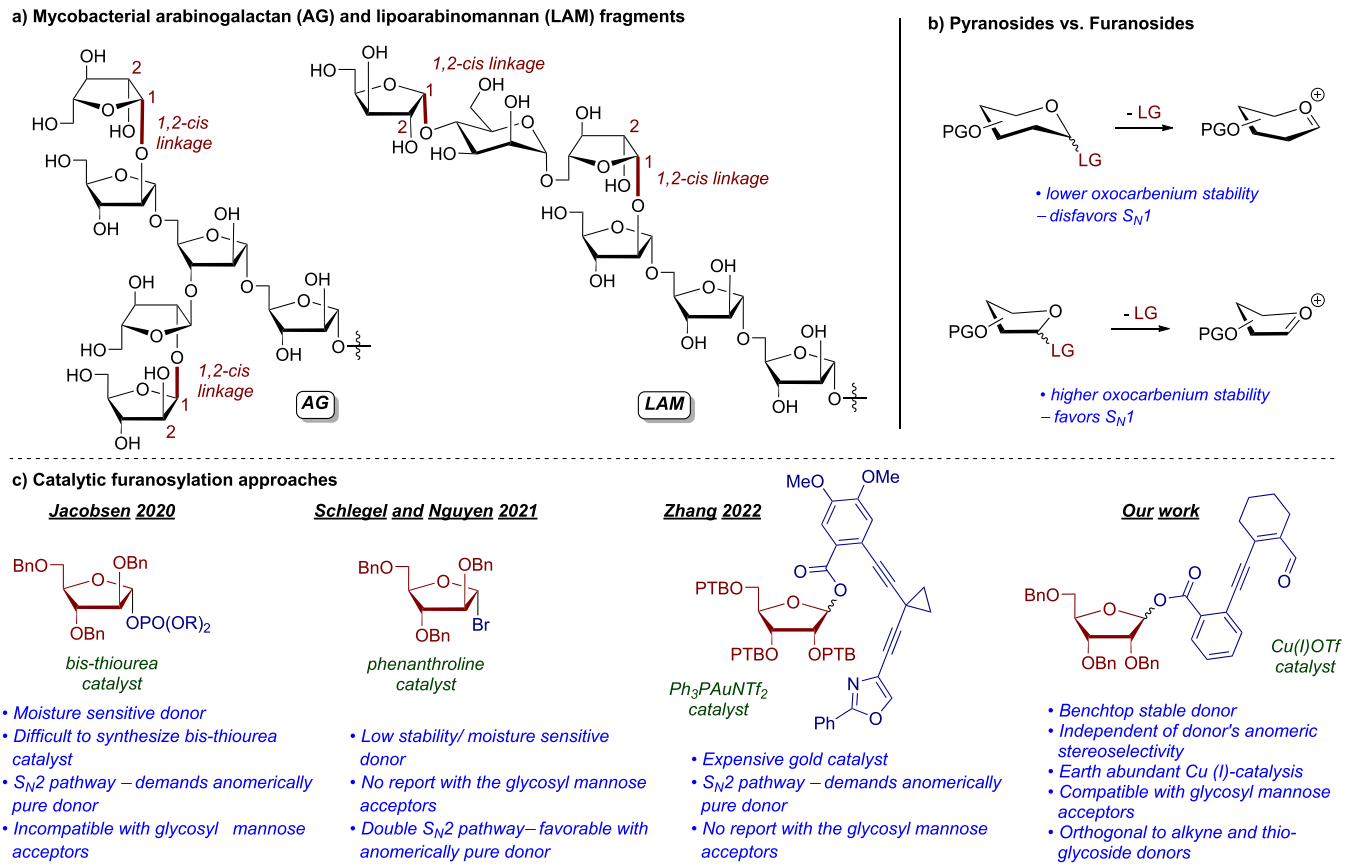

Figure 2. (a) Cell wall hexasaccharide motifs featuring 1,2-*cis*-furanosidic linkages. (b) Differences in reactivity between furanose and pyranose donors. (c) Catalytic furanosylation approaches.

This pyranosylation strategy lacks chemoselectivity and proceeds through two stages: initially, the generation of anomeric sulfonium ylides using a diazo-derived rhodium carbene, followed by protonation of the ylide to provide an oxocarbenium ion, which subsequently engages in glycosylation with alcohol acceptors.

Diazo compounds, however, are mainly activated by using precious rhodium catalysts and hold a reputation for their instability and the safety concerns associated with their regular use. Consequently, significant focus has been placed on identifying sustainable and safe alternatives for generating metal carbenes. Our search led us to the emerging field of enynal and enynone chemistry.[12] These carbene precursors comprise conjugated alkenes, alkynes, and aldehydes or ketones, thus en-yn-al/-one. These compounds maintain numerous benefits when compared to traditional carbene precursors like diazos. For example, these carbene precursors are easy to synthesize and far more stable due to the absence of

https://doi.org/10.1021/acscatal.3c05237
ACS Catal. 2024, 14, 1037−1049

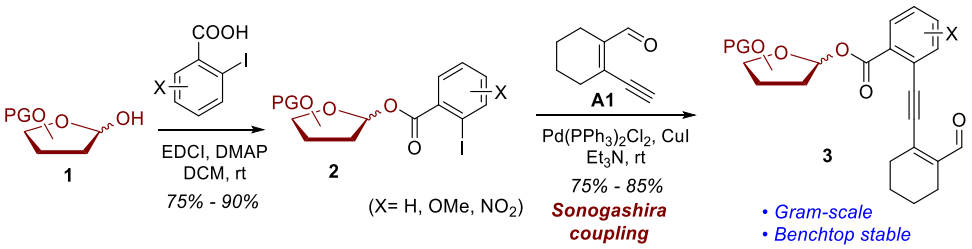

Figure 3. General synthesis of furanosyl enynal donors.

Table 1. Optimization of the Reaction Conditions[a]

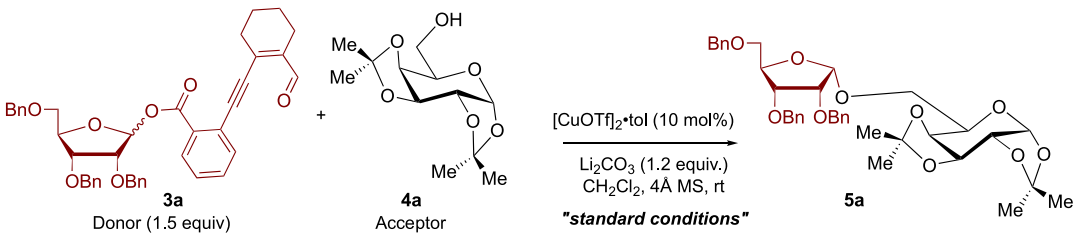

entry	variation from the "standard conditions"	% yield[b]	time	α/β ratio[c]
1	none	78	4	7/1
2	$ZnCl_2$, no $[CuOTf]_2$·tol	20	36	1.5/1
3	$FeCl_3$, no $[CuOTf]_2$·tol	15	36	3/1
4	$ZnOTf_2$, no $[CuOTf]_2$·tol	n.r.	36	n.d.
5[d]	PPh_3AuOTf, no $[CuOTf]_2$·tol, no Li_2CO_3	56	3	7/1
6[e]	$Rh_2(esp)_2$, no$[CuOTf]_2$·tol, no Li_2CO_3	n.r.	36	n.d.
7	$Cu(MeCN)_4PF_6$, no $[CuOTf]_2$·tol	55	4	2/1
8	$Cu(MeCN)_4BF_4$, no $[CuOTf]_2$·tol	<10	24	n.d.
9	THF as solvent	n.r.	24	n.d.
10	ACN as solvent	n.r.	24	n.d.
11	toluene as solvent	<10	24	n.d.
12	TfOH, no Li_2CO_3, no $[CuOTf]_2$·tol	25	2	1/2.5
13	$[CuOTf]_2$·tol, no Li_2CO_3	50	4	5/1
14[f]	$[CuOTf]_2$·tol, DTBMP, no Li_2CO_3	46	10	5/1
15	no $[CuOTf]_2$·tol, Li_2CO_3 only	n.r.	36	n.d.

[a]All furanosylations were conducted with acceptor (0.05 mmol), donor (0.075 mmol), 10 mol % of catalyst, and 1.2 equiv of Li_2CO_3 with respect to the acceptor, CH_2Cl_2 (0.04 M). [b]Yield was determined by ^1H NMR using 1,3,5-trimethoxybenzene as the internal standard. [c]Diastereoselectivity was determined by ^1H NMR. [d]Catalyst was generated by premixing PPh_3AuCl and AgOTf, and the reaction was carried out at −15 °C. [e]Reaction was refluxed at 60 °C. [f]Reaction was heated at 40 °C. n.r. = no reaction; n.d. = not determined.

the high-energy dinitrogen (N_2) motif that causes diazo compounds to have a reputation for instability.[13] Additionally, enynals are recognized for their activation through transition metals via a 5-*exo*-dig cyclization process, leading to the formation of a furyl carbene. We hypothesize that the resulting furyl carbene, derived from enynals, would facilitate the activation of the furanose ester under mild conditions, enabling a stereoselective furanosylation process (Figure 1d).

Furanosides are key constituents of many biomedically relevant carbohydrates. Although less common than their pyranoside-based counterparts, oligo- and polyfuranosides are widely distributed in mammals, plants, bacteria, and parasites.[14] Because of their biological significance, there has been a growing interest in the stereoselective synthesis of furanose-containing glycans.[15] Furanosides are commonly identified as featuring 1,2-*trans* and 1,2-*cis* linkages in oligo-and polysaccharides, and the stereochemistry of these linkages is important for their biological function (Figure 2a). While assembling a 1,2-*trans* linkage through anchimeric assistance from a C2-*O*-acyl protecting group is relatively easy,[16] synthesizing the 1,2-*cis* linkage is much more challenging.[17] Furthermore, the higher stability of the oxocarbenium ion in furanosides when compared to their pyranoside counterparts favors the S_N1 end of the S_N1−S_N2 glycosylation boundary (Figure 2b),[18] making it more challenging to achieve 1,2-*cis*-selectivity in furanosides. Most glycosylation approaches developed for 1,2-*cis* linkages in the pyranoside system do not work well with the furanosides, and similar glycosyl donors in furanosylation reactions provide a mixture of stereoisomers. Several innovative approaches using stoichiometric reagents have been designed to overcome these inherent challenges, such as intramolecular aglycone transport,[19] donors with constrained conformations,[15c,20] and the use of functionalized *O*-protecting groups for hydrogen-bond-mediated aglycone transport.[21] Recently, a few elegant catalytic approaches to 1,2-*cis*-furanosylations have been introduced (Figure 2c). The Jacobsen group reported an elegant method for the activation of phosphorus-based furanoside donors using a bis-thiourea organocatalyst to access 1,2-*cis*-furanosides.[22] However, the bis-thiourea catalysts are difficult to synthesize and highly substrate-specific as they do not tolerate mannosyl alcohols as an acceptor. The group of Schlegel and Nguyen reported a

https://doi.org/10.1021/acscatal.3c05237
ACS Catal. 2024, 14, 1037−1049

Table 2. Reaction of Alcohol Nucleophiles with D-Ribofuranosyl Donor[a]

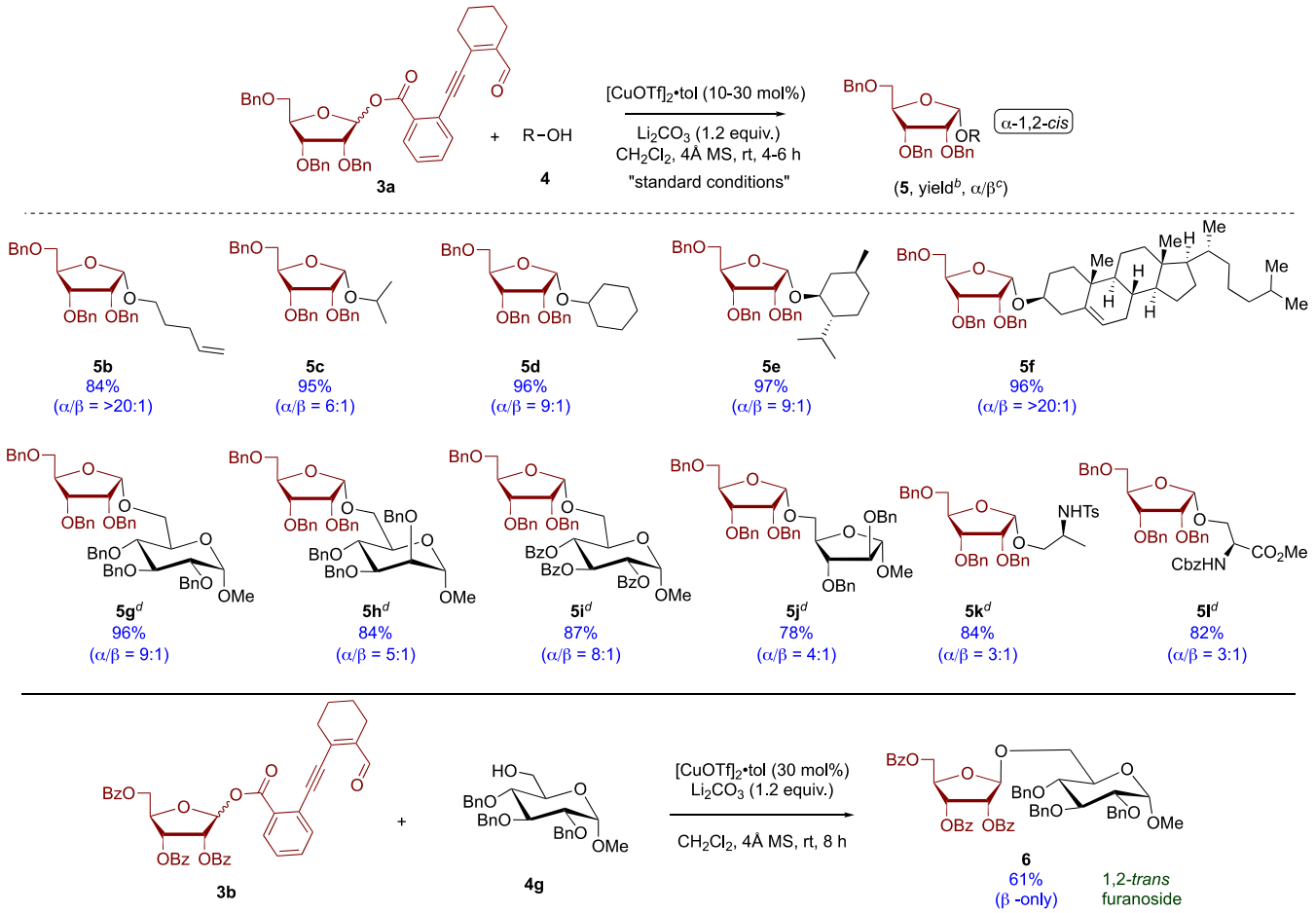

[a]All furanosylations were conducted with donor (0.075 mmol), acceptor (0.05 mmol), 10 mol % of catalyst, and 1.2 equiv of Li_2CO_3 with respect to the acceptor, CH_2Cl_2 (0.04 M). [b]Yield was determined by ^1H NMR using 1,3,5-trimethoxybenzene as an internal standard. [c]Diastereoselectivity was determined by ^1H NMR. [d]30 mol % of catalyst was used.

phenanthroline-supported 1,2-*cis*-furanosylation strategy in which a C1-bromo donor and a phenanthroline organocatalyst direct an acceptor to the *cis* face.[23] Likewise, halo donors are highly susceptible to hydrolysis and must be used immediately after their synthesis. Zhang and co-workers have recently developed an alkyne-based benchtop stable donor that is activated using precious gold-catalysis to undergo a stereoinvertive attack at C1 with an alcohol acceptor, resulting in the formation of 1,2-*cis*-furanosides.[24] Furthermore, these methods require an anomerically pure donor to achieve the desired 1,2-*cis*-selectivity.

To overcome these limitations, there is a need to design a donor where the 1,2-*cis*-selectivity is independent of the anomeric configuration of the donor. Additionally, the donor should have orthogonal reactivity to other donors and be activated using earth-abundant metals (iron, copper, and zinc) rather than precious rare-earth metals such as rhodium, gold, and palladium. Based on our group's experience in metal carbenes,[25] we endeavored to develop an earth-abundant metalcatalyzed carbene-based approach to 1,2-*cis*-furanosylation.

Our methodology commences by synthesizing simple and benchtop stable donors via straightforward EDCI-coupling of iodobenzoic acids with readily accessible anomeric alcohols **1**. The resulting esters **2** were coupled to the enynal moiety using a Sonogashira coupling to provide a variety of enynal donors **3** in high yields (Figure 3; see the Supporting Information for details).

We sought to optimize the reaction conditions by identifying the best component in the reaction in each of three categories: catalyst, acid scavenger, and solvent. We initiated our reaction optimization with the 2,3,5-tri-*O*-benzyl-*α*-D-ribofuranosyl donor **3a** and 1,2:3,4-di-*O*-isopropylidene-*α*-D-galactopyranose acceptor **4a**. Through this study, we found that 10 mol % of copper(I) trifluoromethanesulfonate as the catalyst, lithium carbonate (1.2 equiv) as the acid scavenger, and CH_2Cl_2 as the solvent (0.04 M) at 25 °C with 4 Å molecular sieves led to the highest yield (78%) favoring the desired 1,2-*cis*-diastereoselectivity (7:1, Table 1, entry 1) in the shortest amount of time. Reactions were carried out using 1.5 equiv of the donor as the reaction conditions resulted in a small degree of unproductive decomposition of the donor. Initiating our optimization, we selected catalysts shown to activate enynal systems in the literature.[12f] The earth-abundant catalysts zinc(II) chloride and iron(III) chloride were found to decrease the yield and diastereoselectivity considerably and required more time to reach completion (entries 2 and 3). Other metal triflates, such as zinc(II) triflate and triphenylphosphine gold(I) triflate, did not appear to be effective. While zinc triflate yielded no reaction after 36 h (entry 4), gold triflate displayed a lower

https://doi.org/10.1021/acscatal.3c05237
ACS Catal. 2024, 14, 1037−1049

Table 3. Furanosyl Donor Scope[a]

a) *Reaction of alcohol nucleophiles with D-arabinofuranosyl donor*

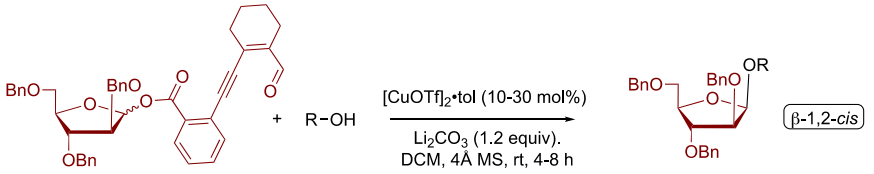

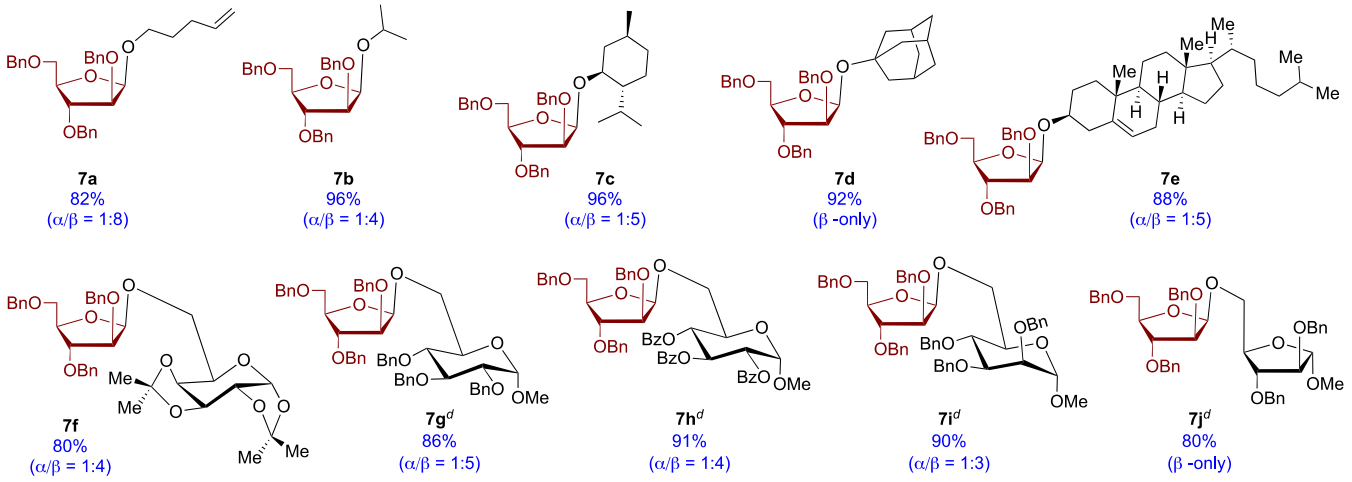

b) *Reaction of alcohol nucleophiles with L-arabinofuranosyl donor*

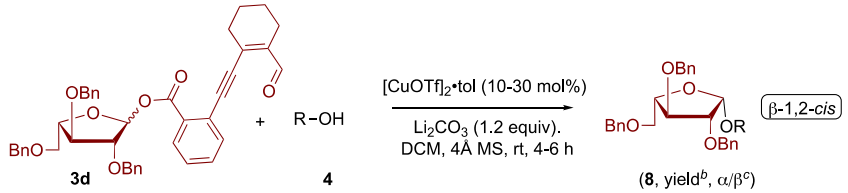

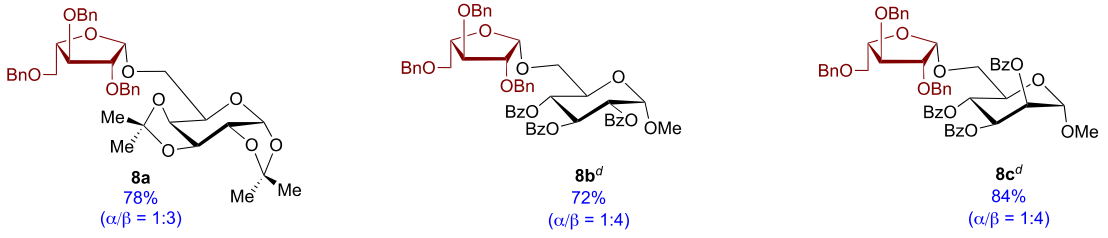

[a]All furanosylations were conducted with donor (0.075 mmol), acceptor (0.05 mmol), 10 mol % of catalyst, and 1.2 equiv of Li_2CO_3 with respect to the acceptor, CH_2Cl_2 (0.04 M). [b]Yield was determined by ^1H NMR using 1,3,5-trimethoxybenzene as an internal standard. [c]Diastereoselectivity was determined by NMR. [d]30 mol % of catalyst was used.

yield but with comparable selectivity to the parent reaction (entry 5). $Rh_2(esp)_2$, which has also been documented to activate enynal compounds,[12f] was unable to initiate the furanosylation (entry 6). Next, we sought to investigate the effect of the counterion present on the copper(I) metal salt. When tetrakis(acetonitrile)copper(I) hexafluorophosphate was selected, the yield fell slightly; however, the selectivity dramatically decreased (entry 7). In the case of tetrakis-(acetonitrile)copper(I) tetrafluoroborate, the reaction proved to be sluggish and yielded nearly no product (entry 8). We then proceeded to optimize the solvent for this reaction. Lewis basic solvents such as THF and acetonitrile were found to produce no reaction, ostensibly due to the coordination of the solvent to the copper catalyst (entries 9 and 10). Toluene, however, did furnish the product, albeit in a significantly decreased yield (10%) and with no selectivity observed (entry 11). From here, we decided to perform control experiments to determine the necessity of each additive. As metal triflates are a mild source of triflic acid,[26] it cannot be discounted that triflic acid could catalyze this reaction. To evaluate this, we added triflic acid instead of lithium carbonate and Cu(I)OTf. In this case, we witnessed a significant decrease in the yield and a complete reversal of diastereoselectivity (entry 12). This result is in accordance with Sharma and Tan's work on $Sc(OTf)_3$-catalyzed spiroketalizations,[26d] where triflic acid can cause the partial decomposition or isomerization of the product from a kinetic product to a more stable thermodynamic product. To probe the impact of the acid scavenger, we executed the reaction without lithium carbonate, which decreased yield and selectivity, probably due to the generation of a small amount of

https://doi.org/10.1021/acscatal.3c05237
ACS Catal. 2024, 14, 1037−1049

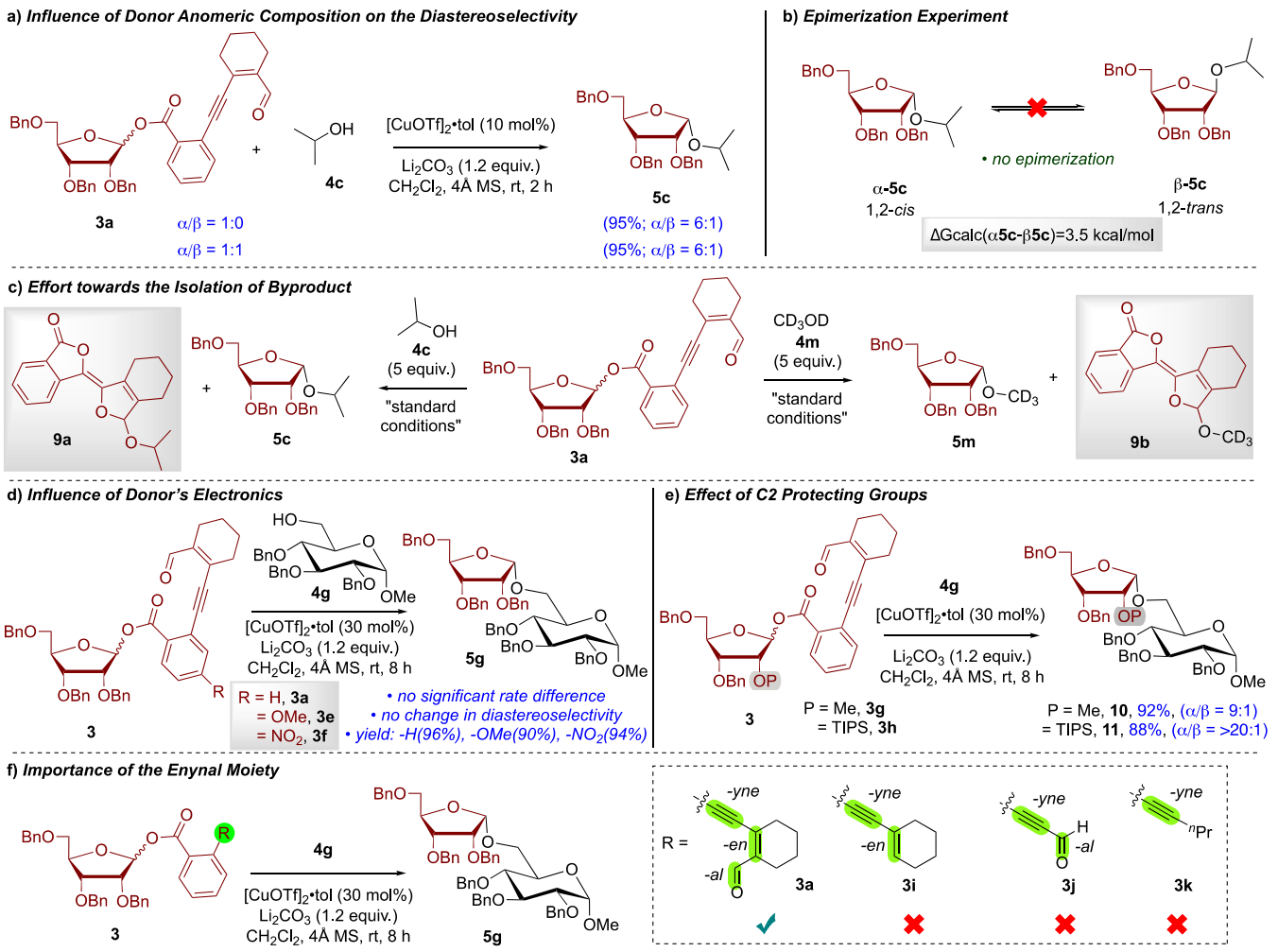

Figure 4. (a) Influence of the donor's anomeric composition. (b) Epimerization experiment. (c) Isolation of the byproduct. (d) Influence of donor electronics on stereoselectivity. (e) Effect of C2 protecting groups. (f) Significance of the donor's -en-yn-al functionality.

triflic acid in the system (entry 13). Selecting 2,6-di-*tert*-butyl-4-methylpyridine (DTBMP) as an alternative acid scavenger led to further declines in output, presumably due to thermal decomposition induced by the higher reaction temperature (entry 14). Finally, we discovered that the presence of a copper catalyst is essential for the reaction to occur (entry 15).

With optimized conditions, a substrate scope consisting of arabinose and ribose donors was built out. A benzyl-protected D-ribofuranosyl donor was selected, and was reacted with various alcohol acceptors. A primary alcohol featuring a terminal olefin was examined. The reaction proceeded smoothly in a high yield with very high *α-cis*-selectivity (Table 2, **5b**). Secondary alcohols, such as isopropanol and cyclohexanol, proceeded rapidly to afford the corresponding products in a >95% yield with high *cis*-selectivity (**5c** and **5d**). Chiral secondary alcohols such as cholesterol and L-menthol were then subjected to the optimized conditions, yielding their respective products with excellent yield and *cis*-selectivity (**5e** and **5f**). It is worth noting that a nearly exclusive *α-cis*-product was observed in the case of cholesterol. Various carbohydrate alcohol acceptors bearing different protecting groups were also screened. Unlike previous acceptors, benzyl-/benzoyl-protected glucopyranosides, as well as benzyl-protected arabinofuranoside acceptors and protected amino acid alcohol acceptors, required higher catalyst loading to provide the intended products in sufficient yields. For example, 10 mol % of the copper catalyst with acceptor **4g** provides 64% yield of product **5g** with a significant amount of unreacted donor, while 20 mol % provides 82% and 30 mol % leads to almost quantitative conversion (96%). However, we did not observe any significant difference in 1,2-*cis*-selectivity. To our delight, reaction yields and selectivity were independent of protecting group influence for benzyl-/benzoyl-protected carbohydrate acceptors (**5g**−**5j**). Notably, the mannosyl acceptor, incompatible with the bis-thiourea catalyst,[22] worked equally well under our optimized conditions to provide the 1,2-*cis*-furanosylation product. Amino acid alcohol acceptors, including tosyl-protected alaninol and protected serine, were also examined, resulting in high yields and good *cis*-selectivity (**5k** and **5l**).

In addition, 1,2-*trans*-glycosidic linkages are also essential in carbohydrate chemistry as they are crucial in determining the biological activity and stability of various glycosides and polysaccharides.[27] Therefore, we decided to examine the compatibility of our optimized reaction conditions to access a 1,2-*trans*-furanosidic linkage via the assistance of neighboring-group participation. We were pleased to observe that benzoyl donor **3b** generated product 6 in a moderate yield (61%) with an exclusive *β-trans*-selectivity.

With the success of the ribose donor, we sought to investigate a substrate scope with an arabinose donor **3c**. 4-

https://doi.org/10.1021/acscatal.3c05237
ACS Catal. 2024, 14, 1037−1049

Penten-1-ol reacted effectively, yielding the desired arabinofuranoside **7a** with high yield and β-*cis*-selectivity (Table 3a, 82%, α/β = 1:8). Simple secondary alcohol isopropanol furnished product **7b** in a high yield with good stereoselectivity (96%, α/β = 1:4). Chiral secondary alcohol L-menthol as the acceptor led to a similarly high yield with even greater selectivity (**7c**, 96%, α/β = 1:5). Tertiary alcohol acceptor 1-adamantanol also resulted in an 88% yield, in line with those previously discussed and with exclusive β-*cis*-selectivity (**7d**, 92%). Similarly, cholesterol underwent a smooth reaction, yielding the corresponding product **7e** with a high yield and *cis*-selectivity. To our pleasure, acetonide, benzyl, and benzoyl-protected glucose acceptors proved facile and reactive in our system with high yields and β-*cis*-selectivity (**7f**–**7h**). As previously described, acceptors derived from mannose were unreactive with the Jacobsen bis-thiourea furanosylation protocol.[22]

To our delight, our method furnished the intended product with the arabinose donor in high yields and selectivity with the mannose acceptor (**7i**, 90%, α/β = 1:3). Finally, the benzyl-protected arabinofuranoside acceptor afforded the desired product **7j** in a respectable yield (80%) and with exclusive β-*cis*-selectivity. Furthermore, we noticed that the *cis*-selectivity of the newly formed furanosidic linkage was not affected by the reactivity of the nucleophilic acceptor. This was evidenced by electron-donating and electron-withdrawing acceptors affording their products with similar selectivity. To demonstrate the compatibility with an opposite enantiomer, L-arabinofuranoside was also examined as a donor with various alcohol acceptors. Reactions with donor **3d** displayed β-*cis*-selectivity, likewise, observed with D-arabinofuranoside. The acetonide and benzoyl-protected glucopyranoside acceptors supplied their intended products in good yield with modest selectivity (Table 3b, **8a** and **8b**). Similarly, the benzoyl-protected mannopyranoside acceptor provided the desired outcome with a good yield and selectivity (**8c**, 84%, α/β = 1:4).

Jacobsen and co-workers reported that the reaction outcome in their bis-thiourea-catalyzed furanosylation was significantly impacted by the anomeric composition of their furanose phosphate donors.[22] Recently, the Zhang group disclosed a gold-catalyzed alkyne donor for 1,2-*cis*-furanosylations,[24] wherein the stereoselectivity also depends on the anomeric purity of the initial donor. This is due to the underlying mechanism of S_N2-like displacement that requires an anomerically pure donor.

To determine the influence of the anomeric configuration of our donor on the stereochemical outcome of the developed protocol, a racemic mixture and an anomerically pure version of the D-ribofuranoside donor were synthesized and implemented in a head-to-head comparison (Figure 4a). Based on the observed results, it is apparent that 1,2-*cis*-diastereoselectivity is independent of the anomeric configuration of the donor, and the reaction proceeds through a common intermediate, ostensibly the oxocarbenium ion of the furanose donor, to produce the desired high 1,2-*cis*-selectivity. Additionally, we examined the epimerization of the α/β-furanoside products using the established reaction conditions (Figure 4b). The product exhibited no signs of epimerization, underscoring the stability and mildness of our developed protocol.

Through initial studies, we found the byproduct of this reaction to be unstable, and so we attempted to isolate an intermediate of the byproduct through a trapping experiment; the reaction was set up with ribose donor **3a** and an excess of alcohol acceptor isopropanol **4c** (5 equiv). We found that this resulted in the synthesis of the expected product **5c** and an isomerized isopropanol trapped byproduct **9a**. Additionally, we performed another reaction with deuterated methanol as the acceptor, and we were able to isolate similarly isomerized deuterated methanol incorporated byproduct **9b** along with product **5m** (Figure 4c) (see Supporting Information for more details).

To evaluate whether ester insertion into the carbene, which leads to the formation of the oxocarbenium ion, is the rate-determining step, we modified the electronic character of the aromatic ring on the donor. Subsequently, D-ribofuranosyl donors **3e** and **3f** were synthesized, featuring a methoxy and a nitro group para to the ester moiety in the aromatic ring. Our observations on the relatively similar rates of their reactions with acceptor **4g** (Figure 4d) led to the hypothesis that insertion of the ester into the generated carbene is not the rate-limiting step. Instead, we believe that the reaction rate depends primarily on the reactivity of the alcohol acceptor, which in turn depends on its steric and electronic properties. Thus, we can infer that the rate of formation of the oxocarbenium ion does not play a significant role in determining the rate of reaction. To investigate the effect of the C2 protecting group on the stereochemical outcome of this reaction, we synthesized ribosyl donors with modified C2 protecting groups (Figure 4e). As copper is known to coordinate with alkenes and alkynes, we replaced the C2 benzyl group with a non-π-aryl coordinating methoxy group (**3g**) to probe the role of the phenyl ring coordination in the benzyl protecting group. To our delight, there was no change in the stereochemical outcome of the product. Additionally, we employed a C2 silyloxy group (**3h**) to monitor coordination to the copper catalyst in ensuring *cis*-selectivity. When subjected to our parent conditions, we found that this silyloxy led to nearly exclusive *cis*-selectivity while maintaining high yields. This suggests that coordination of the copper catalyst to the C2 oxygen is necessary for the observed selectivity.

Subsequently, we explored the significance of the -en, -yn, and -al functionalities within our innovative furanosyl donor (Figure 4f). The absence of the aldehyde functionality in the synthesized en–yn ribosyl donor **3i** led to no reaction in the presence of the copper catalyst. Experimentation was also conducted with the ribosyl yn–al donor **3j**, which notably displayed a complete lack of reactivity in the desired furanosylation reaction. The well-established D-ribosyl -yn donor **3k** was unreactive under our standard reaction conditions. Nonetheless, the literature has shown that gold salts can activate these types of alkyne donors to initiate furanosylation.[28] This further highlights the importance of our copper carbene chemistry and the limitations of the known metal-catalyzed approaches, which require precious rare metals such as gold and rhodium. As described earlier, glycosylation catalyzed by earth-abundant metals has been notably missing from academic discourse, and many new donors are unreactive in the presence of such catalysts. These results also demonstrate the orthogonal reactivity of our donor to literature known alkyne donors, which could be harnessed for a one-pot iterative synthesis.

To further demonstrate the orthogonal reactivity of our donor, we attempted a reaction with propargyl alcohol as an acceptor to access propargyl donor **5n**, known to be reactive under gold(III) catalysis, as described by the Hotha group.[29] We were pleased to observe that the reaction exhibited full

https://doi.org/10.1021/acscatal.3c05237
ACS Catal. 2024, 14, 1037–1049

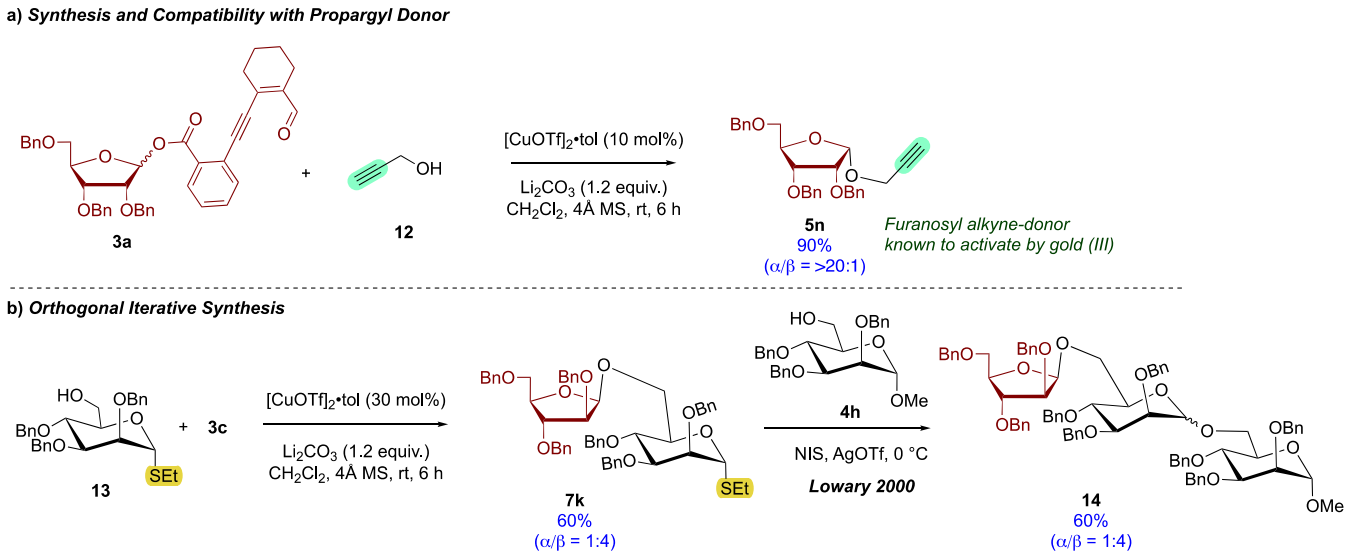

Figure 5. (a) Synthesis and compatibility with propargyl donor. (b) Orthogonal iterative synthesis with a thioglycoside acceptor.

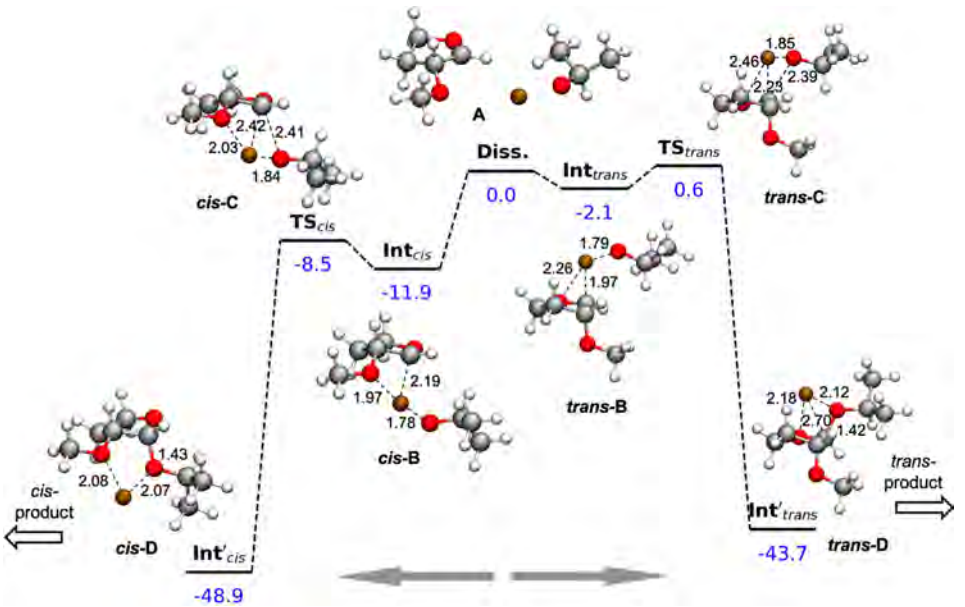

Figure 6. Free energy profile for the reaction of 2-OMe furan oxocarbenium ion with Cu(O^{i}Pr). Energies are given in kcal/mol; atomic distances are given in Å; and atomic colors: O = red, C = gray, H = white, and Cu = bronze.

compatibility with the alkyne group, furnishing a high product yield of 90% with near exclusive α-selectivity. This further highlights the selectivity of the copper catalyst for enynal donors over other alkyne donors known in the literature (Figure 5a).

We next demonstrated the orthogonal reactivity with well-established and widely utilized thioglycoside donors. As expected, acceptor **13**, bearing a thioglycoside moiety, reacted facilely under the optimized copper-catalyzed conditions, highlighting the orthogonal reactivity of these enynal donors. The newly formed thioglycoside product **7k** can be utilized in an established NIS/TfOH method to perform a one-pot iterative synthesis, as demonstrated by Lowary[30] (Figure 5b).

Results from the experimental study provided the following insights into the Cu-catalyzed reaction pathway: ionization of the ribose donor likely is not the rate-limiting step, and the *cis*-stereoselectivity is determined after this step. The latter point is supported by the noninterconvertibility of the isomeric products and the greater stability of the experimentally minor *trans*-isopropoxy product **5c** (ΔG_{calc} = 3.5 kcal/mol), as previously mentioned in Figure 4b. To computationally model the reaction pathway, we considered the likely copper-ligated species Cu(I)XY (X, Y = OR, OTf), which could attack the intermediate oxocarbenium ion. The reactant ratio for CuOTf/ROH/Li_2CO_3 of 0.1/1.0/1.0 and the Cu-anion binding affinities (see the Supporting Information for details) would favor the formation of species such as Cu(OR), Cu(OR)-(OTf)$^-$, and Cu(OR)$_2^-$.[31] Our DFT computational study[32] began by first considering the approaches of Cu-O^{i}Pr to either face of the model 2-methoxyfuran oxocarbenium ion A (Figure 6). Isomeric *cis*- and *trans*-C-bound Cu(III) alkoxide intermediates *cis*-B and *trans*-B, arising from oxidative addition, were found.[33] The *cis*-Cu(III)-C intermediate *cis*-B, which is stabilized by a bonding interaction with the adjacent -OMe

https://doi.org/10.1021/acscatal.3c05237
ACS Catal. 2024, 14, 1037−1049

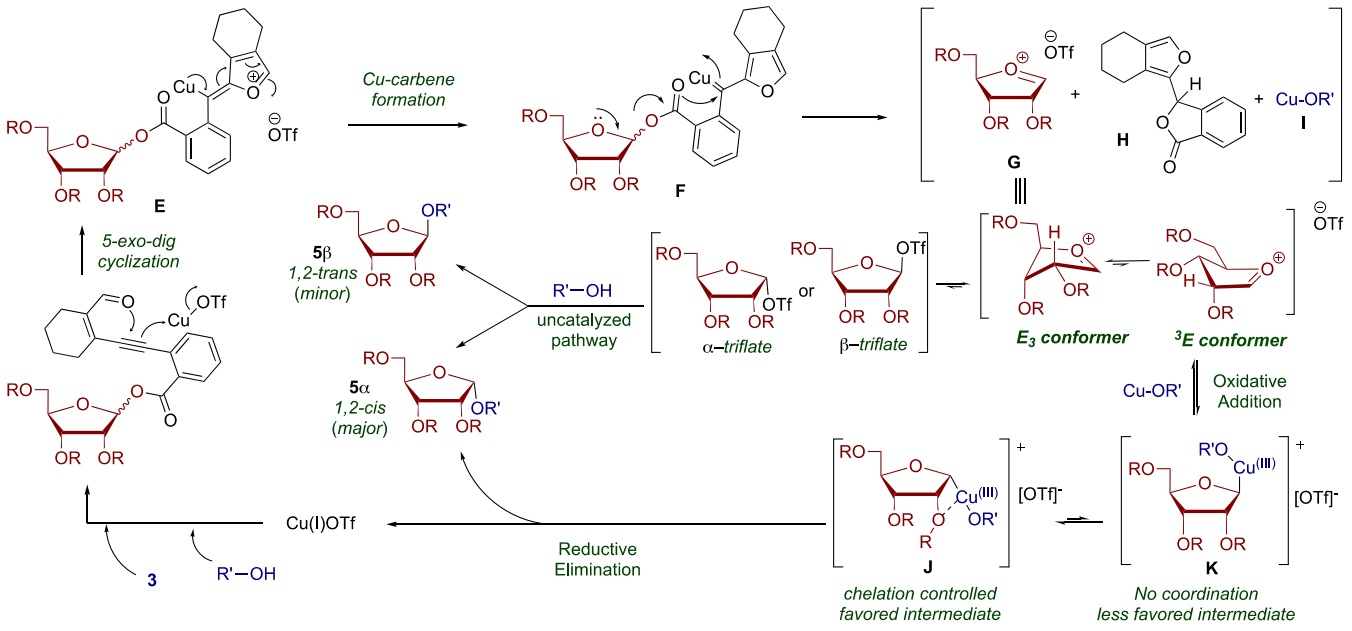

Figure 7. A plausible mechanism for copper-catalyzed ribofuranosylations.

group (Cu-OMe 1.97 Å, Cu-C 2.19 Å), is found to be 9.8 kcal/mol lower in energy (more stable) than the trans intermediate trans-B (Cu-O(furan) 2.26 Å, Cu-C 1.97 Å). Reductive elimination from the intermediates (*cis*-B, *trans*-B) leads to the respective cis- and trans-product complexes (*cis*-D, *trans*-D).[34] The transition states for this process (*cis*-C, *trans*-C) show the O−C bond-making and Cu-O-^{i}Pr bond-breaking: *cis*-TS: Cu-OMe 2.09 Å, Cu-C 2.42 Å, and C-O(^{i}Pr) 1.84 Å; trans-TS: Cu-O (furan) 2.46 Å, Cu-C 2.26 Å, and C-O(^{i}Pr) 1.85 Å. The activation energies for these isomeric transition states are small and quite similar, 3.4 vs 2.8 kcal/mol. According to the energetic profile of Figure 6, the *cis* product complex *cis*-D (and its Cu-free product **5c**) should be the exclusive product. This is qualitatively, but not quantitatively, in agreement with the experimental results. To reconcile the computational and experimental results, we also considered the stereoselectivity of the model carbocation reacting with Cu(O^iPr)$(OTf)^-$ and Cu$(O^i Pr)_2^-$. With these $CuXY^-$ species, the *cis*-oxidative addition intermediate *cis*-B′ (Supporting Information) was only slightly favored or equal energetically to the *trans*-B′ by 0.3 kcal/mol for −Cu(O^iPr)$(OTf)^-$ and −0.0 kcal/mol for −Cu$(O^i Pr)_2^-$. The longer *cis*-Cu-OMe and *trans*-Cu-O(furan) interactions in these cases (see Supporting Information for details) apparently are weaker, probably accounting for their similar stabilities. With both of these $CuXY^-$ species, the trans activation energy is comparable to, or lower (0.5−2.0 kcal/mol) than, the *cis* pathway, predicting a slight preference for the *trans* product. The involvement of these additional pathways would lower the observed cis-selectivity, as would competition with off-the-metal-alcohol attack directly on the oxocarbenium ion.

Based on the above-described results, control experiments, and computational calculations, we hypothesized a plausible mechanism for this copper-catalyzed 1,2-*cis*-furanosylation, as depicted in Figure 7. First, the enynal moiety in the presence of the copper(I)-catalyst forms intermediate E via a 5-*exo*-dig-cyclization. This process is followed by the back-donation from copper, leading to the aromatization of the furan moiety, thereby generating the copper-carbene, intermediate F. The resulting copper carbene activates the anomeric ester to form an oxocarbenium ion G, which is the common intermediate regardless of the anomeric configuration of the starting donor. The resulting oxocarbenium ion G can adopt both E_3 and ^{3}E conformations. Based on the literature, E_3 is identified as the more stable conformation, and an inside attack from the nucleophile to E_3 produces the *cis*-isomer.[35] The furan byproduct H, containing copper, undergoes protodemetalation with the acceptor alcohol, resulting in the formation of copper alkoxide I. This copper alkoxide then undergoes oxidative addition, leading to the formation of intermediates J and K. In the case of intermediate J, stabilization occurs through chelation between the C2 oxygen and copper. In contrast, no such stabilization is observed in intermediate K. Consequently, intermediate J is determined to be more stable than intermediate K. Ultimately, reductive elimination from intermediate J gives rise to the corresponding contra-thermodynamic 1,2-*cis*-furanosylation product (5α). On the other hand, the noncoordinated intermediate K can lead to the corresponding β-1,2-*trans*-product (5β). This proposed mechanism is further supported by the optimization results outlined in Table 1, where the use of the Cu(I)OTf catalyst resulted in a high degree of *cis*-stereoselectivity compared to triflic acid, suggesting the involvement of copper in providing the high anomeric 1,2-*cis*-stereoselectivity. Notably, oxocarbenium intermediate G can also exist in equilibrium as a contact-ion pair. The proximal triflate anion shields the α-face (α-triflate) or β-face (β-triflate) of the furanosyl oxocarbenium ion. A subsequent S_N2 attack on the α-triflate or the β-triflate species would furnish the β- or the α-furanosyl product (5), respectively, without the involvement of the copper catalyst.

CONCLUSIONS

In conclusion, an earth-abundant copper-catalyzed stereoselective furanosylation strategy is developed to access the challenging 1,2-*cis* furanosidic linkages.

This transformation proceeds at room temperature and provides high yields and excellent *cis*-stereoselectivity by utilizing novel benchtop stable enynal-derived furanosyl

https://doi.org/10.1021/acscatal.3c05237
ACS Catal. 2024, 14, 1037−1049

donors. This chemistry accommodates primary, secondary, and tertiary alcohol acceptors, as well as other furanose donors with different substitution and stereochemical patterns. Our control experiments indicate that the observed 1,2-*cis*-stereoselectivity is independent of the anomeric configuration of the starting furanose donors. This method also exhibits orthogonal selectivity with well-established alkyne and thioglycoside donors, enabling a one-pot iterative synthesis. Through experimental and computational studies, we have established that the desired *cis*-stereoselectivity arises from chelation between the C2-oxygen of the furanose donor and the incoming copper alkoxide nucleophile. These findings emphasize the unique capabilities of earth-abundant copper as a catalyst for highly stereoselective furanosylation reactions. Furthermore, applications of this method to other glycosylation reactions are underway and will be reported in due course.

■ ASSOCIATED CONTENT

Supporting Information

The Supporting Information is available free of charge at https://pubs.acs.org/doi/10.1021/acscatal.3c05237.

Experimental procedures, NMR spectroscopic, and analytical data for all compounds (PDF)

■ AUTHOR INFORMATION

Corresponding Author

Indrajeet Sharma − *Department of Chemistry and Biochemistry, University of Oklahoma, Norman, Oklahoma 73019-5251, United States;* orcid.org/0000-0002-0707-0621; Email: isharma@ou.edu

Authors

Bidhan Ghosh − *Department of Chemistry and Biochemistry, University of Oklahoma, Norman, Oklahoma 73019-5251, United States*

Adam Alber − *Department of Chemistry and Biochemistry, University of Oklahoma, Norman, Oklahoma 73019-5251, United States*

Chance W. Lander − *Department of Chemistry and Biochemistry, University of Oklahoma, Norman, Oklahoma 73019-5251, United States*

Yihan Shao − *Department of Chemistry and Biochemistry, University of Oklahoma, Norman, Oklahoma 73019-5251, United States;* orcid.org/0000-0001-9337-341X

Kenneth M. Nicholas − *Department of Chemistry and Biochemistry, University of Oklahoma, Norman, Oklahoma 73019-5251, United States;* orcid.org/0000-0002-5180-1671

Complete contact information is available at: https://pubs.acs.org/10.1021/acscatal.3c05237

Author Contributions

The manuscript was written through the contributions of all authors. All authors have given their approval to the final version of the manuscript.

Funding

This work was supported by NSF CHE-1753187, CHE-2102071, and the Oklahoma Center for the Advancement of Science and Technology (OCAST HR20-078).

Notes

The authors declare no competing financial interest.

■ ACKNOWLEDGMENTS

We thank Dr. Novruz G. Akmedov and Dr. Steven Foster from the Research Support Services, University of Oklahoma, for NMR and mass spectral analyses, respectively. We also thank Dr. Anae Bain and Dr. Prashant Mandal for their helpful discussions.

■ REFERENCES

(1) (a) Hahn, F. E. Introduction: Carbene Chemistry. *Chem. Rev.* **2018**, *118*, 9455−9456. (b) Davies, H. M. L.; Morton, D. Guiding principles for site selective and stereoselective intermolecular C−H functionalization by donor/acceptor rhodium carbenes. *Chem. Soc. Rev.* **2011**, *40*, 1857−1869. (c) Davies, H. M. L.; Nikolai, J. Catalytic and enantioselective allylic C−H activation with donor−acceptor-substituted carbenoids. *Org. Biomol. Chem.* **2005**, *3*, 4176−4187. (d) Zhu, D.; Chen, L.; Fan, H.; Yao, Q.; Zhu, S. Recent progress on donor and donor−donor carbenes. *Chem. Soc. Rev.* **2020**, *49*, 908−950. (e) Davies, H. M. L.; Denton, J. R. Application of donor/acceptor-carbenoids to the synthesis of natural products. *Chem. Soc. Rev.* **2009**, *38*, 3061−3071. (f) Cao, Z.-Y.; Wang, Y.-H.; Zeng, X.-P.; Zhou, J. Catalytic asymmetric synthesis of 3,3-disubstituted oxindoles: diazooxindole joins the field. *Tetrahedron Lett.* **2014**, *55*, 2571−2584. (g) Xia, Y.; Qiu, D.; Wang, J. Transition-metal-catalyzed cross-couplings through carbene migratory insertion. *Chem. rev.* **2017**, *117*, 13810−13889.

(2) (a) Zhu, S.; Perman, J. A.; Zhang, X. P. Acceptor/Acceptor-Substituted Diazo Reagents for Carbene Transfers: Cobalt-Catalyzed Asymmetric Z-Cyclopropanation of Alkenes with α-Nitrodiazoacetates. *Angew. Chem., Int. Ed.* **2008**, *47*, 8460−8463. (b) Nani, R. R.; Reisman, S. E. α-Diazo-β-ketonitriles: Uniquely Reactive Substrates for Arene and Alkene Cyclopropanation. *J. Am. Chem. Soc.* **2013**, *135*, 7304−7311. (c) Zhu, S.; Xu, X.; Perman, J. A.; Zhang, X. P. A General and Efficient Cobalt(II)-Based Catalytic System for Highly Stereoselective Cyclopropanation of Alkenes with α-Cyanodiazoacetates. *J. Am. Chem. Soc.* **2010**, *132*, 12796−12799.

(3) Padwa, A.; Hornbuckle, S. F. Ylide formation from the reaction of carbenes and carbenoids with heteroatom lone pairs. *Chem. Rev.* **1991**, *91*, 263−309.

(4) (a) Yang, M.; Albrecht-Schmitt, T.; Cammarata, V.; Livant, P.; Makhanu, D. S.; Sykora, R.; Zhu, W. Trialkylamines More Planar at Nitrogen Than Triisopropylamine in the Solid State. *J. Org. Chem.* **2009**, *74*, 2671−2678. (b) Moody, C. J.; Taylor, R. J. Rhodium carbenoid mediated cyclisations. Use of ethyl lithiodiazoacetate in the preparation of ω-hydroxy–mercapto-and -boc-amino-α-diazo-β-keto esters. *Tetrahedron Lett.* **1987**, *28*, 5351−5352. (c) Shanahan, C. S.; Truong, P.; Mason, S. M.; Leszczynski, J. S.; Doyle, M. P. Diazoacetoacetate Enones for the Synthesis of Diverse Natural Product-like Scaffolds. *Org. lett.* **2013**, *15*, 3642−3645.

(5) (a) Álvarez, M.; Molina, F.; Pérez, P. J. Carbene-Controlled Regioselective Functionalization of Linear Alkanes under Silver Catalysis. *J. Am. Chem. Soc.* **2022**, *144*, 23275−23279. (b) Jana, S.; Empel, C.; Pei, C.; Aseeva, P.; Nguyen, T. V.; Koenigs, R. M. C. −H. Functionalization Reactions of Unprotected *N*-Heterocycles by Gold-Catalyzed Carbene Transfer. *ACS Catal.* **2020**, *10*, 9925−9931. (c) Jha, N.; Khot, N. P.; Kapur, M. Transition-Metal-Catalyzed C−H Bond Functionalization of Arenes/Heteroarenes via Tandem C−H Activation and Subsequent Carbene Migratory Insertion Strategy. *Chem. Rec.* **2021**, *21*, 4088−4122. (d) He, Y.; Huang, Z.; Wu, K.; Ma, J.; Zhou, Y.-G.; Yu, Z. Recent advances in transition-metal-catalyzed carbene insertion to C−H bonds. *Chem. Soc. Rev.* **2022**, *51*, 2759−2852.

(6) (a) Zhukhovitskiy, A. V.; Kobylianskii, I. J.; Thomas, A. A.; Evans, A. M.; Delaney, C. P.; Flanders, N. C.; Denmark, S. E.; Dichtel, W. R.; Toste, F. D. A Dinuclear Mechanism Implicated in Controlled Carbene Polymerization. *J. Am. Chem. Soc.* **2019**, *141*, 6473−6478. (b) Jellema, E.; Budzelaar, P. H. M.; Reek, J. N. H.; de Bruin, B. Rh-Mediated Polymerization of Carbenes: Mechanism and Stereoregulation. *J. Am. Chem. Soc.* **2007**, *129*, 11631−11641. (c) Li, F.;

Xiao, L.; Li, B.; Hu, X.; Liu, L. Carbene polymerization from the catalyzed decomposition of diazo compounds: Mechanism and modern development. *Coord. Chem. Rev.* **2022**, *473*, 214806.
(7) (a) Patra, S. G.; Das, N. K. Recent advancement on the mechanism of olefin metathesis by Grubbs catalysts: A computational perspective. *Polyhedron* **2021**, *200*, 115096. (b) Huang, J.; Stevens, E. D.; Nolan, S. P.; Petersen, J. L. Olefin Metathesis-Active Ruthenium Complexes Bearing a Nucleophilic Carbene Ligand. *J. Am. Chem. Soc.* **1999**, *121*, 2674−2678. (c) Adlhart, C.; Chen, P. Mechanism and Activity of Ruthenium Olefin Metathesis Catalysts: The Role of Ligands and Substrates from a Theoretical Perspective. *J. Am. Chem. Soc.* **2004**, *126*, 3496−3510. (d) Grau, B. W.; Neuhauser, A.; Aghazada, S.; Meyer, K.; Tsogoeva, S. B. Iron-Catalyzed Olefin Metathesis: Recent Theoretical and Experimental Advances. *Chem.—Eur. J.* **2022**, *28*, No. e202201414.
(8) (a) McGrath, N. A.; Andersen, K. A.; Davis, A. K. F.; Lomax, J. E.; Raines, R. T. Diazo compounds for the bioreversible esterification of proteins. *Chem. Sci.* **2015**, *6*, 752−755. (b) Mix, K. A.; Raines, R. T. Optimized Diazo Scaffold for Protein Esterification. *Org. lett.* **2015**, *17*, 2358−2361. (c) Jun, J. V.; Petri, Y. D.; Erickson, L. W.; Raines, R. T. Modular Diazo Compound for the Bioreversible Late-Stage Modification of Proteins. *J. Am. Chem. Soc.* **2023**, *145*, 6615−6621. (d) Mix, K. A.; Aronoff, M. R.; Raines, R. T. Diazo Compounds: Versatile Tools for Chemical Biology. *ACS Chem. Biol.* **2016**, *11*, 3233−3244. (e) Bernardim, B.; Dunsmore, L.; Li, H.; Hocking, B.; Nuñez-Franco, R.; Navo, C. D.; Jiménez-Osés, G.; Burtoloso, A. C. B.; Bernardes, G. J. L. Precise Installation of Diazo-Tagged Side-Chains on Proteins to Enable In Vitro and In-Cell Site-Specific Labeling. *Bioconjugate Chem.* **2020**, *31*, 1604−1610. (f) Liu, F.-L.; Qi, C.-B.; Cheng, Q.-Y.; Ding, J.-H.; Yuan, B.-F.; Feng, Y.-Q. Diazo Reagent Labeling with Mass Spectrometry Analysis for Sensitive Determination of Ribonucleotides in Living Organisms. *Anal. Chem.* **2020**, *92*, 2301−2309.
(9) (a) Briner, K.; Vasella, A. Glycosylidene Carbenes a new approach to glycoside synthesis. Part 1. Preparation of glycosylidene-derived diaziridines and diazirines. *Helv. Chim. Acta* **1989**, *72*, 1371−1382. (b) Briner, K.; Vasella, A. Glycosylidene carbenes. Part 2. Synthesis of *O*-aryl glycosides. *Helv. Chim. Acta* **1990**, *73*, 1764−1778. (c) Mangholz, S. E.; Vaseha, A. Glycosylidene carbenes. Part 5. Synthesis of glycono-1,5-lactone tosylhydrazones as precursors of glycosylidene carbenes. *Helv. Chim. Acta* **1991**, *74*, 2100−2111. (d) Bozo, E.; Vasella, A. Glycosylidene carbenes. 10. Regioselective glycosidation of 4,6-*O*-benzylidene-D-altropyranosides. *Helv. Chim. Acta* **1992**, *75*, 2613−2633. (e) Briner, K.; Vasella, A. Glycosylidene carbenes. Part 6. Synthesis of alkyl and fluoroalkyl glycosides. *Helv. Chim. Acta* **1992**, *75*, 621−637. (f) Vasella, A.; Uhlmann, P.; Waldraff, C. A. A.; Diederich, F.; Thilgen, C. Fullerenzucker: Herstellung enantiomerenreiner, spiroverknüpfter C-Glycoside von C_{60}. *Angew. Chem.* **1992**, *104*, 1383−1385. (g) Muddasani, P. R.; Bozo, E.; Bernet, B.; Vasella, A. Glycosylidene carbenes. Part 14. Glycosidation of partially protected galactopyranose-glucopyranose-and mannopyranose-derived vicinal diols. *Helv. Chim. Acta* **1994**, *77*, 257−290. (h) Uhlmann, P.; Nanz, D.; Bozo, E.; Vasella, A. Glycosylidene carbenes. Part 18. Insertion of glycosylidene carbenes into the Sn-H bond of tributyl- and triphenylstannane: a synthesis of stannoglycosides. *Helv. Chim. Acta* **1994**, *77*, 1430−1440. (i) Uhlmann, P.; Vasella, A. Glycosylidene carbenes. Part 17. Glycosidation of benzyl *β*-D- and *β*-L-ribopyranosides. Further evidence for the effect of stereoelectronic control on the regioselectivity of glycosidation. *Helv. Chim. Acta* **1994**, *77*, 1175−1192. (j) Vasella, A. *Glycosylidene Carbenes*; Oxford University Press, Inc., 1999, p 56. (k) Wu, J.; Li, X.; Qi, X.; Duan, X.; Cracraft, W. L.; Guzei, I. A.; Liu, P.; Tang, W. Site-Selective and Stereoselective *O*-Alkylation of Glycosides by Rh(II)-Catalyzed Carbenoid Insertion. *J. Am. Chem. Soc.* **2019**, *141*, 19902−19910. (l) Kametani, T.; Kawamura, K.; Honda, T. New entry to the *C*-glycosidation by means of carbenoid displacement reaction. Its application to the synthesis of showdomycin. *J. Am. Chem. Soc.* **1987**, *109*, 3010−3017. (m) Meng, L.; Wu, P.; Fang, J.; Xiao, Y.; Xiao, X.; Tu, G.; Ma, X.; Teng, S.; Zeng, J.; Wan, Q. Glycosylation Enabled by Successive Rhodium(II) and Bronsted Acid Catalysis. *J. Am. Chem. Soc.* **2019**, *141*, 11775−11780.
(10) Mangholz, S. E.; Vasella, A. Glycosylidene Carbenes. Part 21. Synthesis of *N*-tosylglycono-1,4-lactone hydrazones as precursors of glycofuranosylidene carbenes. *Helv. Chim. Acta* **1995**, *78*, 1020−1035.
(11) Edgar, L. J. G.; Dasgupta, S.; Nitz, M. Protecting-Group-Free Synthesis of Glycosyl 1−Phosphates. *Org. lett.* **2012**, *14*, 4226−4229.
(12) (a) Kato, Y.; Miki, K.; Nishino, F.; Ohe, K.; Uemura, S. Doyle−Kirmse Reaction of Allylic Sulfides with Diazoalkane-Free (2-Furyl)carbenoid Transfer. *Org. Lett.* **2003**, *5*, 2619−2621. (b) Jana, R.; Paul, S.; Biswas, A.; Ray, J. K. Copper-catalyzed addition of water affording highly substituted furan and unusual formation of naphthofuran ring from 3-(1-alkenyl)-2-alkene-1-al. *Tetrahedron Lett.* **2010**, *51*, 273−276. (c) Vicente, R.; González, J.; Riesgo, L.; González, J.; López, L. A. Catalytic Generation of Zinc Carbenes from Alkynes: Zinc-Catalyzed Cyclopropanation and Si−H Bond Insertion Reactions. *Angew. Chem., Int. Ed.* **2012**, *51*, 8063−8067. (d) González, M. J.; López, L. A.; Vicente, R. Zinc-Catalyzed Cyclopropenation of Alkynes via 2-Furylcarbenoids. *Org. Lett.* **2014**, *16*, 5780−5783. (e) Ma, J.; Zhang, L.; Zhu, S. Enynal/Enynone: A Safe and Practical Carbenoid Precursor. *Curr. Org. Chem.* **2016**, *20*, 102−118. (f) Ma, J.; Zhang, L.; Zhu, S. Enynal/Enynone: A Safe and Practical Carbenoid Precursor. *Curr. Org. Chem.* **2015**, *20*, 102−118.
(13) Green, S. P.; Wheelhouse, K. M.; Payne, A. D.; Hallett, J. P.; Miller, P. W.; Bull, J. A. Thermal stability and explosive hazard assessment of diazo compounds and diazo transfer reagents. *Org. Process Res. Dev.* **2020**, *24*, 67−84.
(14) (a) Lindberg, B. Components of Bacterial Polysaccharides. In *Adv. Carbohydr. Chem. Biochem.*, Tipson, R. S., Horton, D., Eds.; Vol. *48*; Academic Press, 1990; pp 279−318. (b) Brennan, P. J.; Nikaido, H. The Envelope of Mycobacteria. *Annu. Rev. Biochem.* **1995**, *64*, 29−63. (c) Crick, D. C.; Mahapatra, S.; Brennan, P. J. Biosynthesis of the arabinogalactan-peptidoglycan complex of Mycobacterium tuberculosis. *Glycobiology* **2001**, *11*, 107R−118R. (d) Peltier, P.; Euzen, R.; Daniellou, R.; Nugier-Chauvin, C.; Ferrières, V. Recent knowledge and innovations related to hexofuranosides: structure, synthesis and applications. *Carbohydr. Res.* **2008**, *343*, 1897−1923. (e) Tefsen, B.; Ram, A. F. J.; van Die, I.; Routier, F. H. Galactofuranose in eukaryotes: aspects of biosynthesis and functional impact. *Glycobiology* **2012**, *22*, 456−469. (f) Lowary, T. L. Twenty Years of Mycobacterial Glycans: Furanosides and Beyond. *Acc. Chem. Res.* **2016**, *49*, 1379−1388.
(15) (a) Lowary, T. L. Synthesis and conformational analysis of arabinofuranosides, galactofuranosides and fructofuranosides. *Curr. Opin. Chem. Biol.* **2003**, *7*, 749−756. (b) Richards, M. R.; Lowary, T. L. Chemistry and Biology of Galactofuranose-Containing Polysaccharides. *ChemBioChem* **2009**, *10*, 1920−1938. (c) Imamura, A.; Lowary, T. Chemical Synthesis of Furanose Glycosides. *Trends Glycosci.* **2011**, *23*, 134−152. (d) Tefsen, B.; van Die, I. Glycosyltransferases in Chemo-enzymatic Synthesis of Oligosaccharides. In *Glycosyltransferases: Methods and Protocols*; Brockhausen, I., Ed.; Humana Press, 2013; pp 357−367. (e) Gallo-Rodriguez, C.; Kashiwagi, G. A. Selective Glycosylations with Furanosides. *Selective Glycosylations: Synthetic Methods and Catalysts*; Wiley, 2017; pp 297−326.
(16) (a) Houseknecht, J. B.; Lowary, T. L. Chemistry and biology of arabinofuranosyl- and galactofuranosyl-containing polysaccharides. *Curr. Opin. Chem. Biol.* **2001**, *5*, 677−682. (b) Zhu, S.-Y.; Yang, J.-S. Synthesis of tetra- and hexasaccharide fragments corresponding to the *O*-antigenic polysaccharide of Klebsiella pneumoniae. *Tetrahedron* **2012**, *68*, 3795−3802.
(17) (a) Christina, A. E.; van den Bos, L. J.; Overkleeft, H. S.; van der Marel, G. A.; Codée, J. D. C. Galacturonic Acid Lactones in the Synthesis of All Trisaccharide Repeating Units of the Zwitterionic Polysaccharide Sp1. *J. Org. Chem.* **2011**, *76*, 1692−1706. (b) Imamura, A.; Lowary, T. Chemical Synthesis of Furanose Glycosides. *Trends Glycosci. Glycotechnol.* **2011**, *23*, 134−152. (c) Nigudkar, S. S.; Demchenko, A. V. Stereocontrolled 1,2-*cis* glycosylation as the driving force of progress in synthetic carbohydrate chemistry. *Chem. Sci.*

https://doi.org/10.1021/acscatal.3c05237
ACS Catal. 2024, 14, 1037−1049

2015, *6*, 2687−2704. (d) Mensink, R. A.; Boltje, T. J. Advances in Stereoselective 1,2-*cis* Glycosylation using C-2 Auxiliaries. *Chem.—Eur. J.* **2017**, *23*, 17637−17653.
(18) (a) Satoh, H.; Manabe, S. Design of chemical glycosyl donors: does changing ring conformation influence selectivity/reactivity? *Chem. Soc. Rev.* **2013**, *42*, 4297−4309. (b) Taha, H. A.; Richards, M. R.; Lowary, T. L. Conformational Analysis of Furanoside-Containing Mono- and Oligosaccharides. *Chem. Rev.* **2013**, *113*, 1851−1876. (c) van der Vorm, S.; Hansen, T.; van Rijssel, E. R.; Dekkers, R.; Madern, J. M.; Overkleeft, H. S.; Filippov, D. V.; van der Marel, G. A.; Codée, J. D. C. Furanosyl Oxocarbenium Ion Conformational Energy Landscape Maps as a Tool to Study the Glycosylation Stereoselectivity of 2-Azidofuranoses, 2-Fluorofuranoses and Methyl Furanosyl Uronates. *Chem.—Eur. J.* **2019**, *25*, 7149−7157.
(19) (a) Bols, M.; Hansen, H. C. Long Range Intramolecular Glycosidation. *Chem. Lett.* **1994**, *23*, 1049−1052. (b) Krog-Jensen, C.; Oscarson, S. Stereospecific Synthesis of β-d-Fructofuranosides Using the Internal Aglycon Delivery Approach. *J. Org. Chem.* **1996**, *61*, 4512−4513. (c) Désiré, J.; Prandi, J. Synthesis of methyl β-d-arabinofuranoside 5-[1d (and l)-myo-inositol 1-phosphate], the capping motif of the lipoarabinomannan of Mycobacteriumsmegmatis. *Carbohydr. Res.* **1999**, *317*, 110−118. (d) Bamhaoud, T.; Sanchez, S.; Prandi, J. 1,2,5-ortho esters of d-arabinose as versatile arabinofuranosidic building blocks. Concise synthesis of the tetrasaccharidic cap of the lipoarabinomannan of Mycobacterium tuberculosis. *Chem. Commun.* **2000**, 659−660. (e) Fairbanks, A. J. Intramolecular Aglycon Delivery (IAD): The Solution to 1,2-*cis* Stereocontrol for Oligosaccharide Synthesis? *Synlett* **2003**, *2003*, 1945−1958. (f) Cumpstey, I. Intramolecular aglycon delivery. *Carbohydr. Res.* **2008**, *343*, 1553−1573. (g) Ishiwata, A.; Munemura, Y.; Ito, Y. NAP Ether Mediated Intramolecular Aglycon Delivery: A Unified Strategy for 1,2-*cis*-Glycosylation. *Eur. J. Org Chem.* **2008**, *2008*, 4250−4263.
(20) (a) Zhu, X.; Kawatkar, S.; Rao, Y.; Boons, G.-J. Practical Approach for the Stereoselective Introduction of β-Arabinofuranosides. *J. Am. Chem. Soc.* **2006**, *128*, 11948−11957. (b) Crich, D.; Pedersen, C. M.; Bowers, A. A.; Wink, D. J. On the Use of 3,5-*O*-Benzylidene and 3,5-*O*-(Di-tert-butylsilylene)-2-*O*-benzylarabinothiofuranosides and Their Sulfoxides as Glycosyl Donors for the Synthesis of β-Arabinofuranosides: Importance of the Activation Method. *J. Org. Chem.* **2007**, *72*, 1553−1565. (c) Wang, Y.; Maguire-Boyle, S.; Dere, R. T.; Zhu, X. Synthesis of β-d-arabinofuranosides: stereochemical differentiation between d- and l-enantiomers. *Carbohydr. Res.* **2008**, *343*, 3100−3106. (d) Imamura, A.; Lowary, T. L. β-Selective Arabinofuranosylation Using a 2,3-*O*-Xylylene-Protected Donor. *Org. Lett.* **2010**, *12*, 3686−3689. (e) Tilve, M. J.; Gallo-Rodriguez, C. Glycosylation studies on conformationally restricted 3,5-*O*-(di-tert-butylsilylene)-D-galactofuranosyl trichloroacetimidate donors for 1,2-*cis* α-D-galactofuranosylation. *Carbohydr. Res.* **2011**, *346*, 2838−2848. (f) Lavinda, O.; Tran, V. T.; Woerpel, K. A. Effect of conformational rigidity on the stereoselectivity of nucleophilic additions to five-membered ring bicyclic oxocarbenium ion intermediates. *Org. Biomol. Chem.* **2014**, *12*, 7083−7091. (g) Zhang, L.; Shen, K.; Taha, H. A.; Lowary, T. L. Stereocontrolled Synthesis of α-Xylofuranosides Using a Conformationally Restricted Donor. *J. Org. Chem.* **2018**, *83*, 7659−7671.
(21) (a) Yasomanee, J. P.; Demchenko, A. V. Effect of Remote Picolinyl and Picoloyl Substituents on the Stereoselectivity of Chemical Glycosylation. *J. Am. Chem. Soc.* **2012**, *134*, 20097−20102. (b) Liu, Q.-W.; Bin, H.-C.; Yang, J.-S. β-Arabinofuranosylation Using 5-*O*-(2-Quinolinecarbonyl) Substituted Ethyl Thioglycoside Donors. *Org. Lett.* **2013**, *15*, 3974−3977.
(22) Mayfield, A. B.; Metternich, J. B.; Trotta, A. H.; Jacobsen, E. N. Stereospecific Furanosylations Catalyzed by Bis-thiourea Hydrogen-Bond Donors. *J. Am. Chem. Soc.* **2020**, *142*, 4061−4069.
(23) Xu, H.; Schaugaard, R. N.; Li, J.; Schlegel, H. B.; Nguyen, H. M. Stereoselective 1,2-*cis* Furanosylations Catalyzed by Phenanthroline. *J. Am. Chem. Soc.* **2022**, *144*, 7441−7456.
(24) Ma, X.; Zhang, Y.; Zhu, X.; Zhang, L. An *SN2*-Type Strategy toward 1,2-*cis*-Furanosides. *CCS Chem.* **2022**, *4*, 3677−3685.
(25) (a) Chinthapally, K.; Massaro, N. P.; Sharma, I. Rhodium Carbenoid Initiated O−H Insertion/Aldol/Oxy-Cope Cascade for the Stereoselective Synthesis of Functionalized Oxacycles. *Org. Lett.* **2016**, *18*, 6340−6343. (b) Hunter, A. C.; Chinthapally, K.; Sharma, I. $Rh_2(esp)_2$: An Efficient Catalyst for O−H Insertion Reactions of Carboxylic Acids into Acceptor/Acceptor Diazo Compounds. *Eur. J. Org Chem.* **2016**, *2016*, 2260−2263. (c) Hunter, A. C.; Schlitzer, S. C.; Sharma, I. Synergistic Diazo-OH Insertion/Conia-Ene Cascade Catalysis for the Stereoselective Synthesis of γ-Butyrolactones and Tetrahydrofurans. *Chem.—Eur. J.* **2016**, *22*, 16062−16065. (d) Chinthapally, K.; Massaro, N. P.; Padgett, H. L.; Sharma, I. A serendipitous cascade of rhodium vinylcarbenoids with aminochalcones for the synthesis of functionalized quinolines. *Chem. Commun.* **2017**, *53*, 12205−12208. (e) Hunter, A. C.; Almutwalli, B.; Bain, A. I.; Sharma, I. Trapping rhodium carbenoids with aminoalkynes for the synthesis of diverse *N*-heterocycles. *Tetrahedron* **2018**, *74*, 5451−5457. (f) Massaro, N. P.; Stevens, J. C.; Chatterji, A.; Sharma, I. Stereoselective Synthesis of Diverse Lactones through a Cascade Reaction of Rhodium Carbenoids with Ketoacids. *Org. Lett.* **2018**, *20*, 7585−7589. (g) Chinthapally, K.; Massaro, N. P.; Ton, S.; Gardner, E. D.; Sharma, I. Trapping rhodium vinylcarbenoids with aminochalcones for the synthesis of medium-sized azacycles. *Tetrahedron Lett.* **2019**, *60*, 151253. (h) Hunter, A. C.; Chinthapally, K.; Bain, A. I.; Stevens, J. C.; Sharma, I. Rhodium/Gold Dual Catalysis in Carbene sp2 C−H Functionalization/Conia-ene Cascade for the Stereoselective Synthesis of Diverse Spirocarbocycles. *Adv. Synth. Catal.* **2019**, *361*, 2951−2958. (i) Paymode, D. J.; Sharma, I. Rhodium-Catalyzed [3 + 2]-Annulation of ortho-Diazoquinones with Enol Ethers: Diversity-Oriented Total Synthesis of Aflatoxin B2. *Eur. J. Org Chem.* **2021**, *2021*, 2034−2040. (j) Bain, A. I.; Chinthapally, K.; Hunter, A. C.; Sharma, I. Dual Catalysis in Rhodium(II) Carbenoid Chemistry. *Eur. J. Org Chem.* **2022**, *2022*, No. e202101419.
(26) (a) Tschan, M. J.-L.; Thomas, C. M.; Strub, H.; Carpentier, J. F. Copper(II) Triflate as a Source of Triflic Acid: Effective, Green Catalysis of Hydroalkoxylation Reactions. *Adv. Synth. Catal.* **2009**, *351*, 2496−2504. (b) Sletten, E. T.; Tu, Y.-J.; Schlegel, H. B.; Nguyen, H. M. Are Brønsted Acids the True Promoter of Metal-Triflate-Catalyzed Glycosylations? A Mechanistic Probe into 1,2-*cis*-Aminoglycoside Formation by Nickel Triflate. *ACS Catal.* **2019**, *9*, 2110−2123. (c) Massi, L.; Gal, J.-F.; Duñach, E. Metal Triflates as Catalysts in Organic Synthesis: Determination of Their Lewis Acidity by Mass Spectrometry. *ChemPlusChem* **2022**, *87*, No. e202200037. (d) Sharma, I.; Wurst, J.; Tan, D. S. Solvent-Dependent Divergent Functions of $Sc(OTf)_3$ in Stereoselective Epoxide-Opening Spiroketalizations. *Org. Lett.* **2014**, *16*, 2474−2477.
(27) (a) Varki, A. Biological roles of oligosaccharides: all of the theories are correct. *Glycobiology* **1993**, *3*, 97−130. (b) Dwek, R. A. Glycobiology: Toward Understanding the Function of Sugars. *Chem. Rev.* **1996**, *96*, 683−720. (c) *Essentials of Glycobiology*; Varki, A., Cummings, R. D., Esko, J. D., Stanley, P., Hart, G. W., Aebi, M., Darvill, A. G., Kinoshita, T., Packer, N. H., Prestegard, J. H., Schnaar, R. L., Seeberger, P. H., Eds., Copyright All rights reserved. 2015−2017 by The Consortium of Glycobiology Eds., La Jolla, California; Cold Spring Harbor Laboratory Press, 2015.
(28) (a) Yang, W.; Sun, J.; Lu, W.; Li, Y.; Shan, L.; Han, W.; Zhang, W.-D.; Yu, B. Synthesis of Kaempferol 3-*O*-(3″,6″-Di-*O*-*E*-*p*-coumaroyl)-β-D-glucopyranoside, Efficient Glycosylation of Flavonol 3-OH with Glycosyl *O*-Alkynylbenzoates as Donors. *J. Org. Chem.* **2010**, *75*, 6879−6888. (b) Liu, R.; Hua, Q.; Lou, Q.; Wang, J.; Li, X.; Ma, Z.; Yang, Y. NIS/TMSOTf-Promoted Glycosidation of Glycosyl ortho-Hexynylbenzoates for Versatile Synthesis of *O*-Glycosides and Nucleosides. *J. Org. Chem.* **2021**, *86*, 4763−4778.
(29) Vidadala, S. R.; Gayatri, G.; Sastry, G. N.; Hotha, S. Propargyl/methyl furanosides as potential glycosyl donors. *Chem. Commun.* **2011**, *47*, 9906−9908.

https://doi.org/10.1021/acscatal.3c05237
ACS Catal. 2024, 14, 1037−1049

(30) Chang, G. X.; Lowary, T. L. A Glycosylation Protocol Based on Activation of Glycosyl 2-Pyridyl Sulfones with Samarium Triflate. *Org. Lett.* **2000**, *2*, 1505−1508.
(31) (a) Bellow, J. A.; Yousif, M.; Fang, D.; Kratz, E. G.; Cisneros, G. A.; Groysman, S. Synthesis and Reactions of 3d Metal Complexes with the Bulky Alkoxide Ligand [OC^{t}Bu$_2$Ph]. *Inorg. Chem.* **2015**, *54*, 5624−5633. (b) Cantalupo, S. A.; Lum, J. S.; Buzzeo, M. C.; Moore, C.; DiPasquale, A. G.; Rheingold, A. L.; Doerrer, L. H. Three-coordinate late transition metal fluorinated alkoxide complexes. *Dalton Trans.* **2010**, *39*, 374−383.
(32) DFT calculations used the PBE0 functional; see the Supporting Information p. S18 for more details.
(33) (a) Yu, H.-Z.; Jiang, Y.-Y.; Fu, Y.; Liu, L. Alternative mechanistic explanation for ligand-dependent selectivities in copper-catalyzed *N*-and *O*-arylation reactions. *J. Am. Chem. Soc.* **2010**, *132*, 18078−18091. (b) Fier, P. S.; Hartwig, J. F. Copper-mediated fluorination of aryl iodides. *J. Am. Chem. Soc.* **2012**, *134*, 10795−10798. (c) Jones, G. O.; Liu, P.; Houk, K.; Buchwald, S. L. Computational explorations of mechanisms and ligand-directed selectivities of copper-catalyzed Ullmann-type reactions. *J. Am. Chem. Soc.* **2010**, *132*, 6205−6213. (d) Huffman, L. M.; Stahl, S. S. Mechanistic analysis of trans C−N reductive elimination from a square-planar macrocyclic aryl-copper (iii) complex. *Dalton Trans.* **2011**, *40*, 8959−8963.
(34) (a) Paeth, M.; Tyndall, S. B.; Chen, L.-Y.; Hong, J.-C.; Carson, W. P.; Liu, X.; Sun, X.; Liu, J.; Yang, K.; Hale, E. M.; et al. Csp3−Csp3 bond-forming reductive elimination from well-defined copper (III) complexes. *J. Am. Chem. Soc.* **2019**, *141*, 3153−3159. (b) Casitas, A.; Ribas, X. The role of organometallic copper(III) complexes in homogeneous catalysis. *Chem. Sci.* **2013**, *4*, 2301−2318. (c) Aziz, J.; Frison, G.; Gomez, M.; Brion, J.-D.; Hamze, A.; Alami, M. Copper-catalyzed coupling of N-tosylhydrazones with amines: synthesis of fluorene derivatives. *ACS Catal.* **2014**, *4*, 4498−4503.
(35) (a) van Rijssel, E. R.; van Delft, P.; Lodder, G.; Overkleeft, H. S.; van der Marel, G. A.; Filippov, D. V.; Codée, J. D. C. Furanosyl oxocarbenium ion stability and stereoselectivity. *Angew. Chem., Int. Ed.* **2014**, *53*, 10381−10385. (b) van der Vorm, S.; Hansen, T.; van Rijssel, E. R.; Dekkers, R.; Madern, J. M.; Overkleeft, H. S.; Filippov, D. V.; van der Marel, G. A.; Codée, J. D. C. Furanosyl Oxocarbenium Ion Conformational Energy Landscape Maps as a Tool to Study the Glycosylation Stereoselectivity of 2-Azidofuranoses, 2-Fluorofuranoses and Methyl Furanosyl Uronates. *Chem.—Eur. J.* **2019**, *25*, 7149−7157.

https://doi.org/10.1021/acscatal.3c05237
ACS Catal. 2024, 14, 1037−1049

ACS Catalysis

pubs.acs.org/acscatalysis Research Article

Iron-Carbene Initiated O−H Insertion/Aldol Cascade for the Stereoselective Synthesis of Functionalized Tetrahydrofurans

Prakash Kafle, Bidhan Ghosh,‡ Arianne C. Hunter,‡ Rishav Mukherjee,‡ Kenneth M. Nicholas, and Indrajeet Sharma*

Cite This: ACS Catal. 2024, 14, 1292−1299 Read Online

ACCESS | Metrics & More | Article Recommendations | Supporting Information

ABSTRACT: Given its earth abundance, cost-effectiveness, and ecofriendly qualities, iron serves as a promising alternative to precious metals in catalysis. This article presents an iron carbene-initiated cascade approach for synthesizing highly substituted tetrahydrofurans at the gram scale. This cascade reaction utilizes readily accessible β-hydroxyketones and diazo compounds and works with iron catalyst loading as low as 5 mol %. This reaction proceeds through an O−H insertion into diazo-derived iron carbenes, followed by an intramolecular aldol reaction to access functionalized tetrahydrofurans in high yields and diastereoselectivity. The versatile nature of this domino sequence accommodates diverse β-hydroxyketones and diazo compounds, streamlining access to synthetically challenging spiroethers. Furthermore, this cascade process offers a route to enantiopure tetrahydrofurans by utilizing a diazo ester bearing a chiral auxiliary, 8-phenylmenthol. Postmodifications of the tetrahydrofuran product provide access to various analogues, including a medicinally relevant oxetane motif. Density functional theory (DFT) calculations substantiate a stereospecific mechanism wherein the intramolecular aldol reaction proceeds via a fused six- and five-membered iron−oxygen transition-state complex, yielding the contrathermodynamic *cis*-aldol product.

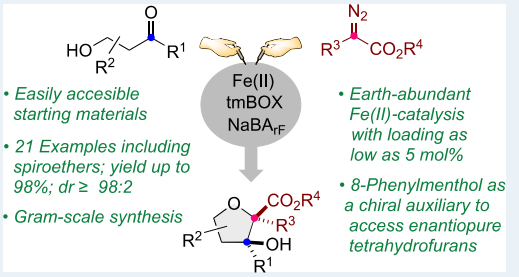

KEYWORDS: *iron catalysis, cascade reactions, diazo compounds, tetrahydrofurans, chiral auxiliary*

Metal catalysts play a pivotal role in synthetic chemistry. Iron (Fe) stands out as the second most abundant metal in the Earth's crust, following only aluminum, with a composition of approximately 4.7% by weight.[1] This abundance, combined with iron's low cost and relative nontoxic nature, positions it as the catalyst of choice for various chemical transformations.[2] Incorporating iron catalysts into synthetic processes can reduce the cost of producing pharmaceuticals, fertilizers, and other essential products, as the expense of reagents directly influences compound cost. Furthermore, iron boasts a commendable safety profile endorsed by regulatory authorities. It is considered "a metal with a minimal safety concern", as 1300 ppm residual iron is deemed acceptable in drug substances. This status represents a distinct advantage compared to the ≤10 ppm prescribed for most other transition metals, including rhodium.[1b] These characteristics elevate iron as a sustainable catalyst for chemical synthesis, presenting economic benefits and enhanced safety features.[2,3] Another crucial factor contributing to cost-effective chemical synthesis involves adopting cascade reactions, which have garnered substantial research interest in recent years.[4] These reactions offer remarkable advantages, encompassing atom economy, a substantial saving in time, labor, resources, and waste management.[5] Cascade reactions introduce notable efficiencies by consolidating multiple transformations within a singular synthetic process. For example, a product traditionally requiring several sequential steps can now be obtained through a singular reaction solvent, workup procedure, and purification phase. In this context, our research group[6] and numerous others have pioneered cascade reactions utilizing diazo-derived rhodium carbenes.[7]

Rhodium is one of the most utilized metals in diazo chemistry.[8] However, due to its high cost and limited availability, we have shifted our focus toward developing cascade reactions utilizing environmentally sustainable, earth-abundant metal catalysts, including iron, copper, and zinc.[9] Despite the decades-long recognition of iron carbene complexes, the utilization of iron in carbene cascade reactions has remained unexplored, likely due to the challenge of identifying an iron catalyst complex that effectively stabilizes the necessary zwitterionic intermediate required to trigger a cascade reaction.[10] To the best of our knowledge, there is no report of a cascade reaction involving diazo-derived iron carbenes. However, multiple research groups have reported N−H, O−H, S−H, and Si−H bond insertion reactions,[11]

Received: October 21, 2023
Revised: December 22, 2023
Accepted: December 26, 2023
Published: January 10, 2024

https://doi.org/10.1021/acscatal.3c05040
ACS Catal. 2024, 14, 1292−1299

cyclopropanations,[12] and C−H functionalization reactions of iron carbenes.[13] We conceived of employing iron as a catalyst within the established carbene-initiated O−H-insertion/aldol cascade as a starting point. This methodology aims to enable access to functionalized tetrahydrofurans, commonly found in naturally occurring bioactive substances spanning diverse classes such as lignans, acetogenins, ionophores, and macrolides.[14] Notable examples include (+)-fragransin A2,[15] caloxylane,[16] and amphidinolide F[17] (Figure 1).

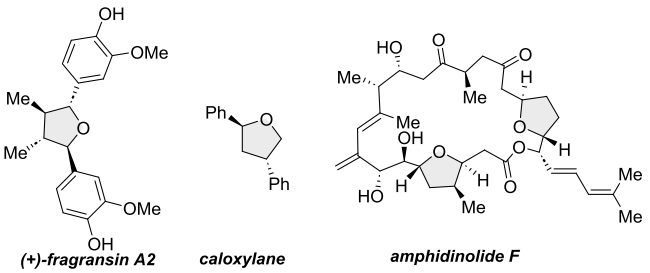

Figure 1. Naturally occurring tetrahydrofurans.

Multiple strategies have been developed to attain the stereoselective synthesis of tetrahydrofurans.[18] Despite significant progress in synthetic methodologies, synthesizing substituted tetrahydrofurans remains formidable, underscoring the need to explore innovative approaches. The Moody and the Hu group reported rhodium(II)-catalyzed reactions of diazocarbonyl compounds with β-hydroxyketones to access highly substituted tetrahydrofurans (Figure 2a).[19] Our group

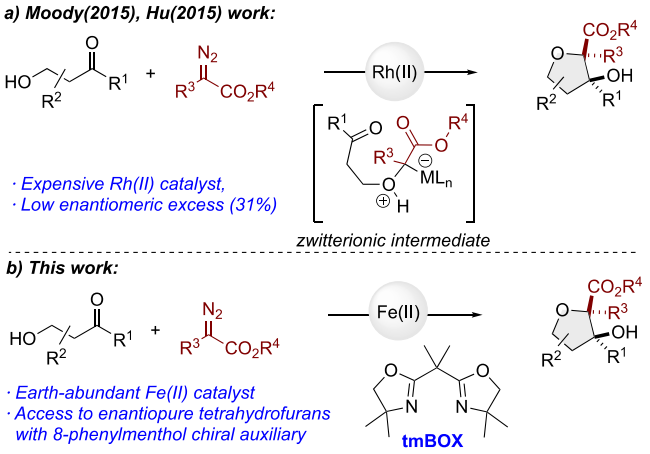

Figure 2. (a) Previously known rhodium-catalyzed approaches. (b) This work: iron catalyzed carbene cascade.

developed a cascade reaction involving O−H insertion/aldol/oxy-Cope sequence to access medium-sized rings.[6b] Taking inspiration from these studies, we introduce an inexpensive iron catalyst in diazocarbene chemistry to synthesize highly substituted tetrahydrofurans (Figure 2b).

Taking inspiration from the Zhou group,[11a] we envisioned that BOX ligand would coordinate and stabilize the Fe(II) catalyst. At the same time, sodium tetrakis(3,5-bis-(trifluoromethyl)phenyl)borate ($NaBAr_F$) would initiate a counterion exchange to create a highly Lewis acidic Fe(II) complex that would effectively decompose the diazo. Therefore, we initiated our optimization studies for the iron-catalyzed cascade reaction with readily available starting materials keto-alcohol **1a**, and diazo **2a** as model substrates to access the desired tetrahydrofurans (Table 1).

Table 1. Optimization of the Reaction Conditions[a]

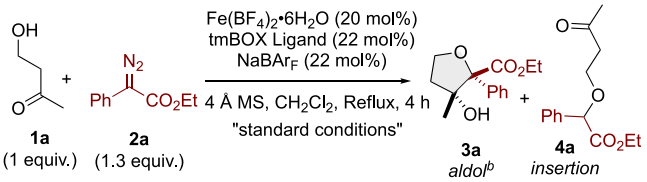

entry	variation from "standard conditions"	% yield[c]	3a/4a[d]
1	none	95%	8:1
2[e]	low catalyst loading (5 mol %)	83%	8:1
3	no 4 Å MS	70%	6:1
4	$FeCl_3$ instead of $Fe(BF_4)_2•6H_2O$	50%	3:1
5	$FeCl_2$ instead of $Fe(BF_4)_2•6H_2O$	n.r.	n.d.
6	no $Fe(BF_4)_2•6H_2O$	n.r.	n.d.
7	no tmBOX	70%	1:1
8	no $NaBAr_F$	75%	1:3
9	44 mol % of $NaBAr_F$	80%	1:2.5
10	44 mol % of tmBOX	20%	1:1
11	$CHCl_3$ as solvent	70%	1:1
12	DCE as solvent	60%	4:1
13	no syringe pump addition	40%	1:1

[a]All reactions were performed by adding diazo compound **2a** (1.3 equiv, 0.15 M CH_2Cl_2) dropwise via syringe pump to a solution of keto-alcohol **1a** (1.0 equiv), $Fe(BF_4)_2•6H_2O$ (20 mol %), $NaBAr_F$ (22 mol %), and tmBOX (22 mol %) in 0.2 M CH_2Cl_2. [b]Diastereomeric ratio (dr) of **3a** was determined by ^1H NMR (dr ≥ 98:2). [c]Yield was determined by ^1H NMR using 1,3,5-trimethoxybenzene as an internal standard. [d]Selectivity (**3a**/**4a**) was determined by ^1H NMR. [e]$Fe(BF_4)_2•6H_2O$ (5 mol %), $NaBAr_F$ (5.5 mol %), and tmBOX (5.5 mol %) was used. n.r. = no reaction; n.d. = not determined.

Following a thorough evaluation of various reaction conditions, we discovered that the optimal results, with a yield of 95% and an aldol/insertion ratio of 8:1, could be obtained by using $Fe(BF_4)_2•6H_2O$ (20 mol %), tetramethyl-bis(oxazoline) (tmBOX) (22 mol %) and $NaBAr_F$ (22 mol %) in methylene chloride with 4 Å molecular sieves. The reaction was carried out by adding a solution of diazo compound **2a** in methylene chloride to the reaction mixture under reflux conditions using a syringe pump for 1.5 h (entry 1). The ^1H NMR analysis confirmed the formation of a single diastereomer (dr ≥ 98:2) of the aldol product. Subsequently, we evaluated the reaction's effectiveness using a low (5 mol %) catalyst loading and were delighted to find a similar outcome as with 20 mol % loading (entry 2). It is noteworthy to mention that we use 20 mol % of iron catalyst in our standard conditions as it is more practical to weigh. Significantly, the absence of 4 Å molecular sieves reduced both the yield and the aldol/insertion ratio (entry 3). $FeCl_3$ also catalyzed the aldol reaction but resulted in low yield and selectivity (entry 4). Conversely, $FeCl_2$ was observed to be unreactive in this context (entry 5). Without $Fe(BF_4)_2•6H_2O$, no desired product was obtained (entry 6). Without the tmBox, the reaction provided a good yield but a lower aldol/insertion ratio for the desired product (entry 7). Likewise, in the absence of $NaBAr_F$, the reaction proceeded with a comparable yield but exhibited an increase in the insertion product (entry 8). Particularly, $NaBAr_F$ has been shown to enhance the Lewis

https://doi.org/10.1021/acscatal.3c05040
ACS Catal. 2024, 14, 1292−1299

acidity and electrophilicity of the iron catalyst by exchanging the counteranion with a bulky and noncoordinating BAr_F anion, resulting in improvements in reaction efficiencies[13b,20] and consequently improving the aldol/insertion ratio. However, augmenting the quantity of $NaBAr_F$ (2 equiv) results in the rapid decomposition of the diazo compound, leading to a faster reaction with an increased amount of the insertion product (entry 9). Additionally, increasing the loading of the tmBox ligand reduced iron's catalytic activity, thereby decreasing the yield, and a lower aldol/insertion ratio was observed (entry 10). Subsequently, our efforts were directed toward optimizing the solvent for this reaction. Chloroform and 1,2-dichloroethane (DCE) demonstrated solvent compatibility, although the yield and aldol/insertion ratio were reduced. Despite this, none of these solvents outperformed dichloromethane, leading to its selection for further investigations (entries 11, 12). We eventually discovered that the slow addition of the diazo compound using a syringe pump over 1.5 h is crucial in achieving the desired yield and a high aldol selectivity (entry 13).

After establishing the optimal conditions, we investigated the scope of α-aryl-α-diazocarbonyl compounds, also known as donor−acceptor diazos[21] (Table 2). At first, substituting the ester group of the diazo compound from ethyl to methyl ester resulted in the formation of the corresponding product **3b** with a comparable yield, and a similar aldol:insertion ratio (10:1) was obtained. Next, we focused on examining different electronic substituents in the aryl group. Notably, electron-donating groups such as methyl and methoxy at the para-position of the phenyl ring provided excellent yields of the desired products (**3c**, **3d**) with favorable aldol/insertion ratios. Similarly, the electron-donating thiophene diazo afforded the corresponding product **3e** in excellent yield with 1:1 aldol/insertion selectivity. Conversely, the electron-withdrawing nitro substituent afforded a lower yield (35%) of desired product **3f** with 4:1 aldol/insertion selectivity.

Moreover, when a halogen was substituted at the *para* position of the phenyl group, the transformation smoothly proceeded to afford the desired product with an outstanding yield (**3g**). Notably, the cyclic diazo compounds proceeded in high yield to provide the desired spiroethers (**3h**), which are challenging to obtain with high stereoselectivity. Diazo compounds derived from tetralone also provided the desired spiroethers in good yield (**3i**).

Next, we aimed to explore the range of substrates for different hydroxyketones (Table 3). We introduced various keto-substituted groups to evaluate their compatibility with diazo substrate **2**. Keto-alcohols **1**, containing substituents such as phenyl, *p*-Me-phenyl, and *p*-Br-phenyl, all underwent smooth reactions with diazo **2** and resulted in the formation of the desired products **3j−l**, with yields ranging from 50 to

Table 2. Scope of Diazo Compounds[a]

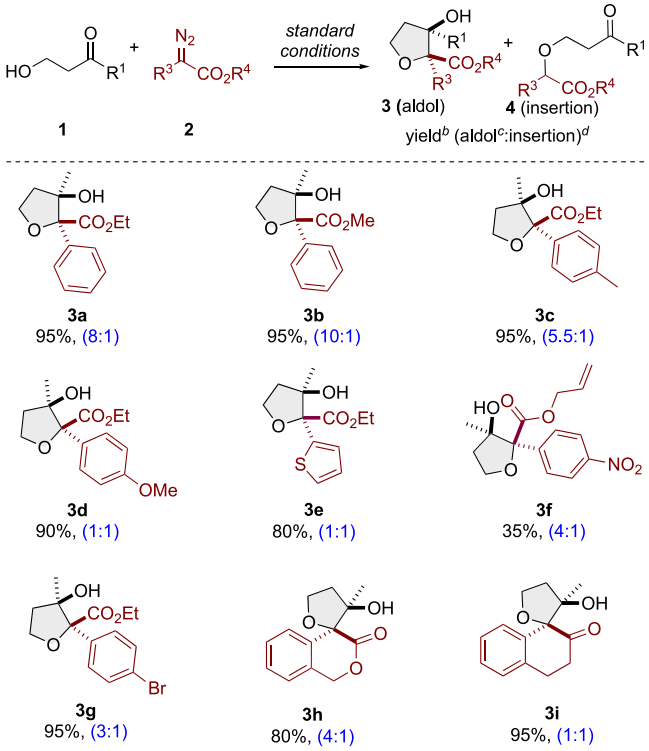

[a]All reactions were performed by adding diazo compound **2** (1.3 equiv, 0.15 M CH_2Cl_2) dropwise via a syringe pump to a solution of keto-alcohol **1** (1.0 equiv), $Fe(BF_4)_2{\bullet}6H_2O$ (20 mol %), $NaBAr_F$ (22 mol %), and tmBOX (22 mol %) in 0.2 M CH_2Cl_2. [b]Yield was determined by ^1H NMR using 1,3,5-trimethoxybenzene as an internal standard. [c]Diastereomeric ratio was determined by ^1H NMR (dr ≥ 98:2). [d]Selectivity was determined by ^1H NMR.

Table 3. Scope of β-Hydroxyketones[a]

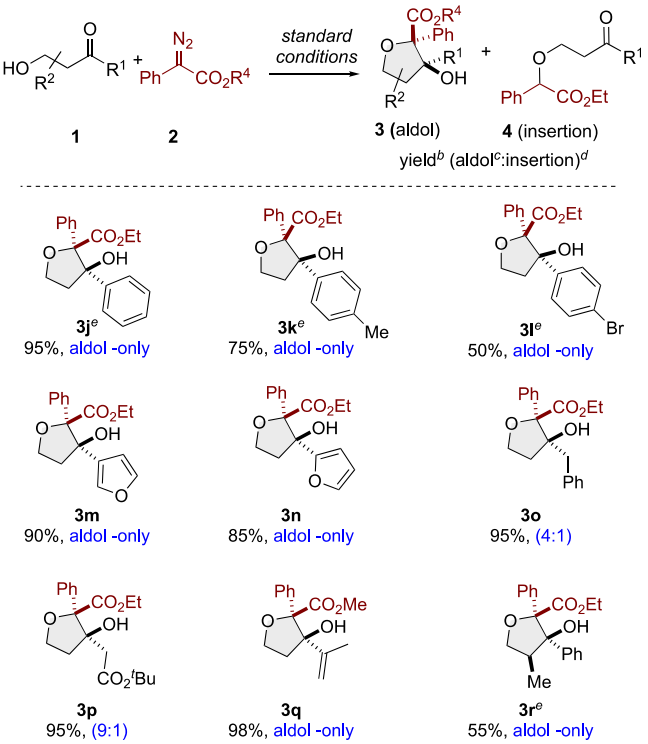

[a]All reactions were performed by adding diazo compound **2** (1.3 equiv, 0.15 M CH_2Cl_2) dropwise via syringe pump to a solution of keto-alcohol **1** (1.0 equiv), $Fe(BF_4)_2{\bullet}6H_2O$ (20 mol %), $NaBAr_F$ (22 mol %), and tmBOX (22 mol %) in 0.2 M CH_2Cl_2. [b]Yield was determined by ^1H NMR using 1,3,5-trimethoxybenzene as an internal standard. [c]Diastereomeric ratio was determined by ^1H NMR (dr ≥ 98:2). [d]Selectivity was determined by ^1H NMR. [e]Diazo compound **2** (1.3 equiv, 0.15 M CH_2Cl_2) dropwise via syringe pump to a solution of keto-alcohol **1** (1.0 equiv), $Fe(BF_4)_2{\bullet}6H_2O$ (30 mol %), $NaBAr_F$ (32 mol %), and tmBOX (32 mol %) in 0.2 M CH_2Cl_2.

https://doi.org/10.1021/acscatal.3c05040
ACS Catal. 2024, 14, 1292−1299

95%. Furthermore, 2- and 3-substituted furan containing hydroxyketones afforded the corresponding tetrahydrofurans with a high yield and exclusive aldol selectivity (**3m**−**n**). It is important to note that the presence of the α,β-unsaturated carbonyl functionality yielded only the aldol product exclusively in every case. Surprisingly, we did not observe any insertion products with these substrates. Ketones bearing acidic α-hydrogens were well tolerated and furnished the corresponding products (**3o**, **p**) with an excellent yield (95%) and a high aldol-selectivity. Pleasantly, substituted vinyl keto-alcohol displayed efficient reactivity, forming the corresponding product **3q** in an excellent yield of 98% and with exclusive formation of the aldol product. Encouragingly, a 2-methyl-substituted keto-alcohol yielded the related aldol product **3r** exclusively, albeit with a moderate yield (55%). Importantly, the methyl and the hydroxyl groups were found to be in the *cis* conformation. This is presumably due to steric interaction arising from the α-methyl and phenyl groups of the β-hydroxyketone in the 5-6-membered fused transition state (see SI page S15 for details).

The stereochemistry of the aldol product was unequivocally established by the single crystal X-ray analysis of compounds **3h** (CCDC 2285941) and **3q** (CCDC 2285940) (Figure 3).[22]

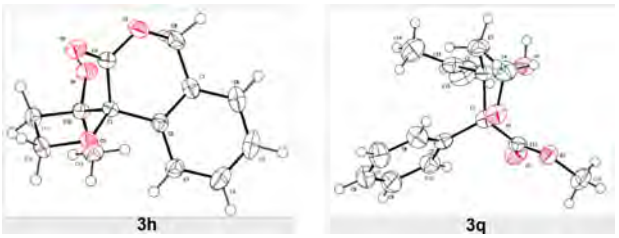

Figure 3. Single crystal X-ray structures of tetrahydrofuran **3h** and **3q**.

Significantly, the newly formed stereocenters in the aldol product have the hydroxyl and ester groups on the same side. This observation suggests a well-organized transition state during the formation of the aldol product.

Next, we focused on synthesizing enantiopure tetrahydrofurans by using chiral ligands on iron. Initially, we employed various chiral BOX-ligands (**L1**−**L3**) to induce enantiomeric excess (ee), as shown in Figure 4a. Although tetrahydrofuran **3a** was obtained in a good yield in all cases, no significant amount of ee was observed. To overcome this challenge, we devised a strategy involving an easily accessible chiral auxiliary that could be conveniently attached through the ester moiety of the diazo compound (Figure 4b).

Consequently, we synthesized esters containing chiral menthol-based auxiliaries **2s** and **2t**. The reaction of hydroxyketone **1a** with L-(−)-menthol diazo **2s** resulted in an aldol-insertion product **3s** with a 15:1 ratio in 84% yield. However, only a 2:1 diastereomeric excess (de) was observed. Significantly, when we employed the bulkier (−)-8-phenylmenthol as the chiral auxiliary, the desired diastereomeric excess was achieved in a 7:1 ratio (**3t**). To our delight, both diastereomers were easy to separate by silica gel flash column chromatography. As expected, the newly formed stereocenters in the major diastereomer had the hydroxyl and ester groups in syn fashion and had an opposite configuration to the alcohol stereocenter of 8-phenylmenthol (see the SI, page S18 for plausible transition states). The absolute stereochemistry of the predominant diastereomer **3t** was established by analyzing its

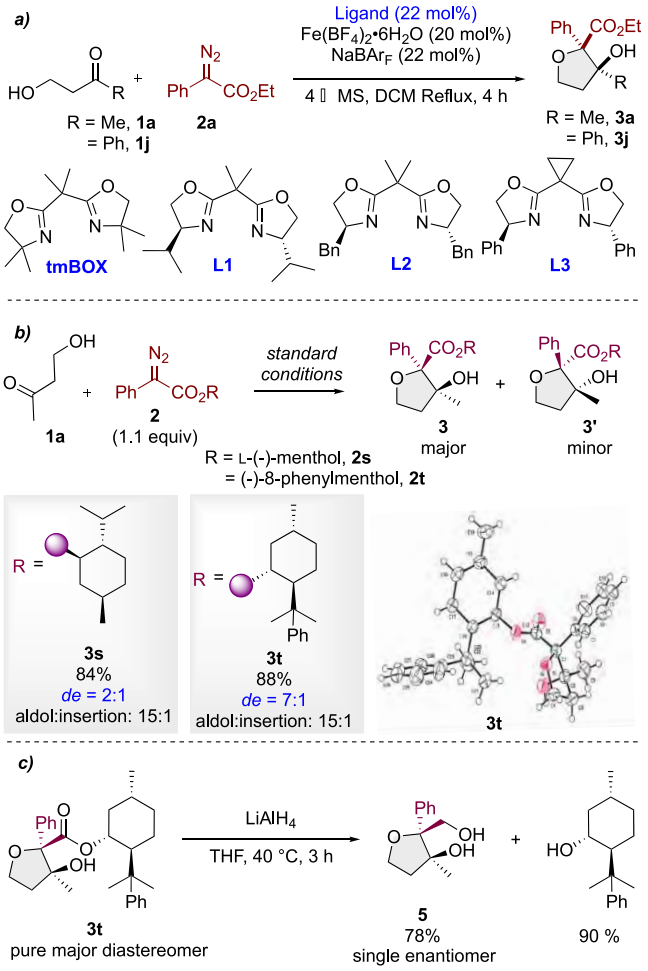

Figure 4. (a) Screening of chiral BOX-ligands. (b) Induction of diastereomeric excess (de) by a chiral auxiliary. (c) Recovery of chiral auxiliary.

crystal structure (CCDC 2285942).[22] Ultimately, the chiral auxiliary, 8-phenylmenthol, could be effectively recovered from the product through $LiAlH_4$ reduction, yielding a 90% recovery with the formation of the pure enantiomer of tetrahydrofuran **5** in 78% yield (Figure 4c).

To demonstrate the practical utility of this approach, the reaction was executed on a 4 mmol scale of β-hydroxyketone **1b**. The reaction involving diazo compound **2u** exhibited efficient progress with a notably lowered iron catalyst loading (5 mol %), affording an 80% yield (1.4 g) of the resulting **3u** compound, as illustrated in Scheme 1.

Additionally, the robustness of this method was demonstrated by successfully applying it to late-stage modifications. The ester moiety of the product was effectively converted to the corresponding alcohol **5u** through diisobutylaluminum hydride (DIBAL-H) reduction. Subsequently, compound **5u** underwent Sonogashira coupling with trimethylsilyl acetylene, forming alkyne **6** in 85% yield. A Sonogashira coupling of **5u** with phenylacetylene afforded alkyne **7** in 60% yield. Treatment of compound **7** with Mitsunobu reaction conditions furnished a dioxabicycloheptane compound **8** bearing an oxetane, which is an important motif in medicinal chemistry due to its physiochemical properties.[23] Additionally, it is important to note that the alkyne functionalities can be further

https://doi.org/10.1021/acscatal.3c05040
ACS Catal. 2024, 14, 1292−1299

Scheme 1. Gram-Scale Synthesis and Post-Modifications

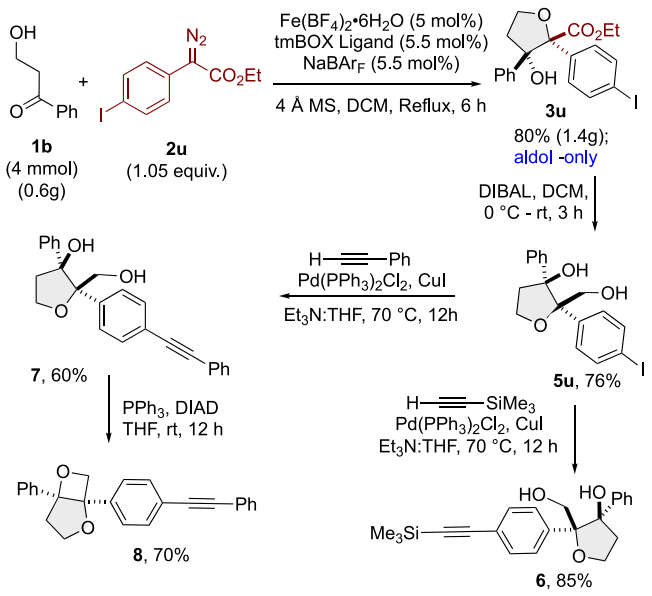

diversified using Click Chemistry to form triazoles found in various bioactive compounds and drug molecules.[24]

To gain further insights into the reaction mechanism, we synthesized the pure insertion product **4a**, following the literature-reported rhodium(II) catalyzed activation protocol, and subjected it to our optimized reaction conditions. However, the reaction did not proceed to yield the corresponding aldol product. DFT calculations also support this observation, as the insertion product **4a** is 8 kcal/mol more stable than the aldol product **3a** (Scheme 2). This experiment suggests the involvement of a metal species in the formation of an *O*-enolate intermediate, which is crucial for the subsequent progression of the aldol step.

Scheme 2. Control Experiment

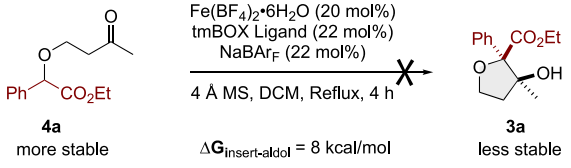

We also performed detailed density functional theory (DFT) calculations using B3LYP//6-31G(d)/LANL2DZ//vac[25] to elucidate the underlying mechanism, as shown in Figure 5.

To economize, the tmBOX ligand was replaced with an electronically similar Me_2-diimine ligand. A combination of $Fe(BF_4)_2$•$6H_2O$, Me_2-diimine, and keto alcohol is expected to produce iron carbene keto-alcohol complex **A** with extrusion of nitrogen. Intermediate **A** can engage in exergonic O−C bond formation with the bound keto alcohol to provide iron η^2-*C*-enolate **B** with the loss of the alcohol (O−H) proton. Alternatively, **B** can undergo exergonic *C*-protonation, leading to the *O*-insertion intermediate **D**. Substrate-assisted decomplexation of **D** provides the thermodynamically favored *O*-insertion product **H**. The η^2-*C*-enolate **B** is in equilibrium with the *O,O,O*-bound iron *O*-enolate **C**, favoring the latter by 7.5 kcal/mol. The *O*-enolate **C** can undergo aldol reaction via a chair-type transition state **E** (ΔG^* = 15.0 kcal/mol) to form the *cis*-iron aldol adduct **F**. Finally, proto-demetalation of **F**

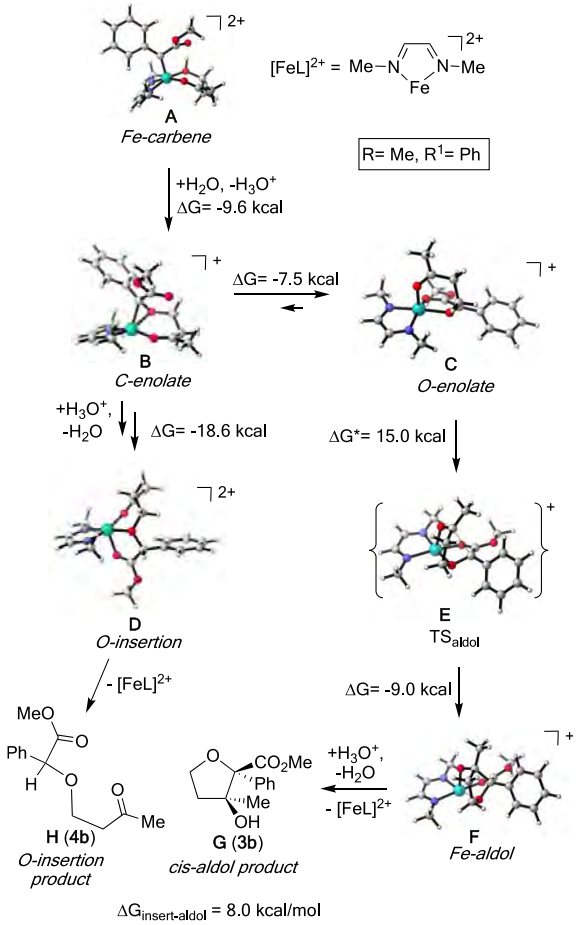

Figure 5. Computational study of the reaction mechanism (B3LYP/6-31G(d)/LANL2DZ/vac).

provides the *cis*-aldol product **G**. The iron *O,O,O*-coordination of **C**, **E**, and **F** strongly favors the experimentally observed *cis*-(OH, CO_2Et) aldol product **G**, despite being nearly isoenergetic with the *trans*-isomer (ΔG = 0.3 kcal/mol). The origin of the interesting R^1-carbonyl group effect on insertion/aldol chemoselectivity (Table 3) is not apparent from our calculations, but it could originate from a high barrier step in the proton transfer **B** to **D** insertion pathway.

Based on the literature precedent,[19a] experimental results, control experiments, and DFT studies, we propose a plausible mechanism for the iron-catalyzed O−H insertion/aldol cascade reaction, depicted in Figure 6.

The initial step involves chelating the tmBOX ligand with $Fe(BF_4)_2$•$6H_2O$ in the presence of $NaBAr_F$, forming iron-tmBOX complex **A**. Subsequently, hydroxyketone **1** coordinates with complex **A**, yielding iron-complex **B**. Next, diazoester **2** reacts with iron-complex **B**, leading to the creation of the iron-carbene intermediate **C**. Following this, insertion of an O−H transpires, generating the zwitterionic intermediate **D**, which may exist in equilibrium with an enol form **E**. Subsequently, intermediate **E** undergoes an intramolecular aldol reaction via a fused five-six-membered chair-type transition state, generating intermediate **F**. This intermediate then experiences protodemetalation, ultimately giving rise to observed tetrahydrofuran product **3** in a *cis*-diastereoselective fashion. It is essential to highlight that intermediate **D** also has the potential to undergo a [1,2]-*H* shift, resulting in the formation of the O−H insertion product **4**. This mechanism is

https://doi.org/10.1021/acscatal.3c05040
ACS Catal. 2024, 14, 1292−1299

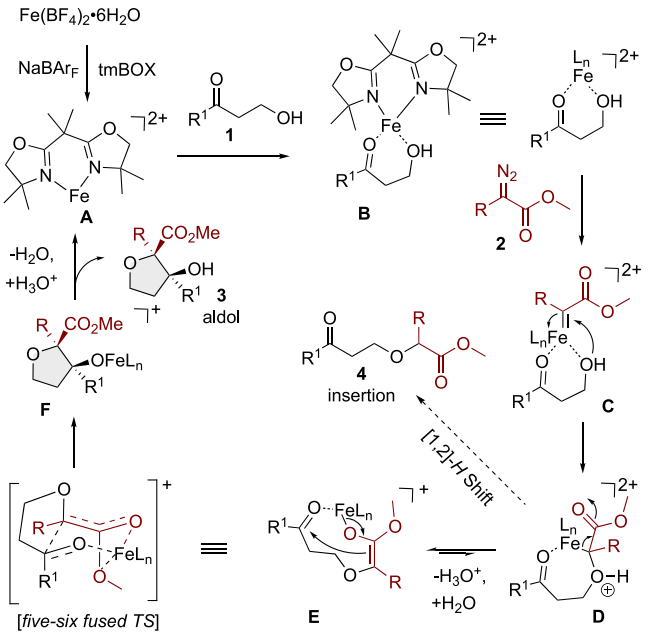

Figure 6. Plausible mechanism.

consistent with the DFT calculations and experimental findings that chiral BOX-ligands in the more stable *O*-enolate form (**E**), are not able to induce enatioinduction in the aldol step due to being far away from the reactive center, as described in the literature.[19a]

In conclusion, we devised a strategy to achieve stereoselective synthesis of highly substituted tetrahydrofurans using an O−H insertion/aldol cascade reaction. This method employs an Earth-abundant iron(II) catalyst and demonstrates tolerance toward a broad range of β-hydroxyketones and diazo compounds. The attainment of enantioselectivity in the reaction is attributed to the utilization of 8-phenylmenthol as a chiral auxiliary. The observed high stereoselectivities in the formation of tetrahydrofurans can be rationalized by proposing a mechanistic pathway supported by DFT calculations involving a fused five-six-membered transition state for the intramolecular aldol reaction. The pragmatic utility of our method has been sustained through a gram-scale synthesis of functionalized tetrahydrofurans, followed by subsequent post-modifications, including the creation of the medicinally relevant oxetane motif. Moreover, understanding iron's role as a catalyst in carbene cascade reactions will undoubtedly pave the way for novel synthetic transformations.

■ ASSOCIATED CONTENT

Supporting Information

The Supporting Information is available free of charge at https://pubs.acs.org/doi/10.1021/acscatal.3c05040.

Experimental procedures, NMR spectroscopy, and analytical data for all compounds (PDF)

Crystal coordinates information (XYZ)

■ AUTHOR INFORMATION

Corresponding Author

Indrajeet Sharma − *Department of Chemistry and Biochemistry, University of Oklahoma, Norman, Oklahoma 73019-5251, United States;* orcid.org/0000-0002-0707-0621; Email: isharma@ou.edu

Authors

Prakash Kafle − *Department of Chemistry and Biochemistry, University of Oklahoma, Norman, Oklahoma 73019-5251, United States*

Bidhan Ghosh − *Department of Chemistry and Biochemistry, University of Oklahoma, Norman, Oklahoma 73019-5251, United States*

Arianne C. Hunter − *Department of Chemistry and Biochemistry, University of Oklahoma, Norman, Oklahoma 73019-5251, United States;* orcid.org/0000-0003-1873-9682

Rishav Mukherjee − *Department of Chemistry and Biochemistry, University of Oklahoma, Norman, Oklahoma 73019-5251, United States*

Kenneth M. Nicholas − *Department of Chemistry and Biochemistry, University of Oklahoma, Norman, Oklahoma 73019-5251, United States;* orcid.org/0000-0002-5180-1671

Complete contact information is available at: https://pubs.acs.org/10.1021/acscatal.3c05040

Author Contributions

‡B.G., A.C.H., and R.M. contributed equally to this work. The manuscript was written through the contributions of all authors. All authors have approved the final version of the manuscript.

Funding

National Science Foundation (NSF) CHE-1753187 and the Oklahoma Center for the Advancement of Science and Technology (OCAST) HR20-078.

Notes

The authors declare no competing financial interest.

■ ACKNOWLEDGMENTS

This work was supported by the NSF CHE-1753187 and the Oklahoma Center for the Advancement of Science and Technology (OCAST HR20-078). We thank Dr. Novruz Akhmedov, Dr. Steven Foster, and Dr. Douglas R. Powell from the Research Support Services, University of Oklahoma, for NMR, mass spectral, and X-ray crystallographic analysis, respectively. We want to thank Anae Bain and Ginny Kim for their helpful discussions. We also acknowledge support from the OU Supercomputing Center for Education & Research (OSCER).

■ REFERENCES

(1) (a) Bolm, C. A new iron age. *Nat. Chem.* **2009**, *1*, 420−420. (b) Bauer, E. B. Iron Catalysis: Historic Overview and Current Trends. In *Iron Catalysis II*, Bauer, E., Ed.; Springer International Publishing, 2015; pp. 1−18.

(2) Enthaler, S.; Junge, K.; Beller, M. Sustainable Metal Catalysis with Iron: From Rust to a Rising Star? *Angew. Chem., Int. Ed.* **2008**, *47*, 3317−3321.

(3) (a) Bolm, C.; Legros, J.; Le Paih, J.; Zani, L. Iron-Catalyzed Reactions in Organic Synthesis. *Chem. Rev.* **2004**, *104*, 6217−6254. (b) Front Matter. In *Iron Catalysis in Organic Chemistry*, 2008; pp I−XV. (c) Sherry, B. D.; Fürstner, A. The Promise and Challenge of Iron-Catalyzed Cross Coupling. *Acc. Chem. Res.* **2008**, *41*, 1500−1511. (d) Carreras, V.; Tanbouza, N.; Ollevier, T. The power of iron catalysis in diazo chemistry. *Synthesis* **2021**, *53*, 79−94.

(4) (a) Muthusamy, S.; Krishnamurthi, J. Heterocycles by Cycloadditions of Carbonyl Ylides Generated from Diazo Ketones. In *Synthesis of Heterocycles via Cycloadditions I*; Hassner, A., Ed.;

Springer: Berlin Heidelberg, 2008; pp 147−192. (b) Nicolaou, K. C.; Chen, J. S. The art of total synthesis through cascade reactions. *Chem. Soc. Rev.* **2009**, *38*, 2993−3009. (c) Padwa, A. A Chemistry Cascade: From Physical Organic Studies of Alkoxy Radicals to Alkaloid Synthesis. *J. Org. Chem.* **2009**, *74*, 6421−6441. (d) Vilotijevic, I.; Jamison, T. F. Epoxide-Opening Cascades in the Synthesis of Polycyclic Polyether Natural Products. *Angew. Chem., Int. Ed.* **2009**, *48*, 5250−5281. (e) Jones, A. C.; May, J. A.; Sarpong, R.; Stoltz, B. M. Toward a Symphony of Reactivity: Cascades Involving Catalysis and Sigmatropic Rearrangements. *Angew. Chem., Int. Ed.* **2014**, *53*, 2556−2591. (f) Ardkhean, R.; Caputo, D. F. J.; Morrow, S. M.; Shi, H.; Xiong, Y.; Anderson, E. A. Cascade polycyclizations in natural product synthesis. *Chem. Soc. Rev.* **2016**, *45*, 1557−1569.

(5) Nicolaou, K. C.; Edmonds, D. J.; Bulger, P. G. Cascade Reactions in Total Synthesis. *Angew. Chem., Int. Ed.* **2006**, *45*, 7134−7186.

(6) (a) Hunter, A. C.; Schlitzer, S. C.; Sharma, I. Synergistic Diazo-OH Insertion/Conia-Ene Cascade Catalysis for the Stereoselective Synthesis of γ-Butyrolactones and Tetrahydrofurans. *Chem.—Eur. J.* **2016**, *22*, 16062−16065. (b) Chinthapally, K.; Massaro, N. P.; Sharma, I. Rhodium Carbenoid Initiated O−H Insertion/Aldol/Oxy-Cope Cascade for the Stereoselective Synthesis of Functionalized Oxacycles. *Org. Lett.* **2016**, *18*, 6340−6343. (c) Massaro, N. P.; Stevens, J. C.; Chatterji, A.; Sharma, I. Stereoselective Synthesis of Diverse Lactones through a Cascade Reaction of Rhodium Carbenoids with Ketoacids. *Org. Lett.* **2018**, *20*, 7585−7589. (d) Hunter, A. C.; Chinthapally, K.; Bain, A. I.; Stevens, J. C.; Sharma, I. Rhodium/Gold Dual Catalysis in Carbene sp2 C−H Functionalization/Conia-ene Cascade for the Stereoselective Synthesis of Diverse Spirocarbocycles. *Adv. Synth. Catal.* **2019**, *361*, 2951−2958.

(7) (a) Soam, P.; Kamboj, P.; Tyagi, V. Rhodium-Catalyzed Cascade Reactions using Diazo Compounds as a Carbene Precursor to Construct Diverse Heterocycles. *Asian J. Org. Chem.* **2022**, *11*, No. e202100570. (b) England, D. B.; Eagan, J. M.; Merey, G.; Anac, O.; Padwa, A. The rhodium(II) carbenoid cyclization−cycloaddition cascade of α-diazo dihydroindolinones for the synthesis of novel azapolycyclic ring systems. *Tetrahedron* **2008**, *64*, 988−1001.

(8) (a) Padwa, A.; Austin, D. J. Ligand Effects on the Chemoselectivity of Transition Metal Catalyzed Reactions of α-Diazo Carbonyl Compounds. *Angew. Chem., Int. Ed.* **1994**, *33*, 1797−1815. (b) Masse, C. E.; Panek, J. S. Diastereoselective Reactions of chiral allyl and allenyl silanes with activated C: X. pi.-Bonds. *Chem. rev.* **1995**, *95*, 1293−1316. (c) Fleming, I.; Barbero, A.; Walter, D. Stereochemical control in organic synthesis using silicon-containing compounds. *Chem. Rev.* **1997**, *97*, 2063−2192. (d) Doyle, M. P.; Forbes, D. C. Recent Advances in Asymmetric Catalytic Metal Carbene Transformations. *Chem. Rev.* **1998**, *98*, 911−936. (e) Davies, H. M.; Nikolai, J. Catalytic and enantioselective allylic C−H activation with donor−acceptor-substituted carbenoids. *Org. Biomol. Chem.* **2005**, *3*, 4176−4187. (f) Moody, C. J. Enantioselective Insertion of Metal Carbenes into N-H Bonds: A Potentially Versatile Route to Chiral Amine Derivatives. *Angew. Chem., Int. Ed.* **2007**, *46*, 9148−9150. (g) Zhang, Z.; Wang, J. Recent studies on the reactions of α-diazocarbonyl compounds. *Tetrahedron* **2008**, *64*, 6577−6605. (h) Davies, H. M.; Denton, J. R. Application of donor/acceptor-carbenoids to the synthesis of natural products. *Chem. Soc. Rev.* **2009**, *38*, 3061−3071. (i) Doyle, M. P.; Duffy, R.; Ratnikov, M.; Zhou, L. Catalytic carbene insertion into C− H bonds. *Chem. Rev.* **2010**, *110*, 704−724. (j) Davies, H. M.; Morton, D. Guiding principles for site selective and stereoselective intermolecular C−H functionalization by donor/acceptor rhodium carbenes. *Chem. Soc. Rev.* **2011**, *40*, 1857−1869. (k) Zhu, S.-F.; Zhou, Q.-L. Transition-metal-catalyzed enantioselective heteroatom−hydrogen bond insertion reactions. *Acc. Chem. Res.* **2012**, *45*, 1365−1377. (l) Gillingham, D.; Fei, N. Catalytic X−H insertion reactions based on carbenoids. *Chem. Soc. Rev.* **2013**, *42*, 4918−4931. (m) Zheng, C.; You, S.-L. Recent development of direct asymmetric functionalization of inert C-H bonds. *RSC Adv.* **2014**, *4*, 6173−6214. (n) Ford, A.; Miel, H.; Ring, A.; Slattery, C. N.; Maguire, A. R.; McKervey, M. A. Modern organic synthesis with α-diazocarbonyl compounds. *Chem. Rev.* **2015**, *115*, 9981−10080. (o) Keipour, H.; Ollevier, T. Iron-Catalyzed Carbene Insertion Reactions of α-Diazoesters into Si−H Bonds. *Org. Lett.* **2017**, *19*, 5736−5739. (p) Boyarskikh, V.; Nyong, A.; Rainier, J. D. Highly diastereoselective sulfonium ylide rearrangements to quaternary substituted indolines. *Angew. Chem., Int. Ed.* **2008**, *47*, 5374−5377.

(9) Ou, C.; Ghosh, B.; Sharma, I. A Non-Diazo Approach to Functionalized (2-Furyl)-2-pyrrolidines through a Cascade Reaction of Enynal-Derived Zinc Carbenoids with β-Arylaminoketones. *Org. Chem. Front.* **2023**, *10*, 5933−5939.

(10) Zhu, S.-F.; Zhou, Q.-L. Iron-catalyzed transformations of diazo compounds. *Natl. Sci. Rev.* **2014**, *1*, 580−603.

(11) (a) Zhu, S.-F.; Cai, Y.; Mao, H.-X.; Xie, J.-H.; Zhou, Q.-L. Enantioselective iron-catalysed O−H bond insertions. *Nat. Chem.* **2010**, *2*, 546−551. (b) Aviv, I.; Gross, Z. Iron porphyrins catalyze the synthesis of non-protected amino acid esters from ammonia and diazoacetates. *Chem. commun.* **2006**, 4477−4479. (c) Aviv, I.; Gross, Z. Iron corroles and porphyrins as very efficient and highly selective catalysts for the reactions of α-diazo esters with amines. *Synlett* **2006**, *2006*, 951−953. (d) Aviv, I.; Gross, Z. Iron (III) Corroles and Porphyrins as Superior Catalysts for the Reactions of Diazoacetates with Nitrogen-or Sulfur-Containing Nucleophilic Substrates: Synthetic Uses and Mechanistic Insights. *Chem.—Eur. J.* **2008**, *14*, 3995−4005. (e) Mbuvi, H. M.; Woo, L. K. Catalytic C− H insertions using iron (III) porphyrin complexes. *Organometallics* **2008**, *27*, 637−645. (f) JaneáWang, Z. Cytochrome P450-catalyzed insertion of carbenoids into N−H bonds. *Chem. sci.* **2014**, *5*, 598−601. (g) Holzwarth, M. S.; Alt, I.; Plietker, B. Catalytic Activation of Diazo Compounds Using Electron-Rich, Defined Iron Complexes for Carbene-Transfer Reactions. *Angew. Chem., Int. Ed.* **2012**, *22*, 5351−5354. (h) Muthusamy, S.; Babu, S. A.; Gunanathan, C. Indium triflate: a mild and efficient Lewis acid catalyst for O−H insertion reactions of α-diazo ketones. *Tetrahedron lett.* **2002**, *43*, 3133−3136. (i) Yue, Y.; Wang, Y.; Hu, W. Regioselectivity in Lewis acids catalyzed X−H (O, S, N) insertions of methyl styryldiazoacetate with benzyl alcohol, benzyl thiol, and aniline. *Tetrahedron lett.* **2007**, *48*, 3975−3977. (j) Yoo, J.; Park, N.; Park, J. H.; Park, J. H.; Kang, S.; Lee, S. M.; Kim, H. J.; Jo, H.; Park, J.-G.; Son, S. U. Magnetically separable microporous Fe−porphyrin networks for catalytic carbene insertion into N−H bonds. *ACS Catal.* **2015**, *5*, 350−355. (k) Zhu, Y.; Liu, X.; Dong, S.; Zhou, Y.; Li, W.; Lin, L.; Feng, X. Asymmetric N-H Insertion of Secondary and Primary Anilines under the Catalysis of Palladium and Chiral Guanidine Derivatives. *Angew. Chem.* **2014**, *126*, 1662−1666. (l) Baumann, L. K.; Mbuvi, H. M.; Du, G.; Woo, L. K. Iron Porphyrin Catalyzed N−H Insertion Reactions with Ethyl Diazoacetate. *Organometallics* **2007**, *26*, 3995−4002.

(12) (a) Lee, W.-C. C.; Wang, D.-S.; Zhu, Y.; Zhang, X. P. Iron(III)-based metalloradical catalysis for asymmetric cyclopropanation via a stepwise radical mechanism. *Nat. Chem.* **2023**, *15*, 1569. (b) Gu, H.; Huang, S.; Lin, X. Iron-catalyzed asymmetric intramolecular cyclopropanation reactions using chiral tetramethyl-1,1′-spirobiindane-based bisoxazoline (TMSI-BOX) ligands. *Org. Biomol. Chem.* **2019**, *17*, 1154−1162. (c) Allouche, E. M. D.; Al-Saleh, A.; Charette, A. B. Iron-catalyzed synthesis of cyclopropanes by in situ generation and decomposition of electronically diversified diazo compounds. *Chem. commun.* **2018**, *54*, 13256−13259. (d) Morandi, B.; Dolva, A.; Carreira, E. M. Iron-Catalyzed Cyclopropanation with Glycine Ethyl Ester Hydrochloride in Water. *Org. Lett.* **2012**, *14*, 2162−2163.

(13) (a) Damiano, C.; Sonzini, P.; Gallo, E. Iron catalysts with *N*-ligands for carbene transfer of diazo reagents. *Chem. Soc. Rev.* **2020**, *49*, 4867−4905. (b) Griffin, J. R.; Wendell, C. I.; Garwin, J. A.; White, M. C. Catalytic C(sp3)−H Alkylation via an Iron Carbene Intermediate. *J. Am. Chem. Soc.* **2017**, *139*, 13624−13627. (c) Batista, V. F.; Pinto, G. A.; D, C.; Silva, A. M. S. Iron: A Worthy Contender in Metal Carbene Chemistry. *ACS Catal.* **2020**, *10*, 10096−10116. (d) Kaur, P.; Tyagi, V. Recent Advances in Iron-Catalyzed Chemical

https://doi.org/10.1021/acscatal.3c05040
ACS Catal. 2024, 14, 1292−1299

and Enzymatic Carbene-Transfer Reactions. *Adv. Synth. Catal.* **2021**, *363*, 877−905.
(14) (a) Faul, M. M.; Huff, B. E. Strategy and Methodology Development for the Total Synthesis of Polyether Ionophore Antibiotics. *Chem. Rev.* **2000**, *100*, 2407−2474. (b) Bermejo, A.; Figadère, B.; Zafra-Polo, M.-C.; Barrachina, I.; Estornell, E.; Cortes, D. Acetogenins from Annonaceae: recent progress in isolation, synthesis and mechanisms of action. *Nat. Prod. Rep.* **2005**, *22*, 269−303. (c) Saleem, M.; Kim, H. J.; Ali, M. S.; Lee, Y. S. An update on bioactive plant lignans. *Nat. Prod. Rep.* **2005**, *22*, 696−716. (d) Lorente, A.; Lamariano-Merketegi, J.; Albericio, F.; Álvarez, M. Tetrahydrofuran-Containing Macrolides: A Fascinating Gift from the Deep Sea. *Chem. Rev.* **2013**, *113*, 4567−4610.
(15) Hattori, M.; Hada, S.; Kawata, Y.; Tezuka, Y.; Kikuchi, T.; Namba, T. New 2, 5-Bis-aryl-3, 4-dimethyltetrahydrofuran Lignans from the Aril of *Myristica fragrans*. *Chem. Pharm. Bull.* **1987**, *35*, 3315−3322.
(16) Llopis, N.; Baeza, A. HFIP-Promoted Synthesis of Substituted Tetrahydrofurans by Reaction of Epoxides with Electron-Rich Alkenes. *Molecules* **2020**, *25*, 3464.
(17) Kobayashi, J.; Tsuda, M.; Ishibashi, M.; Shigemori, H.; Yamasu, T.; Hirota, H.; Sasaki, T. Amphidinolide F, a new cytotoxic macrolide from the marine dinoflagellate Amphidinium sp. *J. Antibiot. (Tokyo)* **1991**, *44*, 1259−1261.
(18) (a) Elliott, M. C. Saturated oxygen heterocycles. *J. Chem. Soc.* **2000**, 1291−1318. (b) Elliott, M. C.; Williams, E. Saturated oxygen heterocycles. *J. Chem. Soc.* **2001**, 2303−2340. (c) Wolfe, J. P.; Hay, M. B. Recent advances in the stereoselective synthesis of tetrahydrofurans. *Tetrahedron* **2007**, *63*, 261−290.
(19) (a) Nicolle, S. M.; Lewis, W.; Hayes, C. J.; Moody, C. J. Stereoselective Synthesis of Highly Substituted Tetrahydrofurans through Diverted Carbene O-H Insertion Reaction. *Angew. Chem., Int. Ed.* **2015**, *54*, 8485−8489. (b) Jing, C.; Xing, D.; Gao, L.; Li, J.; Hu, W. Divergent Synthesis of Multisubstituted Tetrahydrofurans and Pyrrolidines via Intramolecular Aldol-type Trapping of Onium Ylide Intermediates. *Chem.—Eur. J.* **2015**, *21*, 19202−19207.
(20) (a) Yang, J.-M.; Cai, Y.; Zhu, S.-F.; Zhou, Q.-L. Iron-catalyzed arylation of α-aryl-α-diazoesters. *Org. Biomol. Chem.* **2016**, *14*, 5516−5519. (b) Liu, B.; Zhu, S.-F.; Zhang, W.; Chen, C.; Zhou, Q.-L. Highly enantioselective insertion of carbenoids into N− H bonds catalyzed by copper complexes of chiral spiro bisoxazolines. *J. Am. Chem. Soc.* **2007**, *129*, 5834−5835.
(21) Babaahmadi, R.; Dasgupta, A.; Hyland, C. J. T.; Yates, B. F.; Melen, R. L.; Ariafard, A. Understanding the Influence of Donor-Acceptor Diazo Compounds on the Catalyst Efficiency of $B(C_6F_5)_3$ Towards Carbene Formation. *Chem.—Eur. J.* **2022**, *28*, No. e202104376.
(22) *CCDC 2285940 (3q), CCDC 2285941 (3i), CCDC2285942 (3u) contains the supplementary crystallographic data for this paper. These data can be obtained free of charge from the Cambridge Crystallographic Data Centre via* www.ccdc.cam.ac.uk/structures. Published (Date of access: December 18, 2023).
(23) Bull, J. A.; Croft, R. A.; Davis, O. A.; Doran, R.; Morgan, K. F. Oxetanes: Recent Advances in Synthesis, Reactivity, and Medicinal Chemistry. *Chem. Rev.* **2016**, *116*, 12150−12233.
(24) (a) Serafini, M.; Pirali, T.; Tron, G. C. Chapter Three - Click 1,2,3-triazoles in drug discovery and development: From the flask to the clinic? In *Adv. Heterocycl. Chem.*; Meanwell, N. A., Lolli, M. L., Eds.; Academic Press, 2021; Vol. *134*, pp 101−148. (b) Rani, A.; Singh, G.; Singh, A.; Maqbool, U.; Kaur, G.; Singh, J. CuAAC-ensembled 1,2,3-triazole-linked isosteres as pharmacophores in drug discovery: review. *RSC Adv.* **2020**, *10*, 5610−5635.
(25) See the supporting information page S60 for more details.

https://doi.org/10.1021/acscatal.3c05040
ACS Catal. 2024, 14, 1292−1299

OL Organic Letters

pubs.acs.org/OrgLett

Letter

Catalytic Activation of Thioglycosides with Copper-Carbenes for Stereoselective 1,2-*Cis*-Furanosylations

Bidhan Ghosh, Adam Alber, Chance W. Lander, Yihan Shao, Kenneth M. Nicholas, and Indrajeet Sharma*

Cite This: *Org. Lett.* 2024, 26, 9436–9441

Read Online

ACCESS | Metrics & More | Article Recommendations | Supporting Information

ABSTRACT: Thioglycoside activation, crucial for oligosaccharide synthesis, faces challenges with the need for stoichiometric promoters, additives, and cryogenic conditions, particularly in stereoselective 1,2-*cis*-linkage formation. This study introduces a carbene-based catalytic method using $Cu(OTf)_2$ for thioglycoside activation, enabling efficient 1,2-*cis*-furanosylation in ribose and arabinose. The method is orthogonal to conventional thioglycoside and alkyne donors, accommodates sterically demanding acceptors, and achieves stereoselectivity independent of the donor anomeric configuration and C2-protecting groups, with copper chelation playing a key role.

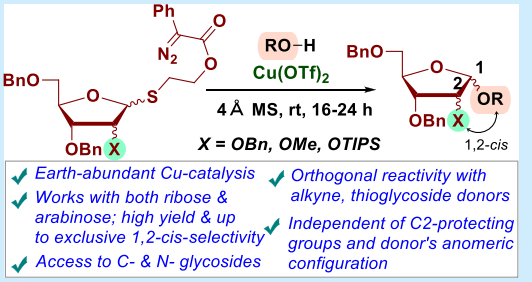

Thioglycosides have been employed for decades as facile glycosyl donors for synthesizing oligosaccharides and glycoconjugates as they hold excellent thermostability and tunable reactivities.[1] Numerous methods have been developed for activating and selectively functionalizing these thioglycoside donors.[1a,2] While elegant, most methods use stoichiometric amounts of harsh and moisture-sensitive reagents, often resulting in undesired side reactions, especially in substrates bearing reactive functionalities.[1f,3] For example, the activating conditions for substrates bearing alkenes are often incompatible and require low temperatures to avoid side reactions.[4] Thus, developing milder methods for thioglycoside activation has been an area of continuous interest. Additionally, catalytic activation of thioglycosides is limited, with most methods utilizing precious rare-earth metals such as rhodium and gold.[5] Furthermore, no catalytic methods for thioglycoside activation are known for synthesizing 1,2-*cis*-furanosides, key constituents of several biomedically relevant carbohydrates.[6] This is likely because constructing a 1,2-*trans* linkage via anchimeric assistance from a C2-*O*-acyl protecting group is relatively straightforward,[2f,7] while achieving the 1,2-*cis* linkage poses a more formidable challenge due to the absence of C2-*O*-participating groups. Additionally, the higher stability of the oxocarbenium ion in furanosides compared to their pyranoside counterparts further complicates the attainment of 1,2-*cis*-selectivity.[8] Therefore, most glycosylation methods developed for 1,2-*cis* linkages in the pyranoside system are ineffective for furanosides, leading to a mixture of stereoisomers with similar glycosyl donors in furanosylation reactions.[9]

A literature review identified an approach by the Wan group using cooperative catalysis with rhodium(II) and Brønsted acid for carbene-based thioglycoside activation (Figure 1a).[5b] This method generates anomeric sulfonium ylides, followed by protonation to form oxocarbenium ions for glycosylation. However, it struggles with 1,2-*cis*-selectivity, likely due to rhodium's inability to form C2-*O* coordination to direct the nucleophile, and it lacks examples of 1,2-*cis*-furanosylations.

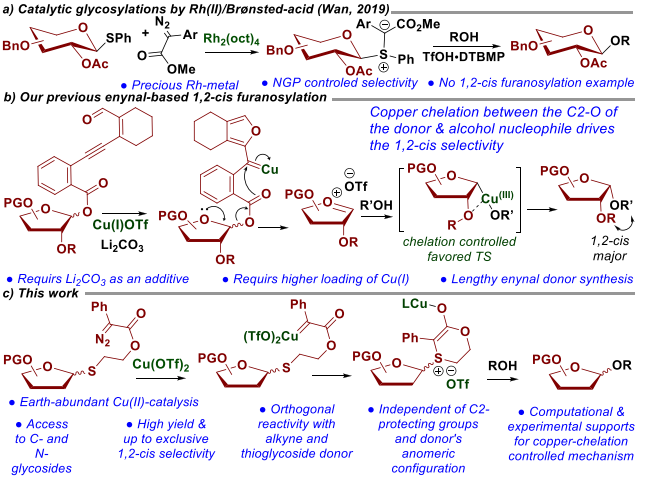

Figure 1. (a) Catalytic glycosylation with Rh-carbene. (b) Enynal derived carbene based 1,2-*cis*-furanosylation. (c) Our approach.

Received: September 2, 2024
Revised: October 17, 2024
Accepted: October 22, 2024
Published: October 28, 2024

https://doi.org/10.1021/acs.orglett.4c03281
Org. Lett. 2024, 26, 9436–9441

To address the challenge of 1,2-*cis*-furanosylations, our group recently developed benzoate donors activated by enynal-derived copper carbenes (Figure 1b).[10] However, the need for higher loadings of copper(I) trifluoromethanesulfonate, the use of a base additive (Li_2CO_3), and the lengthy synthesis required for benzoate donors prompted us to shift our focus to more stable and versatile thioglycoside donors. Drawing inspiration from our previous work and expertise in using earth-abundant metal carbenes,[10,11] we hypothesized that copper carbenes could effectively activate thioglycosides and direct alcohol nucleophiles by coordinating with the C2-ether protecting group, thereby achieving 1,2-*cis*-furanosylation with high stereoselectivity (Figure 1c).

Our approach commences with the activation of a simple thioglycoside donor using an external diazo compound under copper-catalyzed conditions, exploiting the ability of copper to coordinate with furanose C2-*O* and incoming alcohol nucleophiles to achieve 1,2-*cis*-selectivity.[10] The reaction of thioglycoside donor **1a** with diazo compound **2a** and methyl-2,3,4-tri-*O*-benzyl-α-D-glucopyranose acceptor **3a** under copper(I) trifluoromethanesulfonate conditions produced the desired disaccharide **4a** with excellent 1,2-*cis*-stereoselectivity but a low yield (Table 1a, 15%, α/β = 7/1), with most starting materials unreacted. Using copper(II) trifluoromethanesulfonate slightly improved the yield to 20%, though unreacted materials persisted. Stoichiometric copper further improved the yield to 55%, but it also generated multiple byproducts, including carbene dimer, direct alcohol insertion, and other unidentified compounds.

Aiming for an additive-free thioglycoside activation method and addressing the competitive direct attack of the acceptor nucleophile on the diazo-derived carbene, we focused on enhancing the reactivity of the sulfur atom in thioglycosides toward the diazo moiety. To this end, we devised an intramolecular thioglycoside diazo donor, anticipating that the proximity and intrinsic reactivity of the sulfur atom would overcome the competitive reactivity issues observed in intermolecular reactions.

Intramolecular diazo thioglycoside donors can be synthesized in two steps using commercially available starting materials and remain stable for months (see Supporting Information (SI) for details). Optimization of our intramolecular diazo thioglycoside activation began with the 2,3,5-tri-*O*-benzyl-D-ribofuranosyl donor **1b** and the glucopyranose acceptor **3a** (Table 1b). Replicating Rh(II)-catalyzed conditions yielded the desired disaccharide **4a** at ~10% with the formation of major byproduct **5** (entry 1).[5b] Switching to copper salts, 10 mol % copper(I) triflate improved the yield to 37% with excellent 1,2-*cis*-selectivity (9/1) (entry 2). However, using other copper(I) counteranions reduced both yield and selectivity (entries 3, 4). Remarkably, with 10 mol % of copper(II) triflate, the reaction provided an excellent yield (88%) with an α-*cis*-selectivity of 9/1 at room temperature in 20 h (entry 5). Under the reaction conditions, a minor degree of byproduct formation was observed, specifically byproduct **5**, which likely results from the interaction between the oxocarbenium ion and the released oxathian counterpart (see SI page S31 for details).[5b] Since some of the donors followed an unproductive pathway, an increased amount of donor (1.4 equiv) was necessary to fully consume the acceptor. At lower temperatures, the decomposition of diazo compounds slows, which is a critical step in forming copper carbenes. The subsequent reaction steps depend on the successful completion of this initial process. Although byproduct formation decreased, the reaction resulted in a similar yield and selectivity of the desired product **4a** (entries 6, 7). Testing other metal triflates, $Zn(OTf)_2$ gave only the rearrangement byproduct **5**, while $Fe(OTf)_2$ required 50 °C for diazo decomposition with no stereoselectivity (entries 8, 9). Without molecular sieves, both yield and selectivity decreased, leading to increased byproduct formation (entry 10).

With optimized conditions, we explored the substrate scope with the benzyl-protected D-ribofuranosyl donor **1b** (Table 2a). Primary alcohols featuring terminal alkene and alkyne functionalities underwent smooth reactions, providing high yields and α-*cis*-selectivity (**4b**, **4c**). Secondary and tertiary alcohols including chiral alcohol acceptors also afforded corresponding furanosylation products with high yields and α-*cis*-selectivity (**4d**–**4h**). Encouragingly, reaction yields and selectivity with carbohydrate alcohol acceptors were unaffected by protecting groups including acetonide, benzyl, and benzoyl (**4i**–**4l**). Notably, hindered carbohydrate acceptors, which are typically less reactive toward glycosylation, performed equally well with high yields and excellent 1,2-*cis*-selectivity (**4m**, **4n**). A protected amino acid alcohol acceptor also showed high *cis*-selectivity (**4o**). Additionally, our system was successfully applied to synthesize *C*- and *N*-glycosides, achieving high yields and excellent *cis*-selectivity (**4p**, **4q**).

Following this, we expanded the substrate scope using arabinose donor **1c** (Table 2b.) Primary, secondary, and bulkier tertiary alcohol acceptors reacted effectively, producing the desired disaccharides in good yields with excellent β-*cis*-stereoselectivity (**6a**–**6e**). Remarkably, acetonide-protected galactose-, benzyl-, benzoyl-, and acetyl-protected glucose

Table 1. Optimization of the Reaction Conditions[a]

a) Thioglycoside Donor Activation with External Diazo

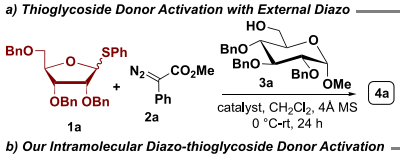

catalyst (mol%)	% yield[b] 4a	α/β ratio[c]
[CuOTf]$_2$·tol (10)	15%	7/1
Cu(OTf)$_2$ (10)	20%	7/1
Cu(OTf)$_2$ (100)	55%	7/1

b) Our Intramolecular Diazo-thioglycoside Donor Activation

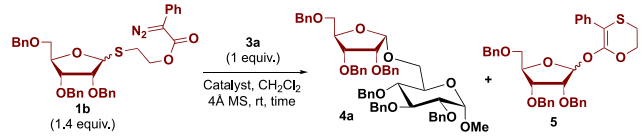

Entry	Catalyst (mol %)	Time	% Yield (4a)[b]	α/β ratio	% Yield (5)[b]
1.	$Rh_2(OAc)_4$ (5%), TfOH·DTBMP	16 h	10%	n.d.	80%
2.	[CuOTf]$_2$·tol (10%)	24 h	37%	9/1	45%
3.	$Cu(MeCN)_4PF_6$ (10%)	24 h	20%	4/1	55%
4.	$Cu(MeCN)_4BF_4$ (10%)	24 h	0%	n.d.	65%
5.	**Cu(OTf)$_2$ (10%)**	20 h	**88%**	9/1	**20%**
6.	Cu(OTf)$_2$ (10%), 0 °C	36 h	65%	9/1	<10%
7.	Cu(OTf)$_2$ (10%), 10 °C	36 h	88%	9/1	20%
8.	Zn(OTf)$_2$ (10%)	36 h	n.r.	n.d.	60%
9.	Fe(OTf)$_2$ (10%), 50 °C	16 h	56%	1/1	40%
10.	Cu(OTf)$_2$ (10%), no 4 Å MS	20 h	58%	7/1	45%

[a]All furanosylations were conducted with acceptor **3a** (0.05 mmol), donor **1b** (0.07 mmol), and CH_2Cl_2 (0.04 M) at 23 °C. [b]Yield was determined by ^{1}H NMR using 1,3,5-trimethoxybenzene as the internal standard, with respective to the acceptor **3a**. [c]Diastereoselectivity was determined by ^{1}H NMR.

https://doi.org/10.1021/acs.orglett.4c03281
Org. Lett. 2024, 26, 9436−9441

Table 2. Scope of 1,2-*cis*-Furanosylations[a]

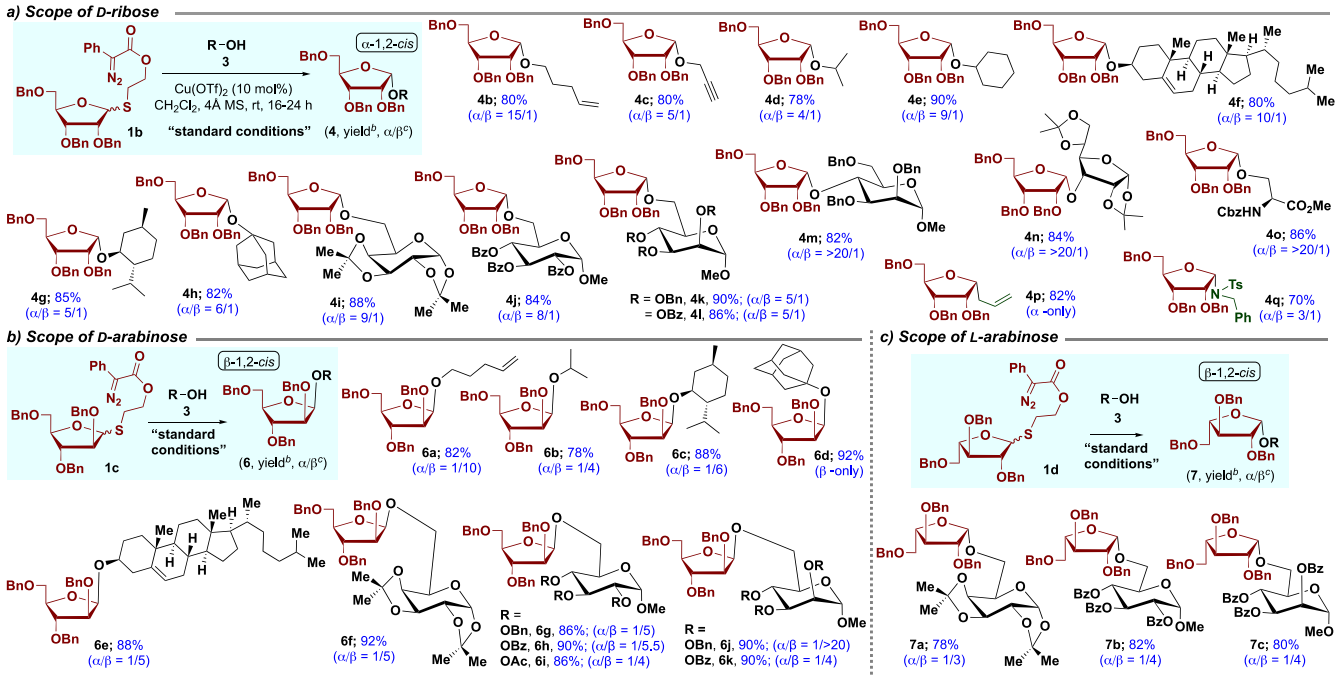

[a]All furanosylations were conducted with acceptor **3** (0.05 mmol), donor **1b**/**1c**/**1d** (0.07 mmol), and CH_2Cl_2 (0.04 M). [b]Yield was determined by ^1H NMR using 1,3,5-trimethoxybenzene as the internal standard. [c]Diastereoselectivity was determined by ^1H NMR.

acceptors demonstrated facile reactivity, furnishing products with good *β-cis*-selectivity and high yields (**6f**–**6i**). Notably, acceptors derived from mannose were unreactive with the Jacobsen bis-thiourea furanosylation protocol.[12] Our method achieved the intended product with high yields and selectivity, adding to the versatility of our approach (**6j**, **6k**).

To demonstrate compatibility with the opposite enantiomer, L-arabinofuranoside donor **1d** was also tested (Table 2c). Reactions with this donor also exhibited *β-cis*-selectivity, likewise D-arabinofuranoside. The acetonide- and benzoyl-protected glucopyranoside acceptors, as well as the benzoyl-protected mannopyranoside acceptor, afforded corresponding products in good yields and *β-cis*-selectivity (**7a**–**7c**).

Recent studies by Jacobsen[12] and Zhang[13] groups showed that donor anomeric composition affects 1,2-*cis*-furanosylation stereoselectivity. We investigated the correlation between the initial anomeric ratio of our diazo thioglycoside donor and the final product's stereoselectivity using both a racemic mixture and an enantiopure ribose donor **1b** (Figure 2a). To our delight, we observed the same yield and stereoselectivity in each trial, suggesting the anomeric composition of the starting diazo donor does not influence the stereoselectivity outcome. Furthermore, testing for potential epimerization of the *α*/*β*-furanoside products under the same conditions revealed no epimerization, demonstrating the mild nature of our protocol.

Next, we investigated the effect of the electronic properties of diazo donors on the reaction kinetics (Figure 2b). Under standard conditions with acceptor **3a**, the *para*-methoxy ribose donor (**1e**) reacted more quickly but produced mainly byproducts, yielding only 34% of the desired product. In contrast, parent donor **1b** provided an 88% yield with minimal byproduct. The *para*-nitro donor (**1f**) was unreactive under the optimized conditions, likely due to the increased stability of the acceptor/acceptor diazo complex.

To investigate the impact of the C2-group, we synthesized donors with various C2 modifications (Figure 2c). We tested whether *cis*-selectivity was driven by copper *π*-aryl coordination or C2 oxygen using a C2 methoxy donor (**1g**), which yielded 92% product with high *α-cis*-selectivity (**8**). Encouraged by this, a C2-OTIPS donor (**1h**), which is suitable for iterative and solid-phase syntheses due to their facile deprotection,[1d,14] provided an excellent yield and *α-cis*-selectivity (**9**). In contrast, the C2 deoxyribose donor (**1i**) decomposed unproductively, indicating that a coordinating group at C2 is crucial for smooth and selective reactivity. Furthermore, to investigate the role of copper in driving *α-cis*-selectivity, we tested the reaction of traditional C2-OTIPS thioglycoside donor (**1h**) under literature-reported NIS/TMSOTf[2n] and NIS/AgOTf[2m] reaction conditions. The reaction produced disaccharides in good yields but without stereoselectivity (Figure 2c). This indicates that copper is likely crucial for achieving the high 1,2-*cis*-selectivity observed in our method.

Building on the success of the C2-TIPS protecting group, we explored furanosylation with various alcohol acceptors, achieving good to excellent yields and exclusive 1,2-*cis*-selectivity (Figure 2d). The method efficiently synthesized phenolic glycosides (**9b**) and showed high yield and exclusive *α-cis*-selectivity with benzoyl-protected glucose and benzyl-protected mannose acceptors (**9c**, **9d**). Furthermore, the donor exhibited orthogonal reactivity with alkynyl and thioglycoside donors (**9e**–**9g**), ideal for iterative oligosaccharide synthesis. We then applied our donor in an iterative synthesis for 1,2-*cis*-selective trisaccharide formation. Using C2-OTIPS donor **1h** with acceptor **3a**, we achieved a 90% yield of the 1,2-*cis* product. Subsequent TBAF deprotection of the C2 silyl group and reaction with additional donor **1h** produced the trisaccharide in 74% yield with *α*-only selectivity.

https://doi.org/10.1021/acs.orglett.4c03281
Org. Lett. 2024, 26, 9436−9441

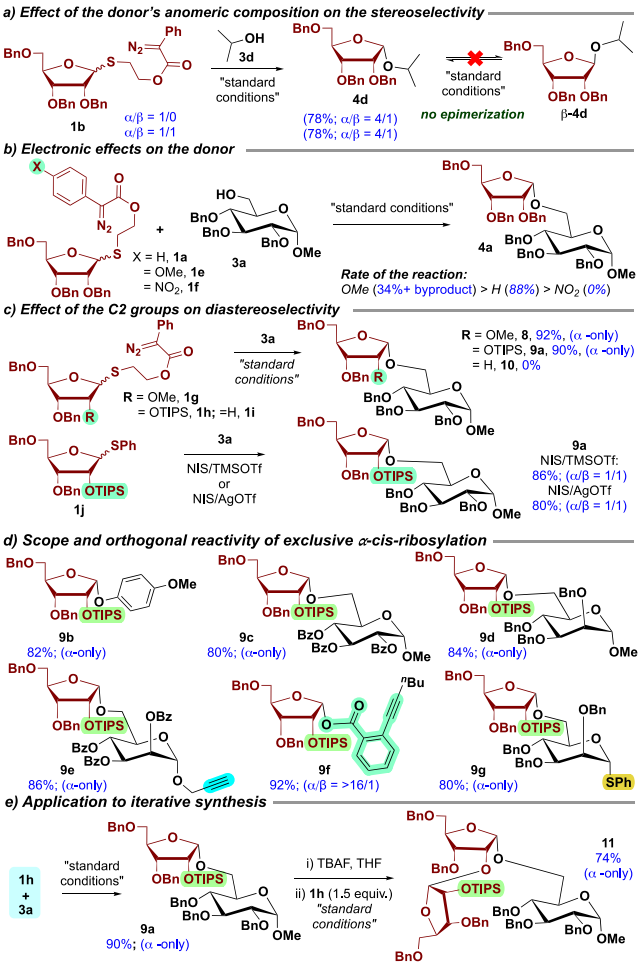

Figure 2. (a) Effect of donor's anomeric configuration on reaction stereoselectivity. (b) Effect of donor's electronics. (c) Effect of the C2-group on reaction diastereoselectivity. (d) Scope and orthogonal reactivity of exclusive 1,2-*cis*-ribosylation. (e) Application to *cis*-selective iterative synthesis.

Mechanistically, the reaction proceeds through an oxocarbenium ion, and the desired 1,2-*cis*-stereoselectivity stems from chelation between the C2-oxygen of the furanose donor and the incoming copper alkoxide nucleophile (see SI page S31 for detailed mechanism and S32 for computational calculations).

In summary, we developed an additive-free, copper(II)-catalyzed 1,2-*cis*-furanosylation, achieving high yields and diastereoselectivity at room temperature. Using benchtop-stable diazo-derived thiofuranosyl donors, the method accommodates diverse alcohol acceptors and furanose donors. Influence of C2 group investigations revealed a very high 1,2-*cis*-selectivity, which was applied in the iterative synthesis of a *cis*-selective trisaccharide. The approach offers stereoselectivity independent of donor anomeric configuration and exhibits orthogonal reactivity with alkyne and thioglycoside donors, broadening its applicability in iterative oligosaccharide synthesis.

■ ASSOCIATED CONTENT

Data Availability Statement

The data underlying this study are available in the published article and its Supporting Information.

Supporting Information

The Supporting Information is available free of charge at https://pubs.acs.org/doi/10.1021/acs.orglett.4c03281.

Experimental procedures, computational studies, NMR spectroscopic and analytical data for all compounds (PDF)

■ AUTHOR INFORMATION

Corresponding Author

Indrajeet Sharma − *Department of Chemistry and Biochemistry, University of Oklahoma, Norman, Oklahoma 73019-5251, United States;* orcid.org/0000-0002-0707-0621; Email: isharma@ou.edu

Authors

Bidhan Ghosh − *Department of Chemistry and Biochemistry, University of Oklahoma, Norman, Oklahoma 73019-5251, United States*

Adam Alber − *Department of Chemistry and Biochemistry, University of Oklahoma, Norman, Oklahoma 73019-5251, United States*

Chance W. Lander − *Department of Chemistry and Biochemistry, University of Oklahoma, Norman, Oklahoma 73019-5251, United States*

Yihan Shao − *Department of Chemistry and Biochemistry, University of Oklahoma, Norman, Oklahoma 73019-5251, United States;* orcid.org/0000-0001-9337-341X

Kenneth M. Nicholas − *Department of Chemistry and Biochemistry, University of Oklahoma, Norman, Oklahoma 73019-5251, United States;* orcid.org/0000-0002-5180-1671

Complete contact information is available at: https://pubs.acs.org/10.1021/acs.orglett.4c03281

Notes

The authors declare no competing financial interest.

■ ACKNOWLEDGMENTS

The NSF CHE-1753187 supported this work. We thank Dr. Novrus G. Akhmedov and Dr. Steven Foster from the Research Support Services, University of Oklahoma, for NMR and mass spectral analyses, respectively.

■ REFERENCES

(1) (a) Escopy, S.; Demchenko, A. V. Transition-Metal-Mediated Glycosylation with Thioglycosides. *Chem.—Eur. J.* **2022**, *28*, No. e202103747. (b) Kaeothip, S.; Akins, S. J.; Demchenko, A. V. On the stereoselectivity of glycosidation of thiocyanates, thioimidates, and thioglycosides. *Carbohydr. Res.* **2010**, *345*, 2146−2150. (c) Codée, J. D. C.; Litjens, R. E. J. N.; van den Bos, L. J.; Overkleeft, H. S.; van der Marel, G. A. Thioglycosides in sequential glycosylation strategies. *Chem. Soc. Rev.* **2005**, *34*, 769−782. (d) Panza, M.; Pistorio, S. G.; Stine, K. J.; Demchenko, A. V. Automated Chemical Oligosaccharide Synthesis: Novel Approach to Traditional Challenges. *Chem. Rev.* **2018**, *118*, 8105−8150. (e) Zhang, Z.; Ollmann, I. R.; Ye, X.-S.; Wischnat, R.; Baasov, T.; Wong, C.-H. Programmable One-Pot Oligosaccharide Synthesis. *J. Am. Chem. Soc.* **1999**, *121*, 734−753. (f) Lian, G.; Zhang, X.; Yu, B. Thioglycosides in carbohydrate research. *Carbohydr. Res.* **2015**, *403*, 13−22.

(2) (a) Nielsen, M. M.; Pedersen, C. M. Catalytic Glycosylations in Oligosaccharide Synthesis. *Chem. Rev.* **2018**, *118*, 8285−8358. (b) Chu, A.-H. A.; Minciunescu, A.; Montanari, V.; Kumar, K.;

Bennett, C. S. An Air- and Water-Stable Iodonium Salt Promoter for Facile Thioglycoside Activation. *Org. Lett.* **2014**, *16*, 1780−1782. (c) Goswami, M.; Ellern, A.; Pohl, N. L. B. Bismuth(V)-Mediated Thioglycoside Activation. *Angew. Chem., Int. Ed.* **2013**, *52*, 8441−8445. (d) Wever, W. J.; Cinelli, M. A.; Bowers, A. A. Visible light mediated activation and *O*-glycosylation of thioglycosides. *Org. Lett.* **2013**, *15*, 30−33. (e) Nicolaou, K.; Seitz, S.; Papahatjis, D. A mild and general method for the synthesis of *O*-glycosides. *J. Am. Chem. Soc.* **1983**, *105*, 2430−2434. (f) Fügedi, P.; Garegg, P. J. A novel promoter for the efficient construction of 1, 2-*trans* linkages in glycoside synthesis, using thioglycosides as glycosyl donors. *Carbohydr. Res.* **1986**, *149*, C9−C12. (g) Veeneman, G.; Van Boom, J. An efficient thioglycoside-mediated formation of α-glycosidic linkages promoted by iodonium dicollidine perchlorate. *Tetrahedron Lett.* **1990**, *31*, 275−278. (h) Veeneman, G.; Van Leeuwen, S.; Van Boom, J. Iodonium ion promoted reactions at the anomeric centre. II An efficient thioglycoside mediated approach toward the formation of 1, 2-*trans* linked glycosides and glycosidic esters. *Tetrahedron Lett.* **1990**, *31*, 1331−1334. (i) Crich, D.; Smith, M. 1-Benzenesulfinyl piperidine/trifluoromethanesulfonic anhydride: a potent combination of shelf-stable reagents for the low-temperature conversion of thioglycosides to glycosyl triflates and for the formation of diverse glycosidic linkages. *J. Am. Chem. Soc.* **2001**, *123*, 9015−9020. (j) Codée, J. D.; Litjens, R. E.; den Heeten, R.; Overkleeft, H. S.; van Boom, J. H.; van der Marel, G. A. Ph_2SO/Tf_2O: a powerful promotor system in chemoselective glycosylations using thioglycosides. *Org. Lett.* **2003**, *5*, 1519−1522. (k) Lu, S.-R.; Lai, Y.-H.; Chen, J.-H.; Liu, C.-Y.; Mong, K.-K. T. Dimethylformamide: an unusual glycosylation modulator. *Angew. Chem., Int. Ed.* **2011**, *50*, 7315−7320. (l) Ferrier, R.; Hay, R.; Vethaviyasar, N. A potentially versatile synthesis of glycosides. *Carbohydr. Res.* **1973**, *27*, 55−61. (m) Konradsson, P.; Udodong, U. E.; Fraser-Reid, B. Iodonium promoted reactions of disarmed thioglycosides. *Tetrahedron Lett.* **1990**, *31*, 4313−4316. (n) Konradsson, P.; Mootoo, D. R.; McDevitt, R. E.; Fraser-Reid, B. Iodonium ion generated in situ from N-iodosuccinimide and trifluoromethanesulphonic acid promotes direct linkage of 'disarmed'pent-4-enyl glycosides. *J. Chem. Soc., Chem. Commun.* **1990**, 270−272. (o) Ito, Y.; Ogawa, T. Sulfenate esters as glycosyl acceptors: A novel approach to O-glycosides from thioglycosides and sulfenate esters. *Tetrahedron Lett.* **1987**, *28*, 4701−4704. (p) Uchiro, H.; Mukaiyama, T. An efficient method for catalytic and stereoselective glycosylation with thioglycosides promoted by trityl tetrakis (pentafluorophenyl) borate and sodium periodate. *Chem. Lett.* **1997**, *26*, 121−122. (q) Damico, A.; Shrestha, G.; Das, A.; Stine, K. J.; Demchenko, A. V. SFox imidates as versatile glycosyl donors for chemical glycosylation. *Org. Biomol. Chem.* **2024**, *22*, 5214−5223.

(3) (a) Qin, Z.-H.; Li, H.; Cai, M.-S.; Li, Z.-J. Bromonium ion-promoted glycosidic bond formation and simultaneous bromination of an activated aryl aglycon. *Carbohydr. Res.* **2002**, *337*, 31−36. (b) Yu, B.; Sun, J.; Yang, X. Assembly of Naturally Occurring Glycosides, Evolved Tactics, and Glycosylation Methods. *Acc. Chem. Res.* **2012**, *45*, 1227−1236. (c) Dulin, M. L.; Noecker, L. A.; Kassel, W. S.; Giuliano, R. M. An unusual course of thioglycoside activation with bromine: synthesis and crystal structure of 4-*O*-acetyl-2-bromo-2,3,6-trideoxy-3-*C*-methyl-3-trifluroacetamido-α-l-altropyranosyl bromide. *Carbohydr. Res.* **2003**, *338*, 1121−1125. (d) Hendel, J. L.; Cheng, A.; Auzanneau, F.-I. Application and limitations of the methyl imidate protection strategy of N-acetylglucosamine for glycosylations at O-4: synthesis of Lewis A and Lewis X trisaccharide analogues. *Carbohydr. Res.* **2008**, *343*, 2914−2923. (e) Codée, J. D. C.; van den Bos, L. J.; Litjens, R. E. J. N.; Overkleeft, H. S.; van Boeckel, C. A. A.; van Boom, J. H.; van der Marel, G. A. Chemoselective glycosylations using sulfonium triflate activator systems. *Tetrahedron* **2004**, *60*, 1057−1064. (f) Krog-Jensen, C.; Oscarson, S. Synthesis of D-Fructofuranosides Using Thioglycosides as Glycosyl Donors. *J. Org. Chem.* **1996**, *61*, 1234−1238.

(4) (a) Demchenko, A. V.; De Meo, C. Semi-orthogonality of *O*-pentenyl and *S*-ethyl glycosides: application for the oligosaccharide synthesis. *Tetrahedron Lett.* **2002**, *43*, 8819−8822. (b) López, J. C.; Gómez, A. M.; Uriel, C.; Fraser-Reid, B. Thioglycoside and trichloroacetimidate donors in regioselective glycosidations. Comparison with n-pentenyl glycosides. *Tetrahedron Lett.* **2003**, *44*, 1417−1420. (c) Mootoo, D. R.; Konradsson, P.; Fraser-Reid, B. n-Pentenyl glycosides facilitate a stereoselective synthesis of the pentasaccharide core of the protein membrane anchor found in Trypanosoma brucei. *J. Am. Chem. Soc.* **1989**, *111*, 8540−8542.

(5) (a) Vibhute, A. M.; Dhaka, A.; Athiyarath, V.; Sureshan, K. M. A versatile glycosylation strategy via Au (III) catalyzed activation of thioglycoside donors. *Chem. Sci.* **2016**, *7*, 4259−4263. (b) Meng, L.; Wu, P.; Fang, J.; Xiao, Y.; Xiao, X.; Tu, G.; Ma, X.; Teng, S.; Zeng, J.; Wan, Q. Glycosylation Enabled by Successive Rhodium(II) and Brønsted Acid Catalysis. *J. Am. Chem. Soc.* **2019**, *141*, 11775−11780.

(6) (a) Mazeau, K.; Pérez, S. The preferred conformations of the four oligomeric fragments of Rhamnogalacturonan II. *Carbohydr. Res.* **1998**, *311*, 203−217. (b) Pérez, S.; Rodríguez-Carvajal, M. A.; Doco, T. A complex plant cell wall polysaccharide: rhamnogalacturonan II. A structure in quest of a function. *Biochimie* **2003**, *85*, 109−121. (c) Matsunaga, T.; Ishii, T.; Matsumoto, S.; Higuchi, M.; Darvill, A.; Albersheim, P.; O'Neill, M. A. Occurrence of the Primary Cell Wall Polysaccharide Rhamnogalacturonan II in Pteridophytes, Lycophytes, and Bryophytes. Implications for the Evolution of Vascular Plants. *Plant Physiol.* **2004**, *134*, 339−351.

(7) Dasgupta, F.; Garegg, P. J. Alkyl sulfenyl triflate as activator in the thioglycoside-mediated formation of β-glycosidic linkages during oligosaccharide synthesis. *Carbohydr. Res.* **1988**, *177*, c13−c17.

(8) (a) Larsen, C. H.; Ridgway, B. H.; Shaw, J. T.; Woerpel, K. A. A Stereoelectronic Model To Explain the Highly Stereoselective Reactions of Nucleophiles with Five-Membered-Ring Oxocarbenium Ions. *J. Am. Chem. Soc.* **1999**, *121*, 12208−12209. (b) van Rijssel, E. R.; van Delft, P.; Lodder, G.; Overkleeft, H. S.; van der Marel, G. A.; Filippov, D. V.; Codée, J. D. C. Furanosyl Oxocarbenium Ion Stability and Stereoselectivity. *Angew. Chem., Int. Ed.* **2014**, *53*, 10381−10385. (c) Xu, H.; Schaugaard, R. N.; Li, J.; Schlegel, H. B.; Nguyen, H. M. Stereoselective 1,2-cis Furanosylations Catalyzed by Phenanthroline. *J. Am. Chem. Soc.* **2022**, *144*, 7441−7456. (d) Gallo-Rodriguez, C.; Kashiwagi, G. A. Selective Glycosylations with Furanosides. *Selective Glycosylations: Synthetic Methods and Catalysts* **2017**, 297−326.

(9) (a) Prévost, M.; St-Jean, O.; Guindon, Y. Synthesis of 1′,2′-*cis*-Nucleoside Analogues: Evidence of Stereoelectronic Control for S_N2 Reactions at the Anomeric Center of Furanosides. *J. Am. Chem. Soc.* **2010**, *132*, 12433−12439. (b) Pierce, J.; Serianni, A. S.; Barker, R. Anomerization of furanose sugars and sugar phosphates. *J. Am. Chem. Soc.* **1985**, *107*, 2448−2456. (c) Adero, P. O.; Amarasekara, H.; Wen, P.; Bohé, L.; Crich, D. The Experimental Evidence in Support of Glycosylation Mechanisms at the S_N1−S_N2 Interface. *Chem. Rev.* **2018**, *118*, 8242−8284.

(10) Ghosh, B.; Alber, A.; Lander, C. W.; Shao, Y.; Nicholas, K. M.; Sharma, I. Catalytic Stereoselective 1,2-*cis*-Furanosylations Enabled by Enynal-Derived Copper Carbenes. *ACS Catal.* **2024**, *14*, 1037−1049.

(11) (a) Ou, C.; Ghosh, B.; Sharma, I. A non-diazo approach to functionalized (2-furyl)-2-pyrrolidines through a cascade reaction of enynal-derived zinc carbenoids with β-arylaminoketones. *Org. Chem. Front.* **2023**, *10*, 5933−5939. (b) Kafle, P.; Ghosh, B.; Hunter, A. C.; Mukherjee, R.; Nicholas, K. M.; Sharma, I. Iron-Carbene Initiated O−H Insertion/Aldol Cascade for the Stereoselective Synthesis of Functionalized Tetrahydrofurans. *ACS Catal.* **2024**, *14*, 1292−1299. (c) Pratap Singh, S.; Ghosh, B.; Sharma, I. Catalytic Orthogonal Glycosylation Enabled by Enynal-Derived Copper Carbenes. *Adv. Synth. Catal.* **2024**, *366*, 1847−1856.

(12) Mayfield, A. B.; Metternich, J. B.; Trotta, A. H.; Jacobsen, E. N. Stereospecific Furanosylations Catalyzed by Bis-thiourea Hydrogen-Bond Donors. *J. Am. Chem. Soc.* **2020**, *142*, 4061−4069.

(13) Ma, X.; Zhang, Y.; Zhu, X.; Zhang, L. An S_N2-Type Strategy toward 1,2-*cis*-Furanosides. *CCS Chem.* **2022**, *4*, 3677−3685.

(14) (a) Yao, W.; Xiong, D.-C.; Yang, Y.; Geng, C.; Cong, Z.; Li, F.; Li, B.-H.; Qin, X.; Wang, L.-N.; Xue, W.-Y.; et al. Automated solution-phase multiplicative synthesis of complex glycans up to a 1,080-mer. *Nat. Synth.* **2022**, *1*, 854−863. (b) Joseph, A. A.; Pardo-Vargas, A.;

https://doi.org/10.1021/acs.orglett.4c03281
Org. Lett. 2024, 26, 9436−9441

Seeberger, P. H. Total Synthesis of Polysaccharides by Automated Glycan Assembly. *J. Am. Chem. Soc.* **2020**, *142*, 8561−8564.

NOTE ADDED AFTER ASAP PUBLICATION

This paper was published October 28, 2024. Figure 1 and the abstract graphic have been updated. The revised version reposted on November 8, 2024.

https://doi.org/10.1021/acs.orglett.4c03281
Org. Lett. 2024, 26, 9436−9441

RESEARCH ARTICLE doi.org/10.1002/adsc.202301207

Advanced Synthesis & Catalysis

Catalytic Orthogonal Glycosylation Enabled by Enynal-Derived Copper Carbenes

Surya Pratap Singh,[+a] Bidhan Ghosh,[+a] and Indrajeet Sharma[a,*]

[a] Department of Chemistry and Biochemistry, University of Oklahoma,
101 Stephenson Parkway, Norman, OK-73019, USA
E-mail: isharma@ou.edu
Homepage: https://indrajeetsharma.com

[+] These authors contributed equally to this work.

Manuscript received: October 21, 2023; Revised manuscript received: January 10, 2024;
Version of record online: March 5, 2024

Supporting information for this article is available on the WWW under https://doi.org/10.1002/adsc.202301207

Abstract: Herein, we present an approach for catalytic orthogonal glycosylation utilizing earth-abundant copper carbenes. This method operates under mild conditions and employs readily accessible starting materials, including benchtop stable enynal-derived glycosyl donors, synthesized at the gram scale. The reaction accommodates a variety of glycosyl acceptors, including primary, secondary, and tertiary alcohols. The enynal-derived copper carbenes exhibit remarkable reactivity and selectivity, allowing for the formation of glycosidic linkages with different protecting groups and stereochemical patterns. This approach provides access to both 1,2-*cis*- and -*trans*-glycosidic linkages. The product stereoselectivity is independent of the anomeric configuration of the glycosyl donor, which also has orthogonal reactivity to widely used alkynes and thioglycoside donors. An iterative synthesis of a trisaccharide further demonstrates the application of this orthogonal reactivity.

Keywords: copper catalysis; 1,2-*cis*-glycosides; stereoselective glycosylation; enynal-derived metal carbenes

Introduction

Carbenes are versatile synthetic intermediates, enabling new transformations for constructing a wide range of scaffolds, including complex molecules and materials.[1] The most common carbene precursors are diazo compounds that generate these species by extruding nitrogen gas. Other precursors besides diazo compounds are hydrazones, triazoles, sulfonium ylides, cyclopropenes, and alkynes (Figure 1).

Carbenes can be easily generated from these precursors using transition metals, heat, and photochemical conditions (UV light, blue LED).[2] They can perform novel reactions such as cyclopropanations,[3] cyclopropenations,[4] heteroatom insertion,[5] C–H functionalization,[6] trifluoromethylations,[7] rearrangements,[8] and dipolar- and cycloadditions.[9] Transition metal carbene complexes act as a catalyst in polymerization,,[10] and olefin metathesis.[11] Furthermore, carbenes are used in labeling biomolecules (proteins, DNA, and RNA) for research and diagnostic applications.[12] Despite the application of carbenes in various fields, these synthons have been underutilized in carbohydrate chemistry.[13]

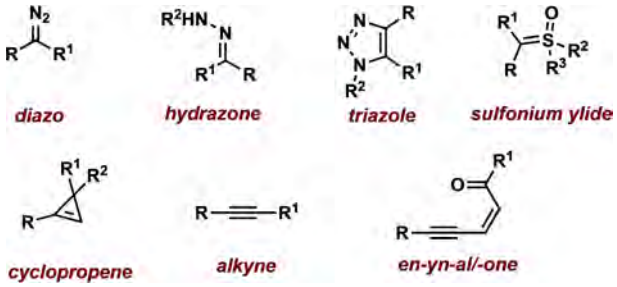

Figure 1. Common carbene precursors.

The first report on the utilization of carbenes in glycosylation goes back to 1989 when the Vasella group synthesized glycosylidene carbenes from the corresponding diazirines.[13a] Because of the instabil-

ity of diazirines, they then employed the anomeric *N*-tosylhydrazone donors, which are benchtop stable carbene precursors. The sodium salts of these *N*-tosylhydrazones under photochemical conditions generate the corresponding anomeric carbenes, which undergo an O–H insertion reaction with alcohols to form *O*-glycosides (Scheme 1a).[13c] A similar anomeric carbene has also been employed in protecting group-free phosphorylations.[14] The requirements of a significant excess of nucleophiles limited the use of highly reactive anomeric carbenes but opened the door for the potential application of carbenes in stereoselective glycosylation. In 2019, the Wan group activated thioglycosides using rhodium carbenoids (Scheme 1b).[13m] However, this glycosylation approach lacks chemo-selectivity and proceeds in two steps: first, the generation of an anomeric sulfonium ylides by employing a diazo-derived rhodium carbenoid,[1f,15] followed by protonation of the ylide to provide the oxocarbenium ion, which undergoes glycosylation with alcohol acceptors. Besides the carbene approach, notable contribution in catalytic glycosylation methods[16] include the pioneering palladium-catalyzed coupling of anomeric stannates,[17] bis-thiourea catalysis,[18] phosphoric acid catalysis,[19] activation of anomeric fluorides using $B(C_6F_5)_3$,[20] and the successful utilization of $Bi(OTf)_3$,[21] phenanthroline catalysts[22] to activate anomeric bromides, halogen-bond assisted radical activation of glycosyl donors.[23] Most of these approaches utilize moisture-sensitive anomeric donors. Among all catalytic methods, a widely studied process employs the benchtop stable alkyne-based donors activated mainly by gold (I/III) and with limited reports of copper catalysts.[24–26] While numerous novel glycosylation techniques have emerged, the process still necessitates laborious fine-tuning and trial-and-error approaches for synthesizing diverse glycans. Additionally, these catalytic approaches have several limitations, such as using precious metals (gold/rhodium), potentially explosive or unsafe diazo compounds, and the need for orthogonality with other donors.

Based on our experience in metal carbene chemistry,[27] we envision addressing these limitations by designing a benchtop stable enynal-derived carbene-based donor for catalytic orthogonal glycosylation. The idea was to activate this enynal using earth-abundant metals such as iron, copper, and zinc. Enynals are carbene surrogates, known to be activated using zinc salts through a 5-*exo*-dig cyclization to form furyl carbene (Scheme 1c).[28] We envisioned that the resulting furyl carbene from enynals would activate the glycosyl ester under mild conditions to enable stereoselective glycosylation (Scheme 1d).

Results and Discussion

To initiate our work, we synthesized benchtop stable enynal donors **3** through the direct EDCI-coupling of iodobenzoic acids with easily accessible anomeric alcohols **1**. The resulting esters **2** were then coupled to the enynal moiety using well-established Sonogashira coupling (Scheme 2; vide SI for details).

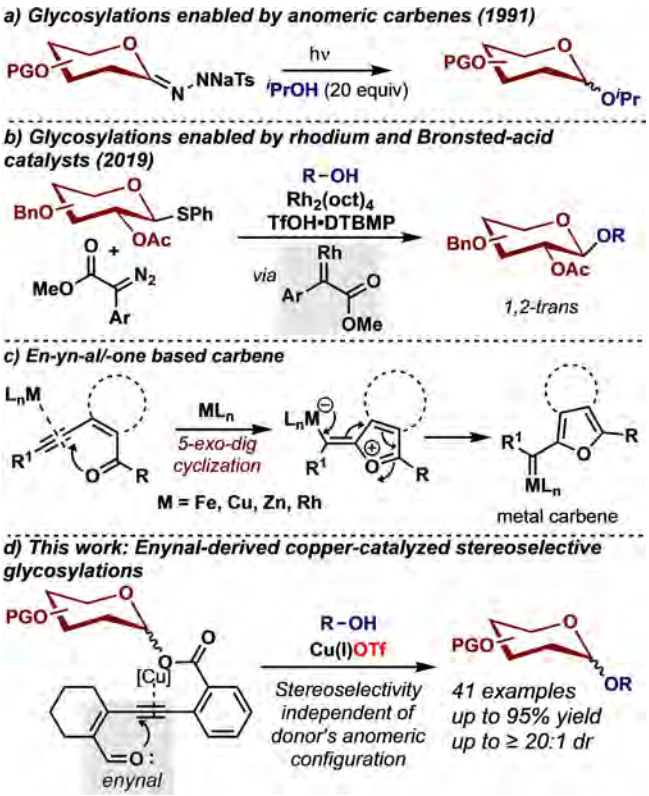

Scheme 1. Carbenes in glycosylations.

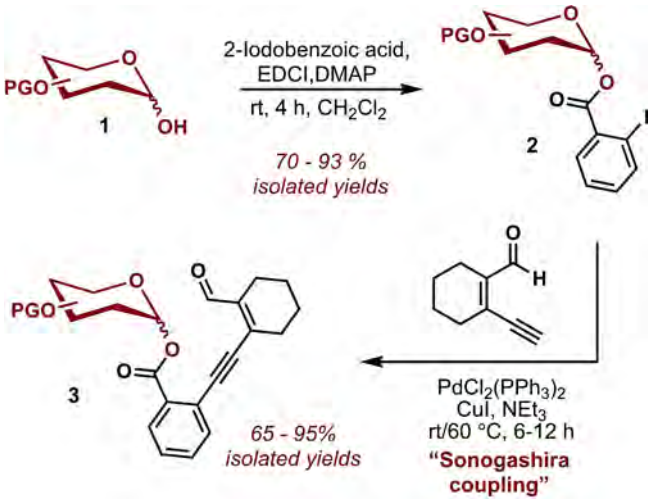

Scheme 2. Synthesis of enynal donors at gram scale.

We initiated our optimization study with the 4,6-*O*-benzylidene-2,3-di-*O*-benzyl-D-mannopyranosyl donor **3 a** to showcase the compatibility of the acid-sensitive acetal moiety under our reaction conditions. Another factor for selecting the donor was the absence of any example in the previously established carbene-based glycosylation (Scheme 1b).[13m] Additionally, the impact of the 4,6-benzylidene locking group is known to enhance the β-1,2-*cis*-selectivity, as previously shown by Sharma and Crich.[29] The methyl-tri-*O*-benzyl-α-D-glucopyranoside **4 a** was selected as the acceptor to optimize the reaction conditions so that the resulting product can undergo global deprotection ($Pd/C + H_2$) to provide the unprotected disaccharide.[30] We focused on identifying the optimal components among earth-abundant metal catalysts, acid scavengers, and solvents (Table 1). Through our studies, we determined that the highest yield (90%) and desired 1,2-*cis*-diastereoselectivity (α:β = 1:8) could be achieved using 30 mol% Cu(I)OTf as the catalyst, lithium carbonate (1.5 equiv.) as the acid scavenger, CH_2Cl_2 as the solvent at 0 °C with 4 Å molecular sieves in 24 h. Through our observations, we found that employing 1.5 equiv. of the donor resulted in the desired glycoside with excellent yield. A higher amount of the donor is attributed to a slight decomposition leading to an unproductive pathway.

Table 1. Optimization of the reaction conditions.[a]

Entry	Deviations from standard conditions	Yield[b]	α/β[c]
1	none	90%	1/8
2	CuI as a catalyst	NR	–
3	$Cu(CH_3CN)_4]PF_6$ as a catalyst	51%	1/1.2
4	$Cu(CH_3CN)_4]BF_4$ as a catalyst	20%	1/1.1
5	$CuCO_3$ as a catalyst, no Li_2CO_3	NR	–
6	−20 °C instead of 0 °C	NR	–
7	−10 °C instead of 0 °C	20%	1/8
8	rt instead of 0 °C	81%	1/5
9	no Li_2CO_3, TfOH instead of $[CuOTf]_2\cdot$tol	NR	–
10	No Li_2CO_3	65%	1/4
11	TTBP, instead of Li_2CO_3	80%	1/4
12	THF or ACN as solvents	NR	–
13	Toluene or CH_2Cl_2/heptane as solvents	45%	1/3
14	$FeCl_3$, instead of $[CuOTf]_2\cdot$tol	<10%	1/2
15	$Zncl_2$ instead of $[CuOTf]_2\cdot$tol	18%	1/2
16	$Zn(OTf)_2$, instead of $[CuOTf]_2\cdot$tol	<10%	1/2
17	$Rh_2(OAc)_4$ instead of $[CuOTf]_2\cdot$tol	NR	–
18	no $[CuOTf]_2\cdot$tol, Li_2CO_3 only	NR	–

[a] Reaction conditions: **3 a** (0.075 mmol), **4 a** (0.05 mmol), catalyst (30 mol%), additive (1.5 equiv.), solvent (0.04 M), 0 °C – rt, 24 h.
[b] Yield was determined by ^{1}H NMR using 1,3,5-trimethoxybenzene as the internal standard.
[c] Diastereoselectivity was determined by ^{1}H NMR. NR = no reaction.

Next, the effect of different copper(I) counteranions was examined. Notably, the triflate counteranion was superior to the corresponding iodide, hexafluorophosphate, and tetrafluoroborate (entries 2–4). Following that, we examine the potential catalytic capability of copper(II) carbonate; nevertheless, no reaction was observed after 24 h (entry 5). Next, we aimed to explore the ideal temperature for the reaction. It was noted that at a lower temperature of −20 °C, the reaction did not occur. Upon raising the temperature to −10 °C, the reaction proceeded at a slower rate, resulting in a reduced yield. However, the selectivity remained comparable to that of the original reaction. (entries 6, 7). Elevating the reaction temperature to room temperature resulted in a diminished yield and selectivity (entry 8). From here, we decided to perform control experiments into the necessity of each additive. As metal triflates can act as a mild source of triflic acid (TfOH),[31] the possibility of triflic acid as a catalyst was probed. With TfOH, we witnessed the complete decomposition of the donor without any desired glycoside (entry 9). A reaction without lithium carbonate decreased the yield and selectivity, highlighting the importance of an acid scavenger (entry 10). 2,4,6-tri-*tert*-butylpyrimidine (TTBP) as an alternative acid scavenger also worked, albeit in lower yield and selectivity (entry 11). Lewis basic solvents like tetrahydrofuran (THF) and acetonitrile (ACN) did not produce any reaction, likely due to solvent coordination with the copper catalyst (entry 12). Likewise, when the reaction solvent was switched to toluene or CH_2Cl_2/heptane (v/v = 1/1), as described by the Zhang group, the yield and α-selectivities were diminished (entry 13). Other catalysts known to activate the enynal systems in the literature, such as iron (III) chloride, zinc (II) chloride, zinc (II) triflate, and rhodium (II) acetate, decreased the product yield and anomeric selectivity (entries 14–17). Finally, no reaction was observed without a copper catalyst, highlighting its importance (entry 18).

With these optimized conditions, we investigated the substrate scope of varying alcohol acceptors with 4,6-*O*-benzylidene-2,3-di-*O*-benzyl-D-mannopyranosyl donor **3 a** (Table 2). Secondary alcohols proceeded smoothly to afford the corresponding products in excellent yields and 1,2-*cis*-selectivity (**5 b**–**5 e**). Electron-rich phenol was glycosylated with excellent yield

Table 2. Scope of enynal donors in 1,2-*cis* glycosylations.[a]

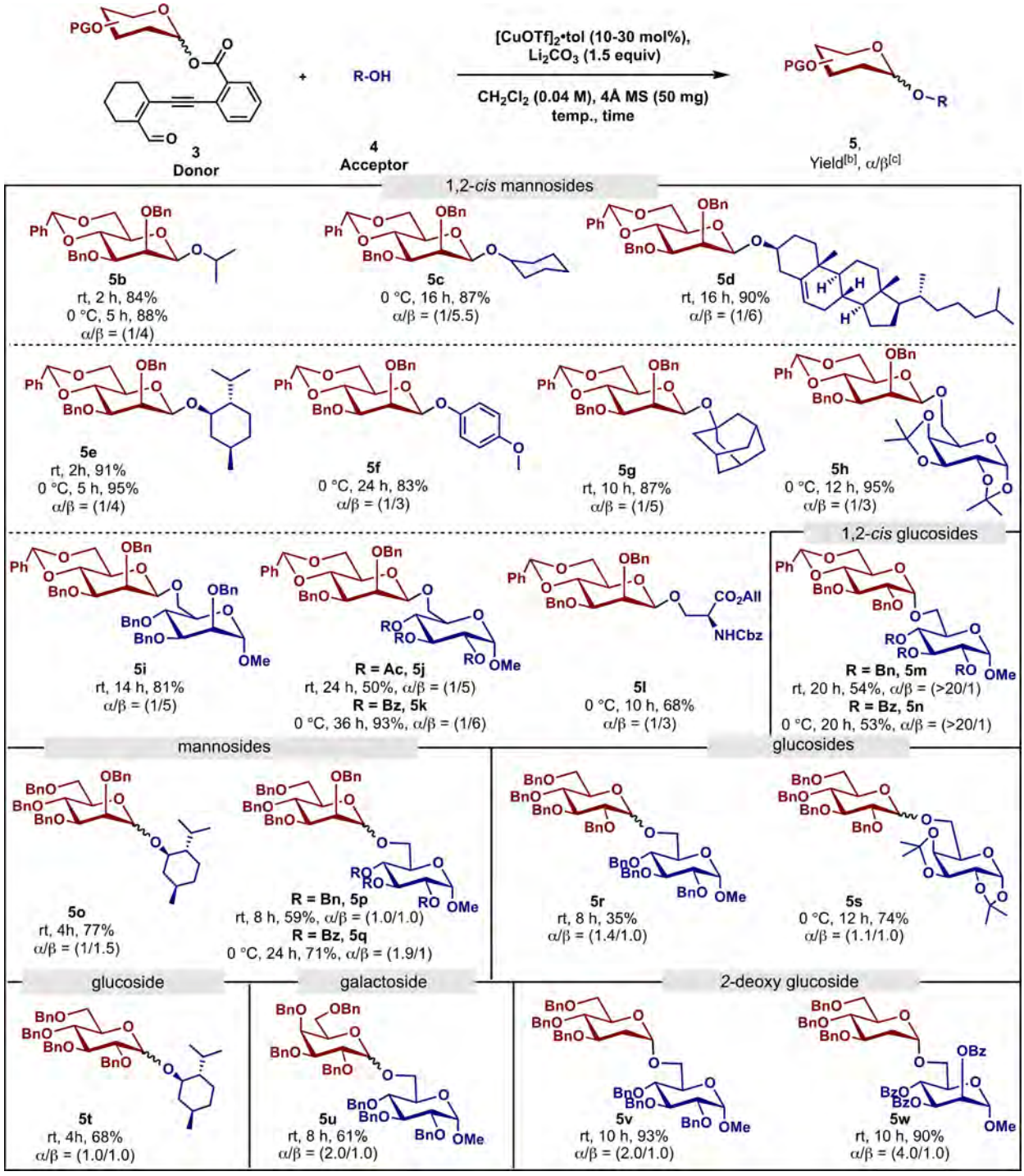

[a] Reaction conditions: **3** (0.075–0.09 mmol), **4** (0.05 mmol), catalyst (10–30 mol%), Li_2CO_3 (1.5 equiv.), solvent (0.04 M).
[b] Yield was determined by ^{1}H NMR using 1,3,5-trimethoxybenzene as the internal standard.
[c] Diastereoselectivity was determined by ^{1}H NMR.
[d] 10 ml% of $[CuOTf]_2 \cdot$tol was used.

and high *cis*-selectivity (**5f**). Bulky tertiary alcohol acceptors like 1-adamantanol also provided good *cis*-selectivity (**5g**). Various carbohydrate alcohol acceptors bearing different protecting groups were then screened. Likewise, acetonide-protected galctopyranoside acceptors, benzyl-/benzoyl-protected manno-

pyranoside acceptors, and acetyl/benzoyl-protected glucopyranoside acceptors provided the intended products in high yields, preferring 1,2-*cis*-selectivity (**5 h**–**5 k**). Notably, reaction yields and selectivity were independent of protecting group influence for benzyl-, benzoyl- and acetyl-protected carbohydrate acceptors. We evaluated the catalytic glycosylation reaction with an amino acid alcohol acceptor, affording the coupling product in good yield and *cis*-selectivity (**5 l**).

Next, we examined the locking effect of 4,6-*O*-benzylidene protection on the D-glucopyranosyl donor **3 b**. We were pleased to observe that the glycosylation reaction with benzyl/benzoyl-protected gluco-pyranoside acceptors afforded the respective products with exclusive 1,2-*cis*-selectivity (**5 m**, **5 n**), albeit in slightly lower yields. We then investigated other donors, such as tetra benzyl-protected glucopyranosyl, mannopyranosyl, galactopyranosyl, and 2-deoxy glucopyranosyl donors, lacking the 4,6-*O*-benzylidene protection. Glycosylation reactions of these synthesized donors with different alcohol acceptors proceeded in good yields; however, no selectivity was observed (**5 o**–**5 w**).

We then focused on synthesizing 1,2-*trans* glycosidic linkages, which play a crucial role in the biological activity of various glycosides and polysaccharides.[32] Additionally, the glycosyl donor containing an acetate group at the C2 encounters multiple limitations, including the concurrent formation of the 1,2-*ortho* ester as an undesired byproduct.[33] Following that, we decided to check the compatibility of our optimized reaction conditions to access 1,2-*trans* glycosidic linkages via the assistance of neighboring group participation. As anticipated, C2 acetyl-protected mannopyranosyl, glucopyranosyl, and galactopyranosyl donors effectively participated in the catalytic glycosylation, producing the desired 1,2-*trans* products with complete stereoselectivity and satisfactory yields (Table 3). For instance, glycosyl-derived acceptors, with diverse stereochemical patterns and protections, bulkier 1-adamantanol, and the phenolic acceptor, successfully underwent the reaction with 2-acetyl mannopyranosyl donor **3 g** to yield the *trans*-glycosides selectively (**6 a**–**6 f**). Significantly, a sterically crowded, less reactive glucose (4-OH) acceptor afforded the glycosylated product in high yield (**6 g**). Likewise, C2-acetyl donors of glucose and galactose exhibited comparable reactivity in the glycosylation reaction (**6 h**–**6 n**). Finally, the reaction was evaluated with a less activated peracylated mannose donor and benzyl-protected glucose acceptor. To our delight, our method furnished the intended product (**6 o**) with high yield.

Next, we investigated the importance of -en, -yn, and -al functionalities within our innovative en-yn-al glycosyl donor. As expected, the synthesized en-yn donor **3 j** and yn-al donor **3 k** exhibited complete stability under the reaction conditions, as shown in Scheme 3a. We then tested the reactivity of a well-established thioglycoside donor (**S-1.4**) under our standard reaction condition. Interestingly, the donor was completely stable, indicating orthogonal reactivity to our designed enynal donor. Likewise, the commonly used alkyne donor **3 l** showed no activity towards the glycosylation reactions under the optimized reaction conditions. We also investigate the effect of aromatic ring electronics on glycosylation by synthesizing the donors (**3 m**, **3 n**) bearing electron-donating (–OMe) and electron-withdrawing (–NO_2) groups *para* to the ester moiety (Scheme 3c). The methoxy donor (*p*-OMe) **3 m** provided a faster reaction (~10 h) compared to the parent (*p*-H) donor (~24 h), while the glycosylation reaction with the nitro donor (*p*-NO_2) **3 n** was sluggish (~36 h). The methoxy (*p*-OMe) afforded a similar yield (88%) to the parent donor (*p*-H), while the nitro donor provided the product with a slightly lower yield (67%). However, there was no change in the anomeric selectivity of the product with either donor (**3 a**, **3 m**, **3 n**), suggesting that the reaction proceeds through a common oxocarbenium ion intermediate in all cases.

Next, we made significant efforts to isolate the plausible leaving group byproduct, which was found to be unstable under the reaction conditions. However, we were able to trap an intermediate of the

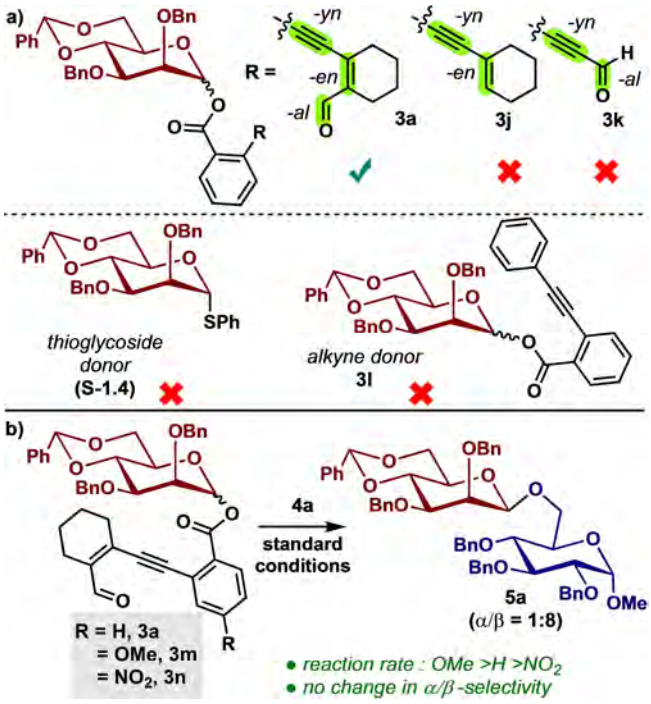

Scheme 3. a) Importance of en-yn-al moiety and reactions of commonly used glycosyl donors under standard conditions. b) Influence of donor's electronics.

Table 3. Scope of enynal donors in 1,2-*trans* glycosylations.[a]

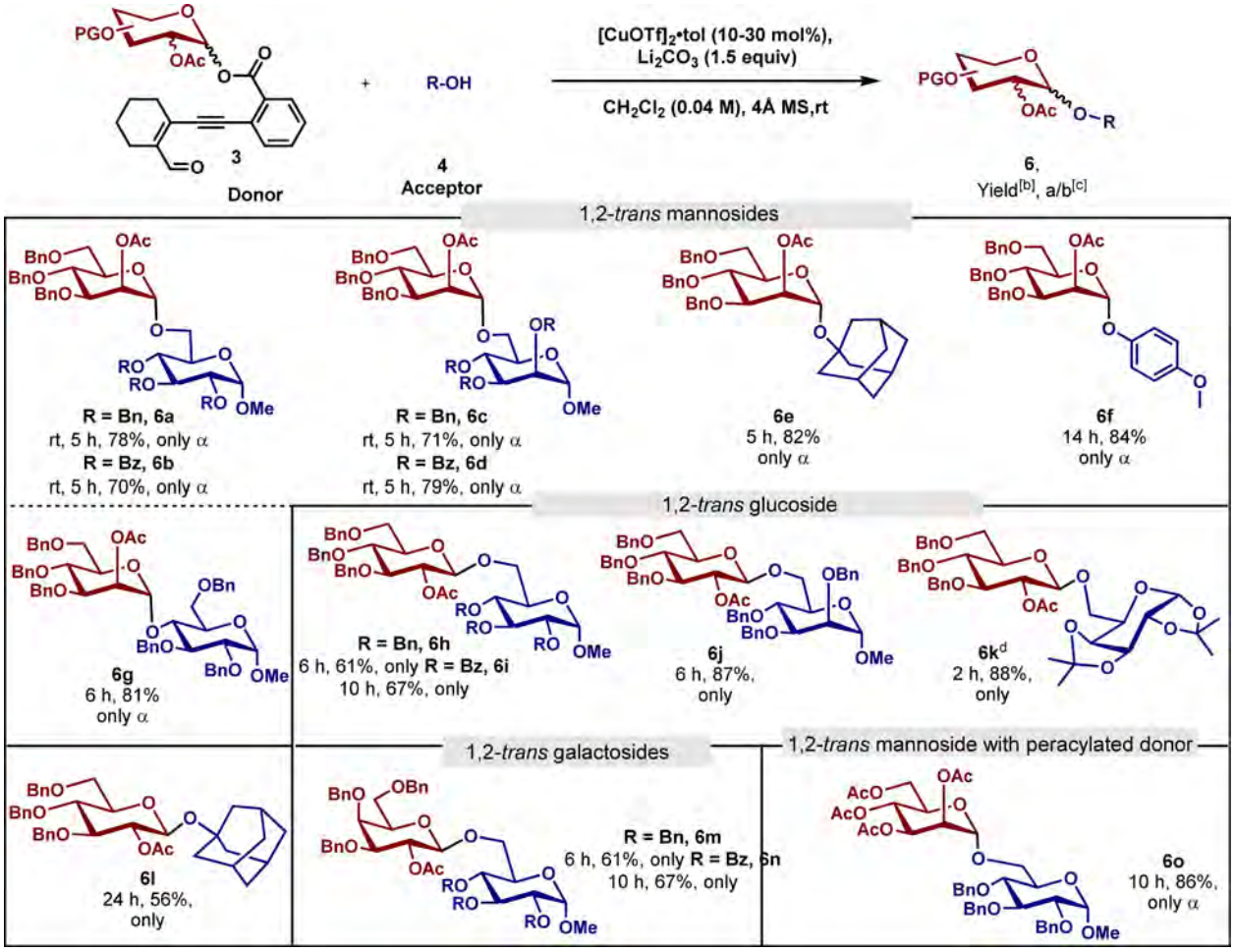

[a] Reaction conditions: **3** (0.075–0.09 mmol), **4** (0.05 mmol), catalyst (10–30 mol%), Li_2CO_3 (1.5 equiv.), solvent (0.04 M).
[b] Yield was determined by ^{1}H NMR using 1,3,5-trimethoxybenzene as the internal standard.
[c] Diastereoselectivity was determined by ^{1}H NMR.
[d] 10 ml% of $[CuOTf]_2 \cdot$tol was used.

byproduct through an excess amount of alcohol acceptor isopropanol **4b** (5 equiv.) along with the anticipated glycosylation product **5b** (Scheme 4). The isomerized isopropanol-trapped byproduct **7** structure was established using extensive NMR and HRMS analysis. This product results from the copper-bound intermediate **9**, and a plausible mechanism has been provided in the SI. Furthermore, the same byproduct has been isolated in our corresponding copper catalyzed 1,2-*cis*-furanosylation studies.[34]

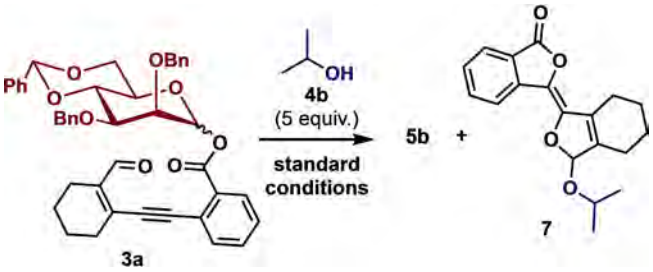

Scheme 4. Isolation of byproduct.

Based on the above-described results, and literature precedence,[29d,35] we hypothesized a plausible mechanism to explain the 1,2-*cis*-selectivity with 4,6-benzylidene donor (Scheme 5). First, the enynal moiety in the presence of copper(I) triflate forms the copper carbene intermediate **8** via a 5-*exo*-dig-cyclization.[36] The resulting copper carbene activates the anomeric ester to form an oxocarbenium ion **11**. The oxocarbenium intermediate **11** exists in equilibrium as a solvent-separated ion pair (SSIP) or contact-ion pair (CIP), or more stable α-covalent triflate **12** (thermodynamic product). In the context of CIP, the proximal triflate anion shields the α-face of

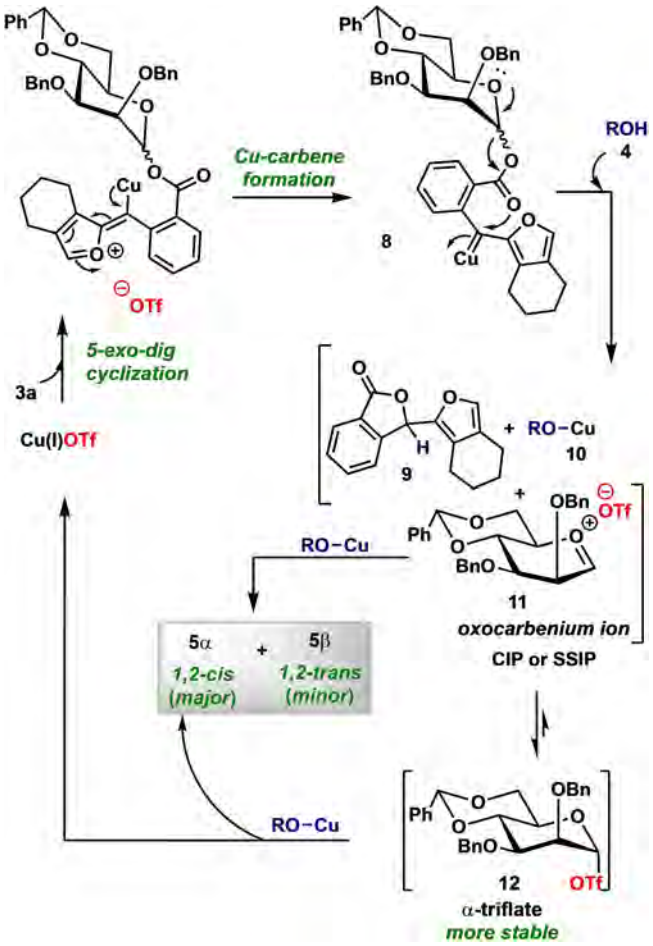

Scheme 5. Plausible reaction mechanism of 1,2-*cis*-selectivity with 4,6-benzylidene donor.

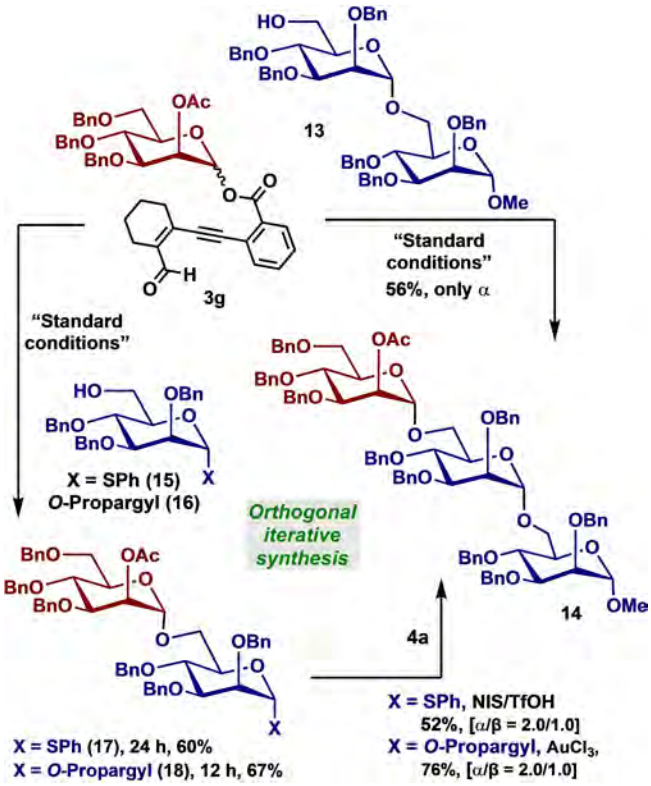

Scheme 6. Orthogonal iterative synthesis of a trisaccharide.

the glycosyl oxocarbenium ion, forming the β-mannopyranosides. On the other hand, in SSIP, the anomeric effect predominantly influences the formation of α- mannopyranosides. A subsequent S_N2 attack on the α-covalent species would furnish the β-anomer. As described by Crich, the role of the 4,6-benzylidene group is to lock the C6–O6 bond in an antiperiplanar conformation to the C5–O5 bond, effectively enhancing its electron-withdrawing effect. This destabilizes the glycosyl oxocarbenium ion and drives the equilibrium strongly toward the covalent triflate form. This shift promotes *cis*-selectivity and facilitates the desired outcome of the reaction. Without the locking effect, the acceptor can capture the oxocarbenium ion intermediate from any face, forming both the α- and β- stereoisomers of the glycosidic bond.

Finally, the application of this methodology was demonstrated with a disaccharide acceptor **13** that resulted in the successful formation of a trisaccharide **14** in good yield (Scheme 6). We further showcased the versatility of our donor by performing an iterative synthesis, taking advantage of its unique orthogonal selectivity. Acceptor **15** reacted smoothly with enynal donor **3g** to provide the disaccharide **17** bearing a thioglycoside moiety that underwent activation with NIS/TMSOTf[37] to give the trisaccharide **14**. Additionally, orthogonal reactivity is harnessed with an alkyne acceptor **16**, which was activated in this iterative sequence with Au-catalyzed condition,[24b] to furnish the trisaccharide **14** with a yield of 76%.

Conclusion

In conclusion, we present an earth-abundant copper metal for catalytic orthogonal glycosylation. This approach involves the utilization of benchtop-stable enynal donors, enabling the synthesis of both 1,2-*cis* and -*trans* linkages. The observed selectivity remains consistent regardless of the donor's anomeric configuration. The applicability of this catalytic system is exemplified through the orthogonal reactivity to thioglycoside and alkyne donors and an iterative synthesis of a trisaccharide. Moreover, the benchtop stability of the glycosyl donors, coupled with their mild activation using earth-abundant copper, renders them well-suited for the automated synthesis of oligosaccharides.[38] Finally, mechanistic insights from this approach will pave the development of

carbene-mediated metal-free glycosylations using blue-LED.

Experimental Section

General Procedure for the Synthesis of 1,2-*cis* (5a–5w), and 1,2-*trans* (6a–6o) glycosylations

A 5 mL dried Schlenk flask was charged with corresponding alcohol acceptor (0.05 mmol, 1.0 equiv.), pyranosyl donor (0.1 mmol, 2.0 equiv.), $[Cu(I)OTf]_2 \cdot tol$ (0.3 mmol, 30 mol%) with respect to the alcohol, Li_2CO_3 (0.06 mmol, 1.5 equiv.), 4 Å molecular sieve and 2 mL CH_2Cl_2. The resulting solution was stirred at 0 °C or room temperature and the progress was monitored by TLC (2–24 h). After completion, saturated $NaHCO_3$ solution was added, the aqueous phase was extracted with CH_2Cl_2 (3x), 1,3,5-trimethoxybenzene (0.05 mmol, 1.0 equiv.) was added, and the organic phases were concentrated *in vacuo*. The product yield and anomeric ratio were determined by ^1H NMR.

Acknowledgements

This work was supported by the NSF CHE-1753187 and the Oklahoma Center for the Advancement of Science and Technology (OCAST HR20-078). We thank Dr. Novruz Akhmedov and Dr. Steven Foster from the Research Support Services, University of Oklahoma, for NMR and mass spectral analyses, respectively. We also thank Dr. Anae Bain and Dr. Prashant Mandal for their helpful discussions.

References

[1] a) D. M. Flanigan, F. Romanov-Michailidis, N. A. White, T. Rovis, *Chem. Rev.* **2015**, *115*, 9307–9387; b) F. E. Hahn, *Chem. Rev.* **2018**, *118*, 9455–9456; c) H. M. L. Davies, D. Morton, *Chem. Soc. Rev.* **2011**, *40*, 1857–1869; d) H. M. L. Davies, J. Nikolai, *Org. Biomol. Chem.* **2005**, *3*, 4176–4187; e) D. Zhu, L. Chen, H. Fan, Q. Yao, S. Zhu, *Chem. Soc. Rev.* **2020**, *49*, 908–950; f) H. M. L. Davies, J. R. Denton, *Chem. Soc. Rev.* **2009**, *38*, 3061–3071; g) Z.-Y. Cao, Y.-H. Wang, X.-P. Zeng, J. Zhou, *Tetrahedron Lett.* **2014**, *55*, 2571–2584.

[2] M. Jia, S. Ma, *Angew. Chem. Int. Ed.* **2016**, *55*, 9134–9166.

[3] a) S. Zhu, J. A. Perman, X. P. Zhang, *Angew. Chem. Int. Ed.* **2008**, *47*, 8460–8463; b) R. R. Nani, S. E. Reisman, *J. Am. Chem. Soc.* **2013**, *135*, 7304–7311; c) S. Zhu, X. Xu, J. A. Perman, X. P. Zhang, *J. Am. Chem. Soc.* **2010**, *132*, 12796–12799.

[4] a) J. F. Briones, H. M. L. Davies, *Org. Lett.* **2011**, *13*, 3984–3987; b) X. Cui, X. Xu, H. Lu, S. Zhu, L. Wojtas, X. P. Zhang, *J. Am. Chem. Soc.* **2011**, *133*, 3304–3307.

[5] a) M. Yang, T. Albrecht-Schmitt, V. Cammarata, P. Livant, D. S. Makhanu, R. Sykora, W. Zhu, *J. Org. Chem.* **2009**, *74*, 2671–2678; b) X. Li, D. P. Curran, *J. Am. Chem. Soc.* **2013**, *135*, 12076–12081; c) C. J. Moody, R. J. Taylor, *Tetrahedron Lett.* **1987**, *28*, 5351–5352; d) C. S. Shanahan, P. Truong, S. M. Mason, J. S. Leszczynski, M. P. Doyle, *Org. Lett.* **2013**, *15*, 3642–3645.

[6] a) M. Álvarez, F. Molina, P. J. Pérez, *J. Am. Chem. Soc.* **2022**, *144*, 23275–23279; b) S. Jana, C. Empel, C. Pei, P. Aseeva, T. V. Nguyen, R. M. Koenigs, *ACS Catal.* **2020**, *10*, 9925–9931; c) N. Jha, N. P. Khot, M. Kapur, *Chem. Rec.* **2021**, *21*, 4088–4122; d) Y. He, Z. Huang, K. Wu, J. Ma, Y.-G. Zhou, Z. Yu, *Chem. Soc. Rev.* **2022**, *51*, 2759–2852.

[7] a) M. Hu, C. Ni, J. Hu, *J. Am. Chem. Soc.* **2012**, *134*, 15257–15260; b) Y. Liu, X. Shao, P. Zhang, L. Lu, Q. Shen, *Org. Lett.* **2015**, *17*, 2752–2755.

[8] a) S. Jana, Y. Guo, R. M. Koenigs, *Chem. Eur. J.* **2021**, *27*, 1270–1281; b) C. Empel, S. Jana, R. M. Koenigs, in *Homologation Reactions*, **2023**, pp. 265–286.

[9] A. Padwa, S. F. Hornbuckle, *Chem. Rev.* **1991**, *91*, 263–309.

[10] a) A. V. Zhukhovitskiy, I. J. Kobylianskii, A. A. Thomas, A. M. Evans, C. P. Delaney, N. C. Flanders, S. E. Denmark, W. R. Dichtel, F. D. Toste, *J. Am. Chem. Soc.* **2019**, *141*, 6473–6478; b) E. Jellema, P. H. M. Budzelaar, J. N. H. Reek, B. de Bruin, *J. Am. Chem. Soc.* **2007**, *129*, 11631–11641; c) F. Li, L. Xiao, B. Li, X. Hu, L. Liu, *Coord. Chem. Rev.* **2022**, *473*, 214806.

[11] a) S. G. Patra, N. K. Das, *Polyhedron* **2021**, *200*, 115096; b) J. Huang, E. D. Stevens, S. P. Nolan, J. L. Petersen, *J. Am. Chem. Soc.* **1999**, *121*, 2674–2678; c) C. Adlhart, P. Chen, *J. Am. Chem. Soc.* **2004**, *126*, 3496–3510; d) B. W. Grau, A. Neuhauser, S. Aghazada, K. Meyer, S. B. Tsogoeva, *Chem. Eur. J.* **2022**, *28*, e202201414.

[12] a) N. A. McGrath, K. A. Andersen, A. K. F. Davis, J. E. Lomax, R. T. Raines, *Chem. Sci.* **2015**, *6*, 752–755; b) K. A. Mix, R. T. Raines, *Org. Lett.* **2015**, *17*, 2358–2361; c) J. V. Jun, Y. D. Petri, L. W. Erickson, R. T. Raines, *J. Am. Chem. Soc.* **2023**, *145*, 6615–6621; d) K. A. Mix, M. R. Aronoff, R. T. Raines, *ACS Chem. Biol.* **2016**, *11*, 3233–3244; e) B. Bernardim, L. Dunsmore, H. Li, B. Hocking, R. Nuñez-Franco, C. D. Navo, G. Jiménez-Osés, A. C. B. Burtoloso, G. J. L. Bernardes, *Bioconjugate Chem.* **2020**, *31*, 1604–1610; f) F.-L. Liu, C.-B. Qi, Q.-Y. Cheng, J.-H. Ding, B.-F. Yuan, Y.-Q. Feng, *Anal. Chem.* **2020**, *92*, 2301–2309.

[13] a) K. Briner, A. Vasella, *Helv. Chim. Acta* **1989**, *72*, 1371; b) K. Briner, A. Vasella, *Helv. Chim. Acta* **1990**, *73*, 1764; c) S. E. Mangholz, A. Vasella, *Helv. Chim. Acta* **1991**, *74*, 2100; d) E. Bozo, A. Vasella, *Helv. Chim. Acta* **1992**, *75*, 2613; e) K. Briner, A. Vasella, *Helv. Chim. Acta* **1992**, *75*, 621; f) A. Vasella, P. Uhlmann, C. A. A. Waldraff, F. Diederich, C. Thilgen, *Angew. Chem.* **1992**, *104*, 1383; g) P. R. Muddasani, E. Bozo, B. Bernet, A. Vasella, *Helv. Chim. Acta* **1994**, *77*, 257; h) P. Uhlmann, D. Nanz, E. Bozo, A. Vasella, *Helv. Chim. Acta* **1994**, *77*, 1430; i) P. Uhlmann, A. Vasella, *Helv. Chim. Acta* **1994**, *77*, 1175; j) A. Vasella, Oxford University Press, Inc., **1999**, p. 56; k) J. Wu, X. Li, X. Qi, X. Duan, W. L. Cracraft, I. A. Guzei, P. Liu, W. Tang, *J. Am. Chem. Soc.* **2019**, *141*, 19902–19910; l) T.

Kametani, K. Kawamura, T. Honda, *J. Am. Chem. Soc.* **1987**, *109*, 3010; m) L. Meng, P. Wu, J. Fang, Y. Xiao, X. Xiao, G. Tu, X. Ma, S. Teng, J. Zeng, Q. Wan, *J. Am. Chem. Soc.* **2019**, *141*, 11775–11780.
[14] L. J. G. Edgar, S. Dasgupta, M. Nitz, *Org. Lett.* **2012**, *14*, 4226–4229.
[15] H. M. L. Davies, *J. Org. Chem.* **2019**, *84*, 12722–12745.
[16] a) M. M. Nielsen, C. M. Pedersen, *Chem. Rev.* **2018**, *118*, 8285–8358; b) S. S. Nigudkar, A. V. Demchenko, *Chem. Sci.* **2015**, *6*, 2687–2704; c) A. Chen, B. Yang, Z. Zhou, F. Zhu, *Chem Catal.* **2022**, *2*, 3430–3470; d) R. Das, B. Mukhopadhyay, *ChemistryOpen* **2016**, *5*, 401–433; e) M. M. Mukherjee, R. Ghosh, J. A. Hanover, *Front. Mol. Biosci.* **2022**, *9*.
[17] a) T. Yang, F. Zhu, M. A. Walczak, *Nat. Commun.* **2018**, *9*, 3650; b) F. Zhu, S. O'Neill, J. Rodriguez, M. A. Walczak, *Chem. Eur. J.* **2019**, *25*, 3147–3155.
[18] A. B. Mayfield, J. B. Metternich, A. H. Trotta, E. N. Jacobsen, *J. Am. Chem. Soc.* **2020**, *142*, 4061–4069.
[19] a) J. Lee, A. Borovika, Y. Khomutnyk, P. Nagorny, *Chem. Commun.* **2017**, *53*, 8976–8979; b) J.-H. Tay, A. J. Argüelles, M. D. DeMars, II, P. M. Zimmerman, D. H. Sherman, P. Nagorny, *J. Am. Chem. Soc.* **2017**, *139*, 8570–8578.
[20] G. C. Sati, J. L. Martin, Y. Xu, T. Malakar, P. M. Zimmerman, J. Montgomery, *J. Am. Chem. Soc.* **2020**, *142*, 7235–7242.
[21] H. B. Steber, Y. Singh, A. V. Demchenko, *Org. Biomol. Chem.* **2021**, *19*, 3220–3233.
[22] H. Xu, R. N. Schaugaard, J. Li, H. B. Schlegel, H. M. Nguyen, *J. Am. Chem. Soc.* **2022**, *144*, 7441–7456.
[23] C. Zhang, H. Zuo, G. Y. Lee, Y. Zou, Q.-D. Dang, K. N. Houk, D. Niu, *Nat. Chem.* **2022**, *14*, 686–694.
[24] a) J. Luo, Q. Wan, in *Carbohydrate Chemistry: Chemical and Biological Approaches, Volume 40, Vol. 40* (Eds.: A. Pilar Rauter, T. Lindhorst, Y. Queneau), The Royal Society of Chemistry, **2014**.; b) S. Hotha, S. Kashyap, *J. Am. Chem. Soc.* **2006**, *128*, 9620–9621; c) G. Sureshkumar, S. Hotha, *Chem. Commun.* **2008**, 4282–4284; d) S. Adhikari, K. N. Baryal, D. Zhu, X. Li, J. Zhu, *ACS Catal.* **2013**, *3*, 57–60; e) Y. Li, Y. Yang, B. Yu, *Tetrahedron Lett.* **2008**, *49*, 3604–3608; f) Y. Tang, J. Li, Y. Zhu, Y. Li, B. Yu, *J. Am. Chem. Soc.* **2013**, *135*, 18396–18405; g) X. Mi, Q. Lou, W. Fan, L. Zhuang, Y. Yang, *Carbohydr. Res.* **2017**, *448*, 161–165; h) F. Yang, Q. Wang, B. Yu, *Tetrahedron Lett.* **2012**, *53*, 5231–5234; i) B. Yu, *Acc. Chem. Res.* **2018**, *51*, 507–516; j) S. R. Vidadala, S. Hotha, *Chem. Commun.* **2009**, 2505–2507; k) A. K. Kayastha, S. Hotha, *Chem. Commun.* **2012**, *48*, 7161–7163.
[25] a) X. Ma, Z. Zheng, Y. Fu, X. Zhu, P. Liu, L. Zhang, *J. Am. Chem. Soc.* **2021**, *143*, 11908–11913; b) X. Ma, Y. Zhang, X. Zhu, Y. Wei, L. Zhang, *J. Am. Chem. Soc.* **2023**, *145*, 22, 11921–11926.
[26] B.-B. Zhan, K.-S. Xie, Q. Zhu, W. Zhou, D. Zhu, B. Yu, *Org. Lett.* **2023**, *25*, 3841–3846.
[27] a) A. I. Bain, K. Chinthapally, A. C. Hunter, I. Sharma, *Eur. J. Org. Chem.* **2022**, *27*, e202101419; b) A. C. Hunter, S. C. Schlitzer, J. C. Stevens, B. Almutwalli, I. Sharma, *J. Org. Chem.* **2018**, *83*, 2744–2752; c) K. Chinthapally, N. P. Massaro, S. Ton, E. D. Gardner, I. Sharma, *Tetrahedron Lett.* **2019**, *60*, 151253; d) D. J. Paymode, I. Sharma, *Eur. J. Org. Chem.* **2021**, *13*, 2034–2040.
[28] a) J. Ma, L. Zhang, S. Zhu, *Curr. Org. Chem.* **2016**, *20*, 102–118; b) M. J. González, L. A. López, R. Vicente, *Org. Lett.* **2014**, *16*, 5780–5783; c) R. Jana, S. Paul, A. Biswas, J. K. Ray, *Tetrahedron Lett.* **2010**, *51*, 273–276; d) C. Ou, B. Ghosh, I. Sharma, *Org. Chem. Front.* **2023**, *10*, 5933–5939.
[29] a) D. Crich, I. Sharma, *Org. Lett.* **2008**, *10*, 4731–4734; b) D. Crich, I. Sharma, *J. Org. Chem.* **2010**, *75*, 8383–8391; c) I. Sharma, L. Bohé, D. Crich, *Carbohydr. Res.* **2012**, *357*, 126–131; d) S. Aubry, K. Sasaki, I. Sharma, D. Crich, in *Reactivity Tuning in Oligosaccharide Assembly* (Eds.: B. Fraser-Reid, J. Cristóbal López), Springer Berlin Heidelberg, Berlin, Heidelberg, **2011**, pp. 141–188.
[30] a) D. Dhara, A. Dhara, P. V. Murphy, L. A. Mulard, *Carbohydr. Res.* **2022**, *521*, 108644; b) V. S. Rao, A. S. Perlin, *Carbohydr. Res.* **1980**, *83*, 175–177.
[31] a) T. C. Wabnitz, J.-Q. Yu, J. B. Spencer, *Chem. Eur. J.* **2004**, *10*, 484–493; b) D. C. Rosenfeld, S. Shekhar, A. Takemiya, M. Utsunomiya, J. F. Hartwig, *Org. Lett.* **2006**, *8*, 4179–4182; c) T. T. Dang, F. Boeck, L. Hintermann, *J. Org. Chem.* **2011**, *76*, 9353–9361.
[32] a) in *Essentials of Glycobiology* (Eds.: A. Varki, R. D. Cummings, J. D. Esko, P. Stanley, G. W. Hart, M. Aebi, A. G. Darvill, T. Kinoshita, N. H. Packer, J. H. Prestegard, R. L. Schnaar, P. H. Seeberger), by The Consortium of Glycobiology Editors, La Jolla, California. All rights reserved., Cold Spring Harbor (NY), **2015**; b) R. A. Dwek, *Chem. Rev.* **1996**, *96*, 683–720; c) A. Varki, *Glycobiology* **1993**, *3*, 97–130.
[33] a) P. H. Seeberger, M. Eckhardt, C. E. Gutteridge, S. J. Danishefsky, *J. Am. Chem. Soc.* **1997**, *119*, 10064–10072; b) D. Crich, Z. Dai, S. Gastaldi, *J. Org. Chem.* **1999**, *64*, 5224–5229.
[34] B. Ghosh, A. Alber, C. W. Lander, Y. Shao, K. M. Nicholas, I. Sharma, *ACS Catal.* **2024**, *14, 2*, 1037–1049.
[35] a) D. Crich, *Acc. Chem. Res.* **2010**, *43*, 1144–1153; b) Y. Fu, L. Bernasconi, P. Liu, *J. Am. Chem. Soc.* **2021**, *143*, 1577–1589; c) P. O. Adero, H. Amarasekara, P. Wen, L. Bohé, D. Crich, *Chem. Rev.* **2018**, *118*, 8242–8284; d) P. R. Andreana, D. Crich, *ACS Cent. Sci.* **2021**, *7*, 1454–1462; e) P. Wen, D. Crich, *J. Org. Chem.* **2015**, *80*, 12300–12310; f) M. Moumé-Pymbock, D. Crich, *J. Org. Chem.* **2012**, *77*, 8905–8912; g) D. Crich, N. S. Chandrasekera, *Angew. Chem. Int. Ed.* **2004**, *43*, 5386–5389; h) D. Crich, O. Vinogradova, *Chem. Informationsdienst* **2007**, *38*, i.
[36] a) K. Miki, Y. Kato, S. Uemura, K. Ohe, *Bull. Chem. Soc. Jpn.* **2008**, *81*, 1158-1165; b) Y. Kato, K. Miki, F. Nishino, K. Ohe, S. Uemura, *Org. Lett.* **2003**, *5*, 2619–2621.

[37] R. Liu, Q. Hua, Q. Lou, J. Wang, X. Li, Z. Ma, Y. Yang, *J. Org. Chem.* **2021**, *86*, 4763–4778.
[38] a) S. Escopy, Y. Singh, K. J. Stine, A. V. Demchenko, *Chem. Eur. J.* **2022**, *28*, e202201180; b) P. H. Seeberger, *Chem. Soc. Rev.* **2008**, *37*, 19–28; c) M. Guberman, P. H. Seeberger, *J. Am. Chem. Soc.* **2019**, *141*, 5581–5592.